Identification and characterization of enzymes responsible for methylglyoxal overproduction in the metabolic syndrome

A Thesis

Submitted to the College of

Graduate Studies and Research

In Partial Fulfillment of the Requirements

For the Degree of Doctor of Philosophy

In the Department of Pharmacology

University of Saskatchewan

Canada

By

Jianghai Liu

PERMISSION TO USE

In presenting this thesis in partial fulfillment of the requirements for a Postgraduate degree from the University of Saskatchewan, I agree that the Libraries of this University may make it freely available for inspection. I further agree that permission for copying of this thesis in any manner, in whole or in part, for scholarly purposes may be granted by the professor or professors who supervised my thesis work or, in their absence, by the Head of the Department or the Dean of the College in which my thesis work was done. It is understood that any copying or publication or use of this thesis or parts thereof for financial gain shall not be allowed without my written permission. It is also understood that due recognition shall be given to me and to the University of Saskatchewan in any scholarly use which may be made of any material in my thesis.

Requests for permission to copy or to make other use of material in this thesis in whole or part should be addressed to:

Head of the Department of Pharmacology

University of Saskatchewan

Saskatoon, Saskatchewan S7N 5E5

Canada

ABSTRACT

Methylglyoxal (MG) is a highly reactive metabolite produced in the cells. Insulin-insensitive vascular cells are the major sites for endogenous MG formation. Elevated levels of MG in vascular tissues were reported in metabolic syndrome with hyperglycemia (such as type 2 diabetes) or without hyperglycemia (such as hypertension), but the underlying mechanism is largely unknown. We observed that in cultured vascular smooth muscle cells (VSMCs), fructose (25 mM) treatment up-regulated gene expression of aldolase B and enhanced MG formation. Glucose (25 mM) treatment of VSMCs activated the polyol pathway and increased fructose formation, leading to aldolase B up-regulation and MG overproduction. In our tested rat models with obesity, hypertension or diabetes, serum and aortic MG and fructose levels were increased, and the expression of aldolase B in the aorta was up-regulated. Our study indicates that aldolase B up-regulation by elevated fructose is a common mechanism for vascular MG overproduction in the metabolic syndrome.

Increased MG accumulation is considered an important molecular mechanism for endothelial cell damage in diabetes. Whether knockdown of aldolase B prevents high glucose-induced MG overproduction and cellular dysfunction was investigated in the cultured endothelial cells. High glucose (25 mM) incubation increased aldolase B mRNA expression and MG formation in endothelial EA. hy926 cells. We found that siRNA knockdown of aldolase B prevented high glucose-elevated MG levels and the activation of multiple metabolic and signaling pathways (i.e. increase in advanced glycation endproducts accumulation, oxidative stress, O-linked N-acetyl glucosamine modification of proteins, membrane protein kinase C activity and nuclear translocation of nuclear factor κB). Our

study further suggests that aldolase B is likely a key target for prevention of MG overproduction and related cellular dysfunction not only in VSMCs but also in vascular endothelial cells in diabetes and its vascular complications.

Recently, MG formation in insulin-sensitive cells has received much attention since high levels of MG have been found to disturb insulin signaling in 3T3-L1 adipocytes and skeletal muscle L6 cells. We, therefore, investigated the mechanisms for MG formation in insulin-sensitive 3T3-L1 adipocytes under physiological and pathological conditions. We found that insulin (100 nM), glucose (25 mM), or their combination has no effect on cellular levels of sorbitol and fructose, in comparison with the control group (5 mM glucose alone). Insulin, glucose (25 mM), or their combination decreased aldolase B mRNA to a similar level. Glucose (25 mM) had no effect on aldolase A gene expression, but insulin (100 nM) markedly increased aldolase A mRNA and protein levels in the absence or presence of 25 mM glucose. Application of insulin (100 nM) increased the levels of basal or glucose (25 mM)-induced MG and glucose 6-phosphate. Knockdown of aldolase A prevented the increased MG levels induced by insulin (100 nM), glucose (25 mM), or their combination. Our data suggest that aldolase A and glycolysis are responsible for the basal and excess MG generation in insulin-sensitive adipose cells, especially under the stimulus of insulin.

In summary, all experiments taken together, show for the first time, that aldolase B is responsible for vascular MG overproduction and aldolase A is responsible for adipose MG overproduction in metabolic syndrome. Increased MG levels in these cells may contribute to endothelial dysfunction, pathogenesis of hypertension and hypertriglyceridemia that characterize the metabolic syndrome.

ACKNOWLEDGEMENTS

I would like to express my deepest appreciation to my supervisor Dr. Lingyun Wu who accepted me as her PhD student and supported me over the years in my study, research and life. I appreciate all her contributions of time, ideas, and funding to make my PhD experience productive. I especially want to thank her for always trusting me and giving me so much time and freedom to pursue the research areas I am interested in. Dr. Wu is a dear and caring lady. She gives me an excellent example as a good scientist and supervisor.

I would also like to thank my co-supervisor Dr. Kaushik Desai for offering me his wide knowledge, many discussions, and lots of comments and corrections throughout the whole thesis work.

A special thank must go to Dr. Rui Wang of Lakehead University for his great help in designing experiments, giving detailed and valuable feedback on my work, and revising manuscripts.

I wish to express my heartiest thanks to my thesis committee: Drs. Steven Richardson, William Roesler, Darrell Mousseau, Lynn Weber, and Peter Yu for their encouragement, insightful comments, and critical questions which always inspired me to better my research.

Our lab is a source of friendships as well as good advice and collaboration. I would like to thank my lab mates: Tuanjie Chang, Arti Dhar, Ali Banigesh, Indu Dhar, Ashley Untereiner, Qian Huang, Hui Wang, Xuming Jia, Xiaoxia Wang and Feng Liang for the discussions, lab assistance and the wonderful time we had working together. In particular, I would like to thank our technician Arlene Drimmie for teaching me technical skills at the

beginning of my program and providing technical assistance whenever needed. Also, thanks to Timothy Chun-Ping Mak, our summer student from McGill University, for his excellent work which contributed in some parts of this thesis.

Thanks to the staff at Department of Pharmacology: Cindy Wruck, Donna Dodge, and Bob Wilcox who helped me greatly in many ways during the past five years.

I cannot finish my PhD thesis without the support of my parents and my wife Xinlei Li. It is their love, dedication, understanding and encouragement in these years that endowed me with the strength to pursue my dream.

Finally, I would like to thank the College of Medicine, Heart and Stroke Foundation of Saskatchewan, and Canadian Institutes of Health Research for their financial support.

DEDICATION

To my wife

Xinlei Li

To my mother

献给我的母亲

For their constant support, encouragement, care, and never ending love

因为她们不断的支持，鼓励，关怀和无尽的爱

To my lost youth

TABLE OF CONTENTS

LIST OF TABLES

LIST OF FIGURES

LIST OF ABBREVIATIONS

2-DG	2-Deoxy-D-glucose
2-MQ	2-methyl quinoxaline
3-DG	3-Deoxyglucosone
5-MQ	5-methyl quinoxaline
8-oxo-dG	8-Oxo-deoxyguanosine
AG	Aminoguanidine
AGEs	Advanced glycation endproducts
ALA	Alagebrium, ALT-711
ANOVA	Analysis of variance
AR	Aldose reductase
BS	Bovine serum
CEL	N(ε)-carboxyethyl-lysine
CML	N(ε)-carboxymethyl-lysine
CYP 2E1	Cytochrome P450 2E1
DADS	Diallyl disulfide
DCF	2',7'-dichlorofluorescein
DHAP	Dihydroxyacetone phosphate
DMEM	Dulbecco's Modified Eagle Medium
ECs	Endothelial cells
eNOS	Endothelial nitric oxide synthase

F-1-P	Fructose 1-phosphate
F-1,6-P_2	Fructose-1,6-bisphosphate
FBS	Fetal bovine serum
GA3P	Glyceraldehyde 3-phosphate
G-6-P	Glucose 6-phosphate
GLUT	Glucose transporter
H_2O_2	Hydrogen peroxide
HPLC	High performance liquid chromatography
iNOS	Inducible nitric oxide synthase
MDL-72974	(E)-2-(4-fluorophenethyl)-3-fluoroallylamine
MG	Methylglyoxal
NF-κB	Nuclear factor kappa B
NO	Nitric oxide
NOS	Nitric oxide synthase
$O_2^{\cdot -}$	Superoxide anions
O-GlcNAc	O-linked N-acetyl glucosamine
$ONOO^-$	Peroxynitrite
o-PD	*o*-phenylenediamine
PBS	Phosphate buffered saline
PCA	Perchloric acid
PKC	Protein Kinase C
ROS	Reactive oxygen species

SD	Sprague-Dawley
SHR	spontaneously hypertensive rats
SOD	Superoxide dismutase
SSAO	Semicarbazide-sensitive amine oxidase
TNF-α	Tumor necrosis factor alpha
VCAM-1	Vascular cell adhesion molecule-1
VSMCs	Vascular smooth muscle cells
WKY	Wistar-Kyoto

CHAPTER 1

INTRODUCTION AND LITERATURE REVIEW

1.1 What is methylglyoxal (MG)?

Methylglyoxal (MG), an α-dicarbonyl compound (Figure 1-1), is also called 2-oxopropanal, pyruvaldehyde, pyruvic aldehyde or 2-ketopropionaldehyde. MG is present mostly in the mono and dihydrate forms [MG-H_2O, 71% and MG-$(H_2O)_2$, 28%], in aqueous solution (*1*). MG can react with and modify cellular macromolecules, including DNA, proteins, peptides, and lipids. In the body, 99% of MG is bound to biomolecules whereas only 1% is in the free form (*2*). The high reactivity of MG is due to the electrophilic carbonyl group and to the O-atoms which increase the positive charge on the carbonyl carbon (*3*). Therefore, MG displays higher reactivity in nucleophilic addition reactions than other dicarbonyl compounds, such as glyoxal and 3-deoxyglucosone (3-DG) (*4*).

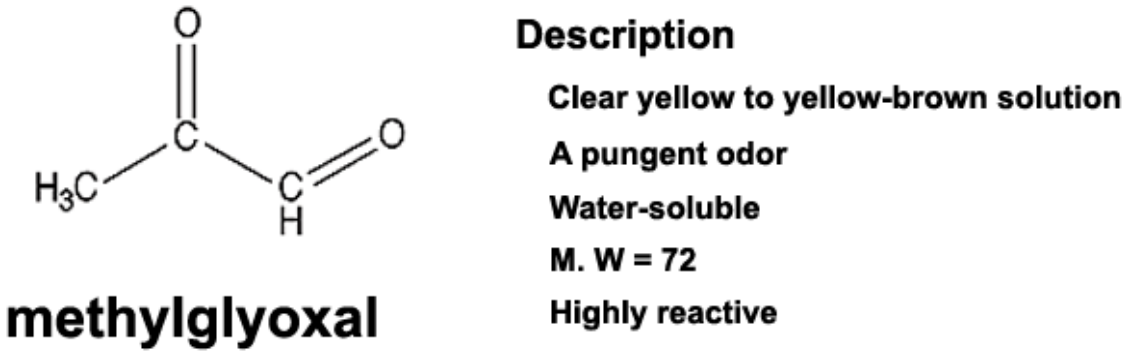

Figure 1-1 Chemical structure and characteristics of methylglyoxal.

1.2 Where does MG come and go?

1.2.1 Sources of endogenous MG

1.2.1.1 MG formation

In living organisms, MG is produced through several metabolic pathways (Figure 1-2). The primary sources for endogenous MG generation are triosephosphates, glyceraldehyde 3-phosphate (GA3P) and dihydroxyacetone phosphate (DHAP) (*5, 6*). GA3P and DHAP are produced during glucose or fructose metabolism in cells. Through glycolysis, glucose is phosphorylated into glucose 6-phosphate (G-6-P) and further metabolized enzymatically into fructose 1,6-bisphosphate (F-1,6-P_2), which is cleaved by aldolase A to generate GA3P and DHAP (*7*). Fructose, either derived from the diet (e.g., table sugar and high fructose corn syrup) or produced from glucose through the polyol pathway (also known as aldose reductase pathway) by the enzymes aldose reductase and sorbitol dehydrogenase, is quickly phosphorylated by fructokinase to fructose 1-phosphate (F-1-P) and subsequently split by aldolase B into glyceraldehyde and DHAP (*7*). Glyceraldehyde is phosphorylated by triose kinase to form GA3P. DHAP and GA3P can be readily inter-converted by triosephosphate isomerase. Both GA3P and DHAP can spontaneously and non-enzymatically degrade to MG (*5, 6*). In addition, DHAP can be also metabolized to MG with the action of MG synthase which is found in many microorganisms, such as *Escherichia coli* and yeast (*8, 9*).

Other important sources for endogenous MG generation include ketone bodies (mainly acetone) derived from fatty acid oxidation and aminoacetone derived from protein catabolism (*10*). Cytochrome P450 2E1 (CYP 2E1) enzymes catalyze a two-step conversion of acetone into MG *via* acetol as an intermediate (*11*). Two other ketone bodies acetoacetic

acid and β-hydroxybutyric acid can spontaneously convert to acetone and may also be the sources for MG formation (*12*). Semicarbazide-sensitive amine oxidase (SSAO) catalyzes MG production *via* deamination of aminoacetone generated from catabolism of threonine and glycine (*13*). SSAO is predominantly expressed in adipose cells, vascular smooth muscle cells (VSMCs), and endothelial cells (*14*). SSAO (also known as vascular adhesion protein 1) is localized on the outer membrane surface. In addition, SSAO is present in the cell cytoplasm and in plasma as soluble SSAO (*14*). Moreover, SSAO stimulates glucose transport into VSMCs and adipocytes *via* glucose transporter GLUT1 (*15*) and GLUT4 (*16*), respectively. The insulin-like effect of SSAO may contribute to MG formation from the increased glucose uptake and metabolism.

1.2.1.2 MG degradation

MG is degraded in cells mainly by the glyoxalase system which consists of two enzymes glyoxalase I and II (*10*) (Figure 1-2). The glyoxalase system is present in all mammalian cells in the cytosol and in cellular organelles, such as mitochondria (*17*). MG is first converted irreversibly by glyoxalase I to (S)-delta-lactoylglutathione using reduced glutathione (GSH) as a cofactor and then to D-lactate by glyoxalase II. A minor pathway for MG catabolism is mediated by aldose reductase which converts MG to acetol using nicotinamide adenine dinucleotide phosphate (NADPH) as a cofactor (*18*). Aldose reductase is an NADPH-dependent aldo-keto reductase that catalyzes the reduction of a variety of aldehydes such as MG. The enzyme activity of aldose reductase on MG metabolism is 40-fold lower than that of glyoxalase I (*19*).

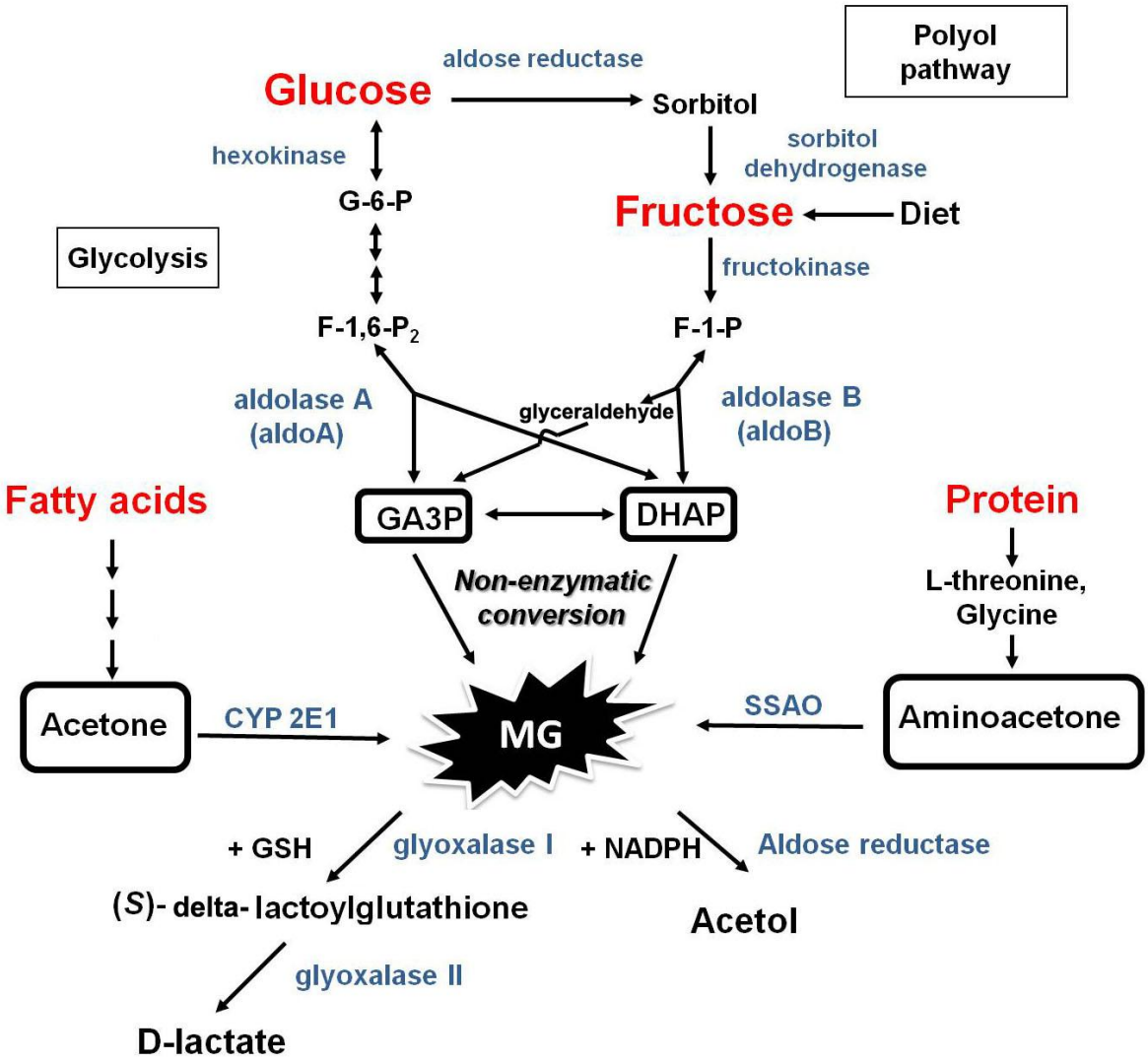

Figure 1-2 Schematic pathways of cellular methylglyoxal (MG) generation and degradation. Triosephosphates glyceraldehyde 3-phosphate (GA3P) and dihydroxacetone phosphate (DHAP) which are produced form glucose through glycolysis or the polyol pathway or produced during fructose metabolism spontaneously and non-enzymatically converts to MG. In addition, acetone from fatty acid oxidation and aminoacetone from protein catabolism are metabolized to MG with the actions of cytochrome P450 2E1 (CYP 2E1) and semicarbazide-sensitive amine oxidase (SSAO), respectively. Cellular MG is degraded by glyoxalase I and glyoxalase II into D-lactate or by aldose reductase into acetol.

Abbreviations: CYP 2E1 – cytochrome P450 2E1; DHAP – dihydroxacetone phosphate; F-1-P – fructose 1-phosphate; F-1,6-P_2 – fructose-1,6-bisphosphate; G-6-P – glucose 6-phosphate; GA3P – glyceraldehyde 3-phosphate; GSH – glutathione; MG – methylglyoxal; NADPH – nicotinamide adenine dinucleotide phosphate; SSAO – semicarbazide-sensitive amine oxidase; TIM – triosephosphate isomerase.

1.2.2 Sources of exogenous MG

MG has been reported to be present in rice, wheat and tobacco (*20*). MG is also present in a broad range of commercial foods and beverages, such as bread, coffee, honey, wine, and beer (*21, 22*). MG can be formed during the industrial processing, home cooking and long-time storage. For example, roasting process increases MG levels in coffee (*23*), and the heating and prolonged storage (20-120 days) increases MG levels in honey (*24*). It was reported that MG was 0.79 mg/kg in bread, 2.5 mg/kg in toast bread, 38-828 mg/kg in manuka honey, 100 mg/kg in instant coffee powder, 0.57 μg/ml in wine and 1.5 μg/ml in Bourbon whiskey (*21, 22*). The MG content in these foods and beverages is not normally harmful, but an excess consumption over a long-time may increase the risk of MG-related diseases, such as hypertension and dibetes (*25, 26*). Moreover, the absorption of orally ingested MG is probably limited.

Carbohydrates in foods and beverages are susceptible to non-enzymatic degradation (mainly through Caramelization and Maillard reaction) during food heat treatment, such as roasting, baking, broiling, frying, and evaporating, leading to the formation of α-dicarbonyl compounds, particularly MG, glyoxal, and 3-DG (Figure 1-3). At the chemical level, caramelization involves ring-opening, enolization of reducing sugars (such as D-glucose), sugar dehydration and MG formation (*23*). The caramelization is normally slow, but becomes significant at high sugar concentrations or at high temperatures (*23*). The Maillard reaction begins with reversible formation of unstable Schiff's base *via* condensation of an amino acid with a reducing sugar. The Schiff's base undergoes a slowly reversible organic transformation known as Amadori rearrangement. Both, the Schiff's base and the Amadori product

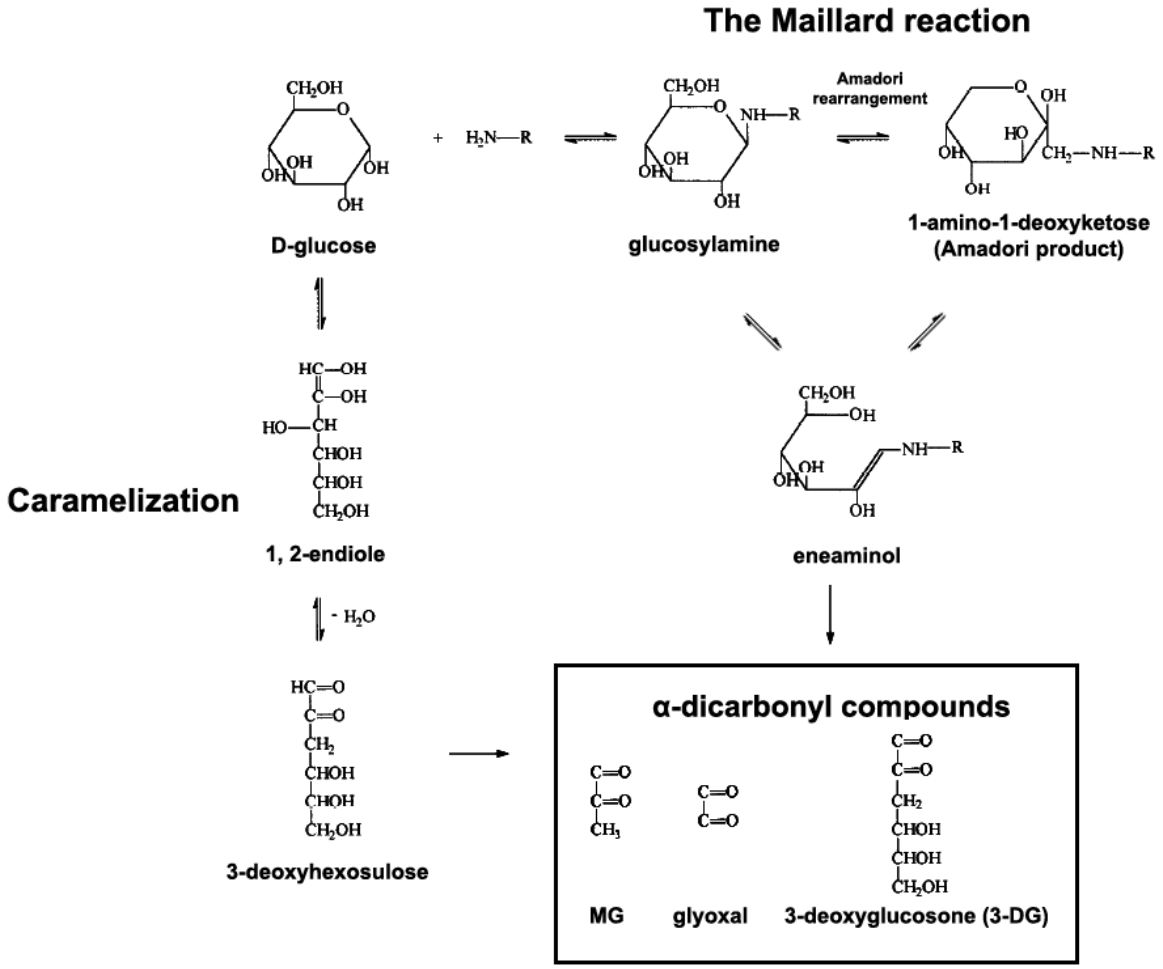

Figure 1-3 Methylglyoxal (MG) formation through caramelization and Maillard reaction. Glucose in foods and beverages non-enzymatically degrades to α-dicarbonyl compounds, such as MG, glyoxal and 3-deoxyglucosone (3-DG), through caramelization and/or Maillard reaction during food heat treatment, such as roasting, baking, broiling, frying, and evaporating.

subsequently degrade into eneaminol and different α-dicarbonyl compounds (*27*, *28*).

Decomposition of lipids caused by storage and processing may also increase MG accumulation in foods. For example, the accelerated storage conditions (60 ℃ for 3 and 7 d) and a cooking condition (200 ℃ for 1 h) enhance MG formation in our dietary oils, such as fish and olive oils (*29*). Photodegradation of lipids, fatty acids and related compounds also yielded MG. Upon ultraviolet irradiation for 10 h, MG amount was increased in squalene and cod liver oils, and to a lesser extent, in ethyl esters of fatty acids, acetaldehyde, acrolein, and propanal (*30*).

In addition, the use of microorganisms in fermentation can also increase MG formation. MG synthase catalyzes the conversation of DHAP to MG and inorganic phosphate in many microorganisms, such as *Escherichia coli* and yeast (*8*, *9*). The release of MG by different microorganisms during fermentation may cause an increase of MG in alcoholic drinks and dairy products.

1.2.3 Cell permeability of MG

Incubation of cells with MG leads to cellular MG accumulation dependent on extracellular MG concentration, incubation time, and cell types. For example, after incubation of L6 skeletal muscle cells with [2-^{14}C] MG (2.5 mM, 30 min), 3% of exogenous MG was incorporated into the cells, in which about 33% partitioned into the cytosolic fraction and 64% was incorporated into the cell membrane fraction (*31*). Incubation of rat aortic smooth muscle cells with [2-^{14}C] MG (160 μM, 15 min), showed that 1.8% of MG was incorporated into the cells (*32*). Incubation of pancreatic beta cell line INS-1E with [2-^{14}C]

MG (0.25-1 mM, 30 min), resulted in 12.5% of MG being incorporated into the cells (*33*). MG can also release into the surrounding environment from cells with increased intracellular MG levels. About 10% of endogenously produced MG was released into the culture medium from Chinese hamster ovary cells after incubation with 100 mM glucose-containing medium for 12 h (*34*). MG may be able to cross cell membranes but the mechanism of MG transport is not known, and it seems dependent on aquaglyceroporin, a subclass of aquaporin water channels (*35*). Extracellular MG was not transported into wild-type *Xenopus* oocytes, but significantly transported into aquaglyceroporin-expressing *Xenopus* oocytes (*35*).

1.3 Effects of MG

1.3.1 MG and advanced glycation endproducts (AGEs)

MG initially reversibly reacts with certain proteins at arginine, lysine, or cysteine residues, and the subsequent irreversible reaction yields AGEs which cause the structural and functional changes of proteins. MG is believed to be the major source of AGEs (*36*) (Figure 1-4). The formation of AGEs is a spontaneous process. Experiments in test tubes showed that incubating purified human insulin with MG (10 μM, 24-72 h) *in vitro* in phosphate buffered saline (PBS, pH 7.4) at 37 ℃ leads to a MG modification of insulin at the arginine residue of the beta chain (*37*), and incubating purified Akt1 with MG (50 μM, 24 h) *in vitro* leads to a MG modification of Akt1 at cysteine 77 (*38*).

Irreversible formation of AGEs on proteins would change their structures, disturbing their physicochemical and biochemical properties as well as their stability. For example, the formation of AGEs on the extracellular matrix molecules, such as fibronectin, laminin, type I

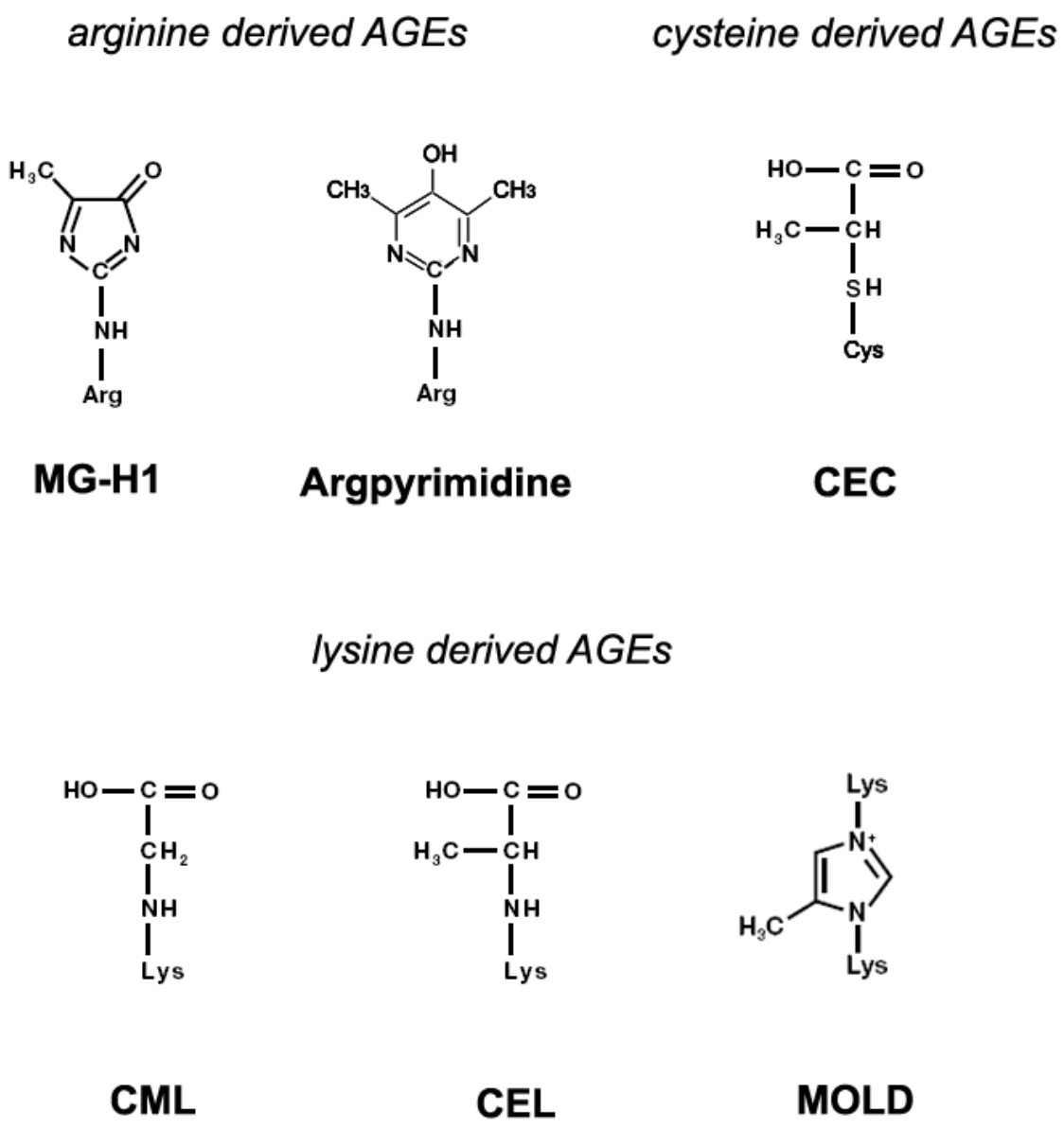

Figure 1-4 Chemical structures of advanced glycation endproducts (AGEs). MG reacts with arginine residue of proteins to form nonfluorescent products 5-hydro-5-methylimidazolone (MG-H1) and the major fluorescent product argpyrimidine (*39*). Upon reaction with lysine residue of proteins, it forms N(ε)-carboxyethyl-lysine (CEL), N(ε)-carboxymethyl-lysine (CML), and methylglyoxal-derived lysine dimer (MOLD) (*40*). MG also reacts with cysteine residue of proteins to generate carboxyethyl cysteine (CEC) (*41*).

and type IV collagens, caused aberrant cross-linking, impaired matrix-matrix interactions, and increased the stiffness of the vasculature (*42*). AGEs formation on extracellular matrix also interferes with matrix-cell interactions. Laminin and collagens are basement membrane components of blood vessels and play key roles in regulating endothelial cell-cell adhesion (*43*). AGE modification of the cell-binding domains of laminin, type I and type IV collagens decreased endothelial cell adhesion and promoted its migration which is important for angiogenesis or large vessel repair (*44*). Arginine, lysine, and cysteine residues are usually involved in active sites of enzymes and AGE formation on these residues may impair enzymes' activities. It was reported that the MG-induced glycation reduced activities of glyceraldehyde-3-phosphate dehydrogenase, glutathione reductase and lactate dehydrogenase (*45, 46*).

Moreover, AGEs can exert multiple effects on cells *via* binding and activating RAGE (receptor for AGEs) on the cell surface. RAGE is a member of the immunoglobulin superfamily present in a wide variety of cell types, such as endothelial cells, VSMCs, and mononuclear phagocytes (*47, 48*). The engagement of RAGE by AGEs leads to perturbation of cellular properties, including excess generation of reactive oxygen species (ROS) through NADPH oxidase and activation of multiple signaling pathways, such as p21 RAS, p38 mitogen-activated protein kinases (MAPK), and the GTPases Cdc42 and Rac (*42, 49*). A key target of RAGE signaling pathways is NF-κB. Binding of AGEs to RAGE induces translocation of NF-κB to the nucleus and up-regulation of its targeted genes, including several growth factors such as vascular endothelial growth factor (VEGF), transforming growth factor-beta (TGF-β) and connective tissue growth factor (CTGF), vasoconstrictors

such as endothelin, proinflammatory cytokines such as interleukin (IL) and tumor necrosis factor-alpha (TNF-α), and cell adhesion molecules such as vascular cell adhesion molecule-1 (VCAM-1) and intercellular adhesion molecule-1 (ICAM-1) (*50, 51*). It was reported that circulating AGEs bound to RAGE on the endothelium enhanced endothelial permeability, stimulated NADPH oxidase and ROS generation, activated NF-κB, and increased vascular inflammation (*42, 49, 52, 53*).

1.3.2 MG and oxidative stress

Oxidative stress is a result of an imbalance between ROS production and anti-oxidant defense. MG is a pro-oxidant (*54, 55*). Dr Wu's group has observed that incubation of cultured aortic VSMCs with MG (10-300 μM) significantly increased superoxide anion ($O_2^{\cdot-}$) production in a concentration- and time-dependent manner (*55*). MG also increased the formation of hydrogen peroxide (H_2O_2) and peroxynitrite ($ONOO^-$), in the same VSMCs (*55*). Moreover, incubation with MG (50–100 μM, 3 h) significantly increased oxidative stress, as determined by the formation of oxidized 2',7'-dichlorofluorescein (DCF, a fluorescent product from the oxidation of the reduced non-fluorescent 2',7'-dichlorodihydrofluorescein diacetate by various forms of ROS, e.g. H_2O_2, $O_2^{\cdot-}$, and $ONOO^-$), in mesenteric artery VSMCs from Sprague-Dawley (SD) rats (*54*). Incubation with MG (50–500 μM, 24 h) significantly increased oxidized-DCF fluorescence in VSMCs isolated from the aorta of Wistar–Kyoto (WKY) rats, and to a higher extent, in VSMCs isolated from the aorta of spontaneously hypertensive rats (SHR) (*56*). The induction of oxidative stress by MG has been also reported in other cell types, such as Jurkat T leukemia cells (*57*) and cultured rat hepatocytes (*58*).

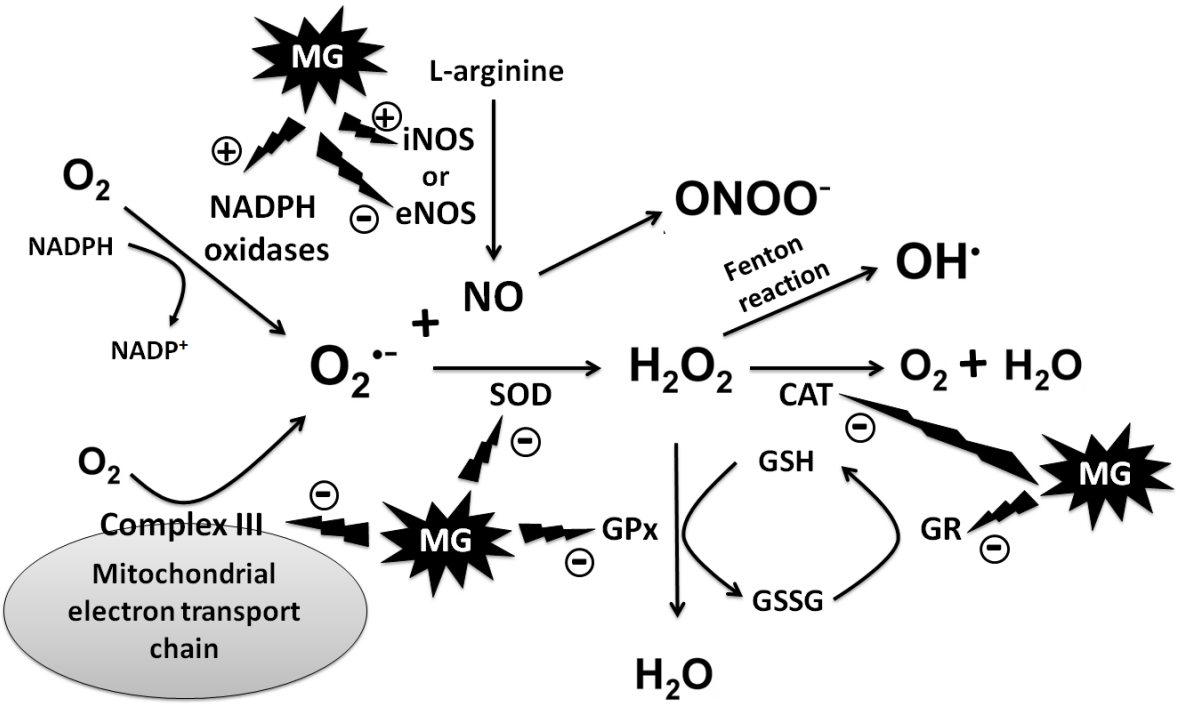

Figure 1-5 Methylglyoxal (MG)-induced reactive oxygen species (ROS) generation. In cells, superoxide ($O_2^{\bullet-}$) is produced predominantly by mitochondrial respiration and the enzyme NADPH oxidase. $O_2^{\bullet-}$ reacts rapidly with nitric oxide (NO), producing peroxynitrite ($ONOO^-$). MG inhibits mitochondrial complex III activities and increases mitochondrial superoxide generation. MG also increases the activities of NADPH oxidases and inducible nitric oxide synthase (iNOS), leading to excess generation of $O_2^{\bullet-}$, NO and $ONOO^-$. Superoxide dismutase (SOD) catalyzes the dismutation of $O_2^{\bullet-}$ into hydrogen peroxide (H_2O_2) and oxygen. H_2O_2 can react with Fe^{2+} to form hydroxyl radicals ($HO^{\bullet}$) via Fenton reaction ($Fe^{2+} + H_2O_2 \rightarrow Fe^{3+} + HO^{\bullet} + OH^-$). H_2O_2 is broken down into water and oxygen by catalase (CAT) or by glutathione peroxidase (GPx) with cofactor reduced glutathione (GSH). MG decreases the activities of SOD, CAT as well as GPx and enhances the accumulation of ROS. Moreover, MG can decrease activities of glutathione reductase (GR) which reduces glutathione disulfide (GSSG) to GSH, leading to a reduction in cellular GSH levels.

Abbreviations: NADPH – nicotinamide adenine dinucleotide phosphate; iNOS and eNOS – inducible or endothelial nitric oxide synthase, respectively;

Numerous *in vitro* and *in vivo* studies have shown that MG stimulates ROS generation by impairing mitochondrial function, activating NADPH oxidases and inducible nitric oxide synthase (iNOS), and inhibiting activities of antioxidant enzymes and reducing cellular antioxidants, such as GSH (*59*) (Figure 1-5).

Mitochondria are the powerhouse of mammalian cells, and also the major sites for the cellular generation of ROS. During mitochondrial respiration, electrons from donors pass through the complexes I – IV of respiration chain (also known as the electron transport chain, ETC). Under physiological conditions, 2-5% of electrons leak out to molecular oxygen and produce 85% of total intracellular superoxide (*60*, *61*). Increasing evidence suggests that mitochondria are important targets of MG. For example, a 5 min incubation with MG (10–200 μM) induced a concentration-dependent reduction in the respiration rate of isolated rat renal mitochondria (*62*). Electron leakage in the ETC mainly occurs at complex I (NADH-ubiquinone oxidoreductase) and complex III (ubiquinol-cytochrome c reductase) (*63*, *64*). Inhibition of complex I or III leads to a significant increase in mitochondrial superoxide generation (*65*). Our recent work found that MG specifically inhibited complex III activity and increased generation of mitochondrial superoxide (*66*) (Figure 1-5).

Another important source for $O_2^{\cdot -}$ generation is the NADPH oxidases-catalyzed transfer of electrons from NADPH to molecular oxygen (Figure 1-5). NADPH oxidases belong to a family of membrane-bound enzymes. In neutrophils, NADPH oxidases are transmembrane proteins expressed on the plasma membrane and $O_2^{\cdot -}$ is produced outside of cells as a defense agent. However, in vascular endothelial cells NADPH oxidases are expressed on the plasma membrane and also in the endosomal compartments, and mainly

produce $O_2^{\cdot-}$ intracellularly (*60*). For example, the isoform NADPH oxidase 1 is expressed on the plasma membrane and NADPH oxidase 4 is expressed in the endoplasmic reticulum of endothelial cells (*67, 68*). By using NADPH oxidase inhibitors, previous work showed that NADPH oxidase mediated MG induced-superoxide production in VSMCs and in rat kidney mesangial cells (*55, 69*). More recently, our lab found that incubation with MG (30 μM, 24 h) directly increased NADPH oxidase activity and ROS production in human umbilical vein endothelial cells and in rat aortic endothelial cells (*70*).

MG causes increased nitric oxide (NO) and $ONOO^-$ production through its actions on iNOS (Figure 1-5). In cells, NO is produced from the oxidation of L-arginine catalyzed by constitutive NOS isoforms, such as neuronal NOS (nNOS) and endothelial NOS (eNOS), or by iNOS (*71*). eNOS is primarily expressed in endothelial cells while iNOS is primarily expressed in macrophages, VSMCs and other cell types (*71*). Dr Wu's group previously found that iNOS expression and NO production were increased in the aorta of 14-week old SHR as compared to WKY rats, which was associated with elevated aortic and plasma MG levels in SHR. However, in the same SHR, aortic eNOS expression was reduced (*72*). More recent work showed that MG (30 μM, 24 h) decreased eNOS activity and decreased basal and bradykinin (10 μM)-stimulated NO production in endothelial cells (*70*). Furthermore, MG (10 μM, 6 h) up-regulated iNOS expression and enhanced NO production and $ONOO^-$ formation in VSMCs (*73*). These studies indicate that the effects of MG on NOS and NO production vary in different cell types, but the NO bioavailability in both endothelial cells and VSMCs is reduced by MG either *via* reducing NO production or *via* increasing the formation of $ONOO^-$, respectively. In addition, mitochondrial NOS (mtNOS) may contribute

to MG-induced NO production in VSMCs, as MG (30 μM, 18 h)-increased NO production in A-10 cells was inhibited by the addition of the mtNOS inhibitor 7-nitroindazole (*66*).

MG can further augment intracellular oxidative stress *via* inactivating different antioxidant enzymes and reducing cellular antioxidants (Figure 1-5). The superoxide produced in cells is dismutated by copper-zinc superoxide dismutase (CuZn SOD) or mitochondrial superoxide dismutase (Mn SOD) to H_2O_2 (*60*), which is further decomposed to water and oxygen by catalase or glutathione peroxidase (GPx) (*74*). MG has been found to inactivate SOD, catalase, and GPx. After incubation with MG in test tubes, the activities of the purified CuZn SOD and GPx were inhibited (*75, 76*). When VSMCs were treated with MG, activities of Mn SOD and GPx were significantly decreased (*66*). Incubation of mice liver homogenate with MG (0.1-10 mM) inhibited activities of SOD and catalase (*77*). Moreover, animal studies showed that Swiss albino male mice which were administered MG (50-400 mg/kg body wt, i.p.) had lower SOD and catalase activities in the liver than control mice (*77*). GSH is an important antioxidant in the cells and plasma. GSH effectively scavenges various ROS including H_2O_2, $ONOO^-$, and hydroxyl radical, through direct interactions or indirect enzyme-catalyzed reactions (*78*). In these processes, GSH is oxidized to form glutathione disulfide (GSSG). Glutathione reductase (GR) recycles GSSG to GSH (*78*). Chronic MG infusion (60 mg/kg/day) by minipump significantly reduced GSH levels in the plasma, pancreas, and skeletal muscle in SD rats (*26*). MG can directly inactivate GR in test tubes (*79*). Cell studies demonstrated that incubation of MG significantly decreased GR protein expression and reduced GSH levels in VSMCs and endothelial cells (*56, 70*).

MG increases oxidative stress partially through the formation of AGEs. Previous

studies observed that the formation of AGEs in the mitochondria increased mitochondrial ROS generation (*80*, *81*). AGEs also impaired functions of antioxidant enzymes, such as CuZn SOD and GPx (*75*, *76*), Moreover, binding of AGEs to RAGEs activates NADPH oxidases and promotes the generation of ROS (*82*). Our recent work showed that the AGEs breaker alagebrium completely decreased AGE formation but only partially reduced MG-increased mitochondrial superoxide generation and intracellular nitrotyrosine, products of tyrosine nitration in proteins mediated by peroxynitrite, in VSMCs (*66*). These studies indicate that MG modification of proteins or AGEs formation may in part contribute to MG-induced oxidative stress.

1.4 Increased MG accumulation in metabolic syndrome

Metabolic syndrome is a cluster of metabolic abnormalities associated with obesity, type 2 diabetes, and hypertension, including abdominal obesity, hyperglycemia, glucose intolerance, insulin resistance, dyslipidaemia, and high blood pressure (*83*). Over the past two decades, the number of people with metabolic syndrome has strikingly increased, and it has become one of the major public-health challenges worldwide (*83*). A large and growing number of studies suggest that MG is an important cause for the development of diabetes and hypertension, although its role in obesity has not yet been established.

1.4.1 MG, diabetes and its vascular complications

1.4.1.1 Increased MG accumulation and MG-induced AGEs in diabetes

Plasma MG levels in healthy human subjects are 1-3 μM (*72*, *84*) and in rats the

normal levels are approximately 1 μM (*26, 85*). In patients with type 2 diabetes, plasma MG levels are two to four-fold elevated (*86*). This increase is positively correlated with levels of fasting plasma glucose, glycosylated hemoglobin, and the ratio of urine albumin to creatinine (*86*). Increased AGEs formation in the blood and tissues occurs with aging and is exaggerated by hyperglycemia in diabetes (*86*). The MG levels were increased in the kidney and retina, the major sites of diabetic microvascular complications, but not in the liver and skeletal muscles in streptozotocin (STZ)-induced diabetic rats (*87*). Immunohistochemical analyses showed that in diabetic rats or mice, AGE levels are increased in the aorta (*88*), mesenteric vessels (*89*) and retinal vessels (*90*). Diabetes-associated accumulation of AGEs in blood vessels is linked to the development of diabetic vascular complications. In patients with type I diabetes, levels of AGEs in the kidney and the retina were associated with the degree of nephropathy and retinopathy, respectively (*91*). For example, in these patients with type 1 diabetes, AGE levels were significantly elevated in the kidney as urinary albumin increased during the early phase of nephropathy (*91*). In diabetic rats, increased renal AGE levels were associated with the morphological abnormalities of diabetic nephropathy, such as glomerular basement membrane thickening (*92*), and of diabetic retinopathy, such as abnormal endothelial cell proliferation (*93*). Moreover, in the STZ-induced diabetic apolipoprotein E-deficient (apoE-/-) mouse (a model of diabetes-associated atherosclerosis), levels of AGEs in the plasma and the aorta were elevated and associated with an increase of atherosclerotic plaque area (*88*). In addition, clinical studies in patients with type 2 diabetes showed that the increased levels of blood MG or AGEs were correlated with decreased endothelium-dependent vasodilation (*94*) and the degree of intima-media thickness of blood vessels,

vascular stiffness, and systolic blood pressure (*95*). These data suggest that increased generation of MG is a cause for the vascular complications of diabetics (*95*).

1.4.1.2 MG and other molecular mechanisms for hyperglycemic damage

1.4.1.2a MG, glucose and oxidative stress

High glucose increases superoxide generation from mitochondrial respiratory chain and NADPH oxidases and reduces the activity of SOD and levels of antioxidants such as GSH and vitamin E in VSMCs and endothelial cells (*96-98*). Superoxide can be converted to hydroxyl radical and H_2O_2 (Figure 1-5). Oxidative stress due to increased ROS generation leads to oxidation of biological macromolecules such as DNA, lipids, and proteins. Moreover, high glucose also stimulates the expression of iNOS and promotes the formation of NO which reacts with superoxide to produce the highly reactive $ONOO^-$ (*99*). $ONOO^-$ can react with amino acids such as tyrosine to form nitrotyrosine (*100*). In addition, the reaction of NO and superoxide during hyperglycemia reduces NO availability and impairs endothelium-dependent vasodilation (*101*). Furthermore, excess ROS activates different signaling pathways and alters gene expression (*102*). For example, in VSMCs, cytosolic ROS such as H_2O_2 and superoxide activated p38 MAPK and ERK 1/2 signaling pathways and mitochondrial ROS activated the JAK/STAT signaling pathway, causing cell proliferation, protein synthesis and hypertrophy (*103*). In vascular endothelial cells, hyperglycemia-induced generation of ROS activated the JNK/SAPK pathway, causing cell apoptosis (*104*), while activation of activator protein-1 (AP-1) caused a decrease in eNOS expression (*105*). As mentioned earlier, MG can enhance the formation of superoxide, NO

and peroxynitrite in VSMCs and endothelial cells, however, whether MG is the key mediator for high glucose-induced ROS is largely unsettled.

1.4.1.2b MG and activation of the hexosamine pathway

Through the hexosamine pathway, the glycolytic metabolite fructose-6 phosphate is first converted to glucosamine-6 phosphate and then to uridine diphosphate N-acetyl glucosamine (UDP-GlcNAc), catalyzed by fructose 6-phosphate amidotransferase (GFAT). O-linked N-acetyl glucosamine (O-GlcNAc) modification or O-GlcNAcylation is a process in which in the presence of O-GlcNAc transferase (OGT), the GlcNAc from UDP-GlcNAc is transferred to the serine and threonine residues of various nuclear and cytosolic proteins (*106*). With O-GlcNAc modification proteins will lose their normal function. Hyperglycemia-increased flux through the hexosamine pathway has been implicated in the pathogenesis of diabetic complications (*106*). For example, high glucose enhanced UDP-GlcNAc formation and increased O-GlcNAc modification of nuclear transcription factors, such as Sp1, leading to up-regulated gene expression of plasminogen activator inhibitor-1 (PAI-1) and transforming growth factor-beta 1 (TGF-β1) in aortic endothelial cells (*107*). The high glucose-increased O-GlcNAc modification of eNOS in aortic endothelial cells leads to a significant reduction in eNOS activity (*108*). Inhibition of glutamine:fructose-6-phosphate amidotransferase (GFAT) in porcine glomerular mesangial cells prevented high glucose-increased formation of glucosamine metabolites (glucosamine-6 phosphate and UDP-GlcNAc) and inhibited TGF-β1 gene expression, bioactivity and its effects on cell proliferation and matrix production (*109*).

There is some indirect evidence that implicates MG in the high glucose-activated hexosamine pathway. For example, O-GlcNAc modification of the proteasome was increased in the kidney of glyoxalase-1 knockout mice (*110*), and over-expression of glyoxalase-1 in endothelial cells reduced high glucose-induced O-GlcNAc modification of transcription factor Sp3 (*111*). However, whether MG increases O-GlcNAc modification remains to be clarified.

1.4.1.2c MG, AGEs and activation of protein kinase C (PKC) isoforms

PKC is a family of protein kinase enzymes that phosphorylate serine and threonine residues of intracellular proteins and play important roles in a variety of cellular functions such as signal transduction (*112*). PKC is activated by signals such as diacylglycerol (DAG) and calcium or by ROS such as H_2O_2 (*113*). Upon activation, PKC is translocated into the plasma membrane where PKC catalyzes phosphorylation of various substrates and mediates a diverse variety of biological processes (*114*).

The PKC activities were increased after incubation with high glucose in VSMCs and endothelial cells (*115*). In the endothelial cells, PKC activation affects the production of endothelium-dependent vasodilators and vasoconstrictors (i.e. deceasing NO and prostacyclin but increasing thromboxane and endothelin-1) and increases cell permeability and angiogenesis *via* the expression of vascular endothelial growth factor (*113*). In VSMCs, PKC activation alters the smooth muscle contractility and hormone responsiveness (*116*) and promotes cell migration and proliferation (*117*). PKC activation also contributes to high glucose-induced activation of NADPH oxidases and generation of ROS in VSMCs and

endothelial cells (*112*). Moreover, activation of PKC was found to up-regulate gene expression of TGF-β1, fibronectin and collagen, and to increase accumulation of microvascular matrix proteins in glomeruli of diabetic rats (*118*). Clinical trials have shown the benefits of PKC inhibitors in the therapy of diabetic vascular complications. For example, pre-treatment with the PKC-β inhibitor LY333531 prevented the reduction in endothelium-dependent vasodilation induced by hyperglycemic clamp in healthy people (*119*), and treatment with ruboxistaurin, an orally administered PKC-β inhibitor, decreased the vision loss in patients with diabetic retinopathy (*120*).

MG seems to activate PKC through the formation of AGEs. PKC can be activated by AGEs directly (*121*) or indirectly through activation of AGEs receptors or generation of ROS (*122*). Inhibition of AGEs decreased the high glucose-increased PKC expression and activation in cultured VSMCs and in the kidney of STZ-diabetic rats (*123*).

1.4.1.2d Activation of nuclear factor κB (NF-κB)

NF-κB is present in the cytosol as an inactive heterodimeric complex, consisting of the p50 and p65 subunits associated with an inhibitory protein κB (IκB), in the resting cells. Divergent stimuli such as hyperglycemia, ROS, proinflammatory cytokines, AGEs, and PKC activate NF-κB through a common mechanism, IκB kinase-mediated phosphorylation and subsequently proteasome-mediated degradation of IκB (*42, 97, 124, 125*). Activated NF-κB (p50/p65 dimer) is translocated to the nucleus and regulates the expression of a large number of genes involved in the immune and inflammatory response, apoptosis, cell proliferation and differentiation, such as growth factors (i.e. VEGF), proinflammatory cytokines (i.e. TNF-α

and IL-1β), RAGE and adhesion molecules (i.e. vascular cell adhesion molecule-1) (*125*). Activation of NF-κB by high glucose has been observed in VSMCs and endothelial cells and in different vascular tissues of diabetic rats, and implicated in the pathogenesis of diabetes and its associated complications (*126-128*).

MG is a stimulus for NF-κB activation. Previous studies with cultured VSMCs and retinal capillary pericytes demonstrated that MG treatment directly activated NF-κB (*56, 129*). Moreover, incubation with AGEs induced NF-κB activation in cultured endothelial cells (*130*). As mentioned earlier, AGEs bound to RAGE induce translocation of NF-κB into the nucleus and NF-κB–mediated gene expression.

1.4.2 MG and hypertension

1.4.2.1 Increased MG accumulation and MG-induced AGEs in hypertension

Plasma MG levels are elevated in hypertension without hyperglycemia. Wang et al. found that in 20-week-old SHR, plasma MG levels were two-times higher than those in age-matched control non-hypertensive WKY rats (*131*). Increased MG and MG-induced AGEs in plasma and/or the aorta correlated with the development of hypertension in SHR (*131, 132*). As SHR developed hypertension, MG levels in the aorta increased in an age-dependent fashion, although there was no difference in blood glucose levels between the SHR and WKY rats (*131*). In the same SHR, AGEs formation, such as CEL and CML, was also elevated in the aorta and the mesenteric arteries when compared with WKY rats (*72, 131*). Along with the elevated levels of MG and AGEs in VSMCs, in the aorta and kidney of 13-week-old SHR, ROS generation was increased and levels of GSH and activities of GR and

GPx were lowered in these cells or tissues when compared with WKY rats (*56, 72, 131, 132*). However, the mechanisms for vascular MG overproduction or accumulation are unknown.

1.4.2.2 MG-induced vascular remodeling in hypertension

Vascular remodeling includes the changes in wall thickness, lumen diameter, cross-sectional area, and media-to-lumen ratio of blood vessels. There are three types of vascular remodeling. Hypertrophic remodeling refers to the increase of cross-sectional area, eutrophic remodeling refers to no change of cross-sectional area, and hypotrophic remodeling refers to a decrease of cross-sectional area. These forms of remodeling can be inward and outward, representing the decrease and increase of lumen diameter, respectively. Current evidence suggests that MG can induce hypertrophic inward remodeling of the vasculature (aorta and mesenteric artery) (73). This vascular remodeling is associated with increased levels of MG and MG-induced AGEs in the aorta and mesenteric arteries of 13-week-old SHR (*72*). Similarly, increased MG and AGEs with mesenteric artery vascular remodeling and hypertension were also observed in SD rats after chronic feeding with the MG precursor fructose for 16 weeks (*25*). A clinical study on hypertensive human subjects showed that the increase in plasma AGEs was related to the increase of aortic stiffness (*133*). A recent study in our lab on VSMCs (A-10 cell line) found that MG treatment increased DNA synthesis and cell proliferation by modifying Akt1 at Cys77 and activating Akt1 signaling pathways (*38*). MG treatment of SD rats through chronic infusion with an implanted minipump for 4 weeks augmented phospho-Akt1 (the active form of Akt1) levels in the aorta (*38*).

Moreover, MG treatment increases the expression of growth factors, such as TGF-β1

and CTGF, and expression of extracellular matrices, leading to progressive thickening of blood vessels (*50, 51, 134*). In Wistar rats treated with MG (i.p., 50-75 mg/kg per day, 7 weeks), the pro-matrix expansion growth factor CTGF was over-expressed, and luminal matrix contents, luminal occlusion and wall thickness were increased in cutaneous arteries (*134*). On the other hand, MG modifies extracellular matrix proteins, leading to inter-protein crosslinking and subsequent arterial stiffness (*106*). For example, oral administration of MG (50 mg/kg in drinking water, 5 months) increased total collagen content in the kidney of mice but the solubility of these collagens was significantly decreased due to the increase of cross linking (*135*).

1.4.2.3 MG-induced endothelial dysfunction in hypertension

Endothelial dysfunction is considered a key event in the pathogenesis of hypertension and vascular complications of diabetes (*136*). It is commonly defined as reduced endothelium-dependent vascular relaxation, resulting from decreased NOS expression, NO bioavailability and NO-mediated muscle relaxation in blood vessels (*137*). As mentioned earlier, NO is produced from L-arginine by the action of eNOS in the endothelium. Different stimuli, such as acetylcholine, bradykinin, insulin, VEGF, shear stress and isometric contraction, can activate eNOS and promote NO production. For example, eNOS requires calcium for its activity and BK can increase intracellular calcium and activates eNOS, while insulin can stimulate phosphorylation of eNOS (phospho-eNOS, the active form of eNOS) (*138, 139*). NO generated within the endothelium diffuses to the VSMCs where it activates soluble guanylate cyclase, increases generation of cyclic guanosine monophosphate (cGMP)

and causes vascular smooth muscle relaxation (*139*).

Treatment with MG (0.2% to 0.8% in drinking water, 18 weeks) decreased serum NO levels and increased blood pressure (*140*). When WKY rats were treated with a MG precursor, fructose (4% in drinking water), systolic blood pressure was continuously increased during 1-5 weeks of treatment, and after 11 weeks of treatment, the mean blood pressure in fructose-fed rats was significantly higher than that in control rats (*141*). Our lab found that acetylcholine-induced endothelium-dependent relaxations were significantly impaired in small mesenteric arteries from 13-week-old SHR in comparison with that from WKY rats (*72*). Treatment of cultured endothelial cells with MG (30 μM, 24 h) reduced basal and bradykinin -stimulated NO production, cellular cGMP levels, and eNOS phosphorylation (at Ser-1177) and activity (*70*). Moreover, when the isolated aortic rings from SD rats were incubated with MG (30 or 100 μM, 2 h), the acetylcholine-induced endothelium-dependent relaxation was inhibited significantly (*70*). These results are consistent with a recent study which showed that incubation of isolated rat mesenteric arteries with MG (0.33 or 1 mM for 1 h, or 10 or 50 μM for 2 h) resulted in significant impairment of acetylcholine-induced vascular relaxation (*142*). The deleterious effects of MG are attributed to the MG-increased oxidative stress, especially superoxide, which reacted with NO and subsequently reduced bioavailability of NO in the isolated blood vessels and in cultured endothelial cells (*70*). The MG-impaired endothelium-dependent relaxation in the isolated aorta or mesenteric arteries was prevented by application of antioxidants, such as SOD mimetics or N-acetyl-l-cysteine (*70, 142*). More recently, our lab found that MG reacted with H_2S, a natural vasodilator, which implicates MG in the pathogenesis of hypertension (*143*).

1.5 MG overproduction and possible mechanisms

1.5.1 MG formation in insulin-insensitive vascular cells and insulin-sensitive adipocytes

Vascular smooth muscle and endothelial cells are considered major sites for endogenous MG production. A study on MG distribution in normal SD rats showed that MG formation is highest in the aorta, which is 2-6 fold higher than that in the lung, brain, liver, kidney, heart, and spleen (*85*). A similar result was reported by Randell *et al*. that MG levels in the aorta of normal SD rats are 3-4 times higher than that in the heart, liver and the kidney (*144*). Increased MG formation occurs with the increased availability of its upstream metabolites, such as glucose. Most glucose enters insulin-insensitive cells, such as VSMCs and endothelial cells, through an insulin-independent glucose transporter 1 (GLUT1) (*145*). High glucose significantly elevated cellular MG levels in VSMCs and in endothelial cells (*70, 146*). Increased MG production in vascular tissues has been considered an important mechanism for the development of diabetes and diabetic vascular complications (*106*).

Recent *in vitro* studies showed that treatment with MG impaired insulin signaling in cultured 3T3-L1 adipocytes (*147*) or skeletal muscle L6 cells (*31*). Moreover, MG modified insulin molecule and impaired its biological functions, such as its stimulation of glucose uptake in adipocytes (*37*). These observations raise a great interest in MG formation in the insulin-sensitive cells. Glucose enters adipose and skeletal muscle cells mainly through an insulin-responsive glucose transporter 4 (GLUT4) (*145*). Insulin can promote membrane translocation of GLUT4 and stimulate glucose transport in adipose and skeletal muscle cells (*148*). High levels of insulin can also enhance glycolysis *via* up-regulating the transcription of glycolytic enzymes, such as hexokinase II, phosphofructokinase, and glyceraldehyde

3-phosphate dehydrogenase (GAPDH) (*149, 150*). It is of great significance and interest to investigate MG formation in insulin-sensitive cells under the conditions of high insulin.

1.5.2 MG and hyperglycemia

1.5.2a Aldolase A-glycolysis pathway

Spontaneous non-enzymatic fragmentation of GA3P and DHAP are considered the major sources for endogenous MG generation (*5, 6*). Most of the glucose is physiologically metabolized through glycolysis in which glucose is first phosphorylated to glucose 6-phosphate by the enzyme hexokinase and further enzymatically converted to fructose 1,6-bisphosphate (F-1,6-P2) (*7*). Aldolase A cleaves F-1,6-P2 to generate GA3P and DHAP (*7*). Aldolase A can also split F-1-P into glyceraldehyde (whch is phosphorylated by triose kinase to form GA3P) and DHAP, but its activity on the cleavage of F-1-P is 50-fold less than the cleavage of fructose F-1,6-P2 (*7*). Aldolase A is one of three structurally distinct forms of aldolases. Two other aldolase isozymes are aldolase B and brain-specific aldolase C (*7, 151*). Aldolase A is an important glycolytic enzyme ubiquitously expressed in many tissues, such as skeletal muscle, adipose tissue, liver, kidney, and the intestine (*151*).

1.5.2b Increased polyol pathway flux during hyperglycemia

Glucose can be metabolized to fructose through the polyol pathway in which aldose reductase reduces glucose to sorbitol, and then sorbitol dehydrogenase oxidizes sorbitol to fructose (*106*). Under physiological conditions, most glucose is metabolized through the glycolytic pathway since hexokinase has a much higher affinity for glucose than aldose

reductase (*152*). However, in diabetes with hyperglycemia, glucose can quickly enter VSMCs and endothelial cells through insulin-independent GLUT1, and this glucose influx saturates hexokinase and activates the polyol pathway. It was reported that aldose reductase was up-regulated and up to 30% of the glucose was channeled into the polyol pathway under hyperglycemic conditions (*153, 154*). Fructose is phosphorylated to F-1-P by fructokinase and subsequently cleaved to yield glyceraldehyde and DHAP by aldolase B (*7*). Glyceraldehyde is phosphorylated by triose kinase to form GA3P. Gene expression of aldolase B was previously detected in the liver, kidney and small intestine (*155*). Aldolase B is the key enzyme responsible for fructose metabolism. Aldolase B has high specific activity toward the substrate F-1-P (*155*). Deficiency of aldolase B due to gene mutations results in hereditary fructose intolerance in humans (*156, 157*).

1.5.3 MG and aldolase B-fructose pathway

Fructose is a monosaccharide found in fruits, vegetables (including sugar cane), and honey. Fructose is also present in sucrose or table sugar that contains equal parts of glucose and fructose and in high-fructose corn syrup (HFCS), a synthetically manufactured sweetener used in the food industry containing between 55–90% fructose. In the past 30 years, dietary fructose consumption has increased markedly due to the increased use of sucrose and HFCS (*158*). Individual consumption of fructose in the western world was only 0.5 lb/year in 1970 but rose to in 62.4 lb/year by 1997 (*159*). The excessive intake of fructose is one proposed cause of metabolic disturbance including insulin resistance, weight gain, hyperlipidemia, hypertension and heart diseases in humans and in animal models (*158-161*).

Using gas chromatography/mass spectrometry (GC/MS), Kawasaki *et al.* reported that the physiological concentration of fructose in serum is about 8.1 ± 1.0 μM in healthy humans and about 12.0 ± 3.8 μM in diabetic patients (*162*). The serum concentration of fructose in diabetic patients with ketoacidosis reaches 205 μM and higher (*163*). It should be noted, however, that the reported fructose levels in serum or plasma of healthy humans varies widely depending on the analytical method used, and were from μM range measured by GC/MS (*162, 164, 165*) to mM range measured by enzymatic methods (*166-169*). Using enzymatic methods, the concentration of blood fructose is 0.1-0.5 mM under physiological conditions, but can increase to 1-2 mM after consumption of fructose or sucrose (*166, 170*).

Dietary fructose rapidly diffuses into blood vessels from the intestine through a specific fructose transporter, GLUT5, on the intestinal epithelium (*171*). The main portion of absorbed fructose is metabolized in the liver where fructose is converted by highly expressed fructokinase and aldolase B to GA3P and DHAP, as illustrated in Figure 1-2. It was reported that the liver metabolized about 50% of fructose injected intravenously in humans (*172*). Fructose can up-regulate the gene expression of gluconeogenic enzymes (such as fructose 1,6-bisphosphatase and glucose 6-phosphatase) and lipogenic enzymes (such as pyruvate kinase, fatty acid synthase and glyceraldehyde 3-phosphate acyltransferase) in the liver. The major portion of GA3P and DHAP produced from fructose can be subsequently converted into glucose, glycogen and lipid (*161, 173, 174*). The left portion of absorbed fructose (approx. 30-45%) is available for extraction and utilization by other tissues expressing GLUT5, such as the kidney, adipose tissue and skeletal muscle (*175*). Whether there is expression of GLUT5 and fructose transport in VSMCs and vascular ECs is not known, but

our lab previously found that incubation with fructose significantly increased MG formation in VSMCs (*73, 146*).

Studies from clinical and basic researches have indicated that a diet high in fructose or sucrose can induce hypertension, insulin resistance, hyperinsulinemia, and diabetes, although the underlying mechanisms are unclear (*25, 176-182*). Some suggestions have been linked to elevated serum uric acid and C-reactive protein expression, endothelial dysfunction, and oxidative stress in adipocytes (*183, 184*). In a human study, the consumption of sucrose at 152 g/day mostly as beverages for 10 weeks resulted in weight gain and a rise in systolic blood pressure (*185*), while under the same conditions consumption of artificial sweeteners with zero sucrose caused no such changes. An increase in diastolic blood pressure was also reported in healthy adults after 6 weeks of 33% sucrose diets (*177*). As in humans, rats fed with fructose displayed metabolic syndrome (*186*) and developed renal hypertrophy, afferent arteriolar thickening, glomerular hypertension, and cortical vasoconstriction (*182*).

Our lab recently found that the development of vascular remodeling, endothelial dysfunction and high blood pressure in fructose-fed SD rats was associated with the high fructose-elevated MG levels in serum, aorta and the mesenteric artery (*25*). Moreover, an age-dependent elevation of MG levels in the plasma and the aorta has been observed in SHR that had normal blood glucose (*131*). Whether blood fructose is increased and is responsible for aortic MG overproduction in SHR is unknown.

1.5.4 MG and Insulin

High levels of insulin can increase glucose transport and cellular glucose

concentrations in adipocytes under normal glucose conditions (*187*). Moreover, insulin can up-regulate the gene expression of glycolytic enzymes independent of extracellular glucose concentrations (*149, 150*), as mentioned earlier. It is well known that people or experimental animals (i.e. rats and mice) with obesity or hypertension have higher blood insulin levels than healthy controls, although their blood glucose remains in a normal range (*188-191*). Studies with rat models of obesity showed that adipose cells are normally insulin sensitive at the early stage of obesity but become insulin resistant at the late stage (*192, 193*). However, whether high insulin enhances MG formation in insulin-sensitive adipocytes is not known.

The fructose transport in cells is independent of insulin stimulation, but high levels of insulin have been reported to up-regulate GLUT5 gene expression in some cell types, such as skeletal muscle cells (*194*). However, whether GLUT5 is up-regulated by insulin and contributes to MG overproduction in VSMCs is not clear. Moreover, little else is known about GLUT5 regulation and MG formation in the aorta of rats with hypertension or obesity.

1.6 Strategies to inhibit MG accumulation and MG-induced AGEs

Currently, no specific and potent scavengers against MG are available although N-acetyl-cysteine, guanidine compounds (such as aminoguanidine and metformin), and alagebrium have claimed their capability to react with or detoxify MG (*195, 196*). These pharmacological compounds are either non-specific for MG or associated with harmful side effects. The clinical trials of aminoguanidine (AG) have proved disappointing due to its nonselective inhibition of neuronal, endothelial and inducible NOS (*197, 198*). Alagebrium is thought to be the only AGE crosslink breaker, yet the results of preclinical (*199-201*) and

clinical (*202-204*) trials remain ambiguous (*205*) and the AGE-breaking ability of alagebrium is not consistently validated (*206*).

1.6.1 MG scavengers

Guanidine compounds, such as AG and metformin, are the most widely used MG scavengers. However, guanidine compounds are not specific since their guanidine residues can interact with the carbonyl in MG or in other carbonyl compounds, such as glyoxal, 3-DG and malondialdehyde (MDA) (*205*).

1.6.1.1 Aminoguanidine (AG)

AG, also known as pimagedine, directly reacts with MG and thereby prevents the related AGEs formation. An *in vitro* study showed that AG can react with MG in the test tube to form 3-amino-5-methyl-1,2,4-triazine and 3-amino-6-methyl- 1,2,4-triazine, which are identified by UV spectra and proton nuclear magnetic resonance spectroscopy (*207*). It has been reported that treatment with AG (100 μM) significantly reduced cellular MG levels in glucose (25 mM) or MG (30 or 100 μM)-treated endothelial cells (*70*). Numerous studies have shown that AG can prevent or reduce vascular remodeling in diabetic or hypertensive rats. Treatment of STZ-diabetic rats with AG (1 g/L in drinking water, 3 weeks or 8 months) prevented the diabetes-induced over-expression of TGF-β and collagens as well as increase of media-to-lumen ratio in mesenteric vessels without effects on food intake (*89*). AG treatment retarded the AGE modification of aortic collagen and decreased arterial wall protein cross-linking and aortic stiffening in diabetic rats (*208-210*). In SHR treated with AG, the

decreased lumen diameter and increased wall thickness and media-to-lumen ratio in the aorta and mesenteric arteries were prevented (*72*). Treatment with AG (0.5-1 g/L in drinking water, 4 weeks) reduced ventricular hypertrophy and diastolic stiffness constants in DOCA-salt hypertensive rats (*211*).

However, the benefit of AG on endothelial dysfunction is controversial. AG is also an inhibitor of NOS (*212*). Incubation with AG at 1 mM inhibited activities of iNOS and constitutive NOS (*212*). Chronic administration of AG (15 mg/ kg/day in drinking water, 9 weeks) reduced the aortic iNOS expression and plasma NO production in SHR (*213*). Some reports showed that AG treatment (25-50 mg/kg/day, s.c., or 250-750 mg/L in drinking water, 6 weeks) did not prevent the decrease in vasodilatory responses to acetylcholine in skeletal muscle arterioles, aorta and the mesenteric arteries of STZ-diabetic rats (*214-216*). Other reports indicated that pre-treatment with AG (250 mg/kg/day by oral gavage, 7 d before the induction of diabetes) partially prevented the time-dependent progression of impaired aortic vasodilatation to acetylcholine in STZ-diabetic rats (*217*), and 3-month treatment with AG (50 mg/kg/day in the drinking water) restored eNOS expression and partially improved the cetylcholine-induced vascular relaxation of mesenteric arteries in type 2 diabetic mice (*218*). Treatment with AG (1 g/L in drinking water, 9 weeks) restored acetylcholine-induced vascular relaxation in mesenteric arteries, increased eNOS expression and reduced iNOS expression in the aorta, and partially attenuated the increase in blood pressure in SHR (*72*).

Aminoguanidine also irreversibly inhibits SSAO, an enzyme which catalyzes the conversion of aminoacetone to MG, as mentioned earlier (*219*). When the SSAO isolated from the rat aorta and human umbilical artery was incubated with AG at a concentration of 10

μM or 1 mM for 30 min, SSAO activity was reduced by 20% or totally inhibited (*219*). An *in vivo* study showed that Wistar rats after treatment with AG (10 mg/kg i.p., 3 h) reduced their aortic SSAO activity by > 90% (*219*). However, SSAO is still considered a minor contributor for MG formation. Moreover, AG can react directly with ROS, such as H_2O_2, hydroxyl radical and $ONOO^-$ (*220*). *In vitro*, AG reduced H_2O_2, hydroxyl radical, and $ONOO^-$ levels at a concentration of 10, 1 and 0.1 μM, respectively (*220*).

1.6.1.2 Metformin

Metformin is an oral hypoglycemic agent for the treatment of type 2 diabetes. Metformin has been found to react with MG directly to form stable triazepinone derivatives in the test tube and in plasma samples of type 2 diabetic patients (*221, 222*). However, a high dose of metformin is required to achieve its MG and AGEs lowering effect (*196, 198*). Treatment with high-dosage metformin (1-2.5 g/day orally, 3 months) significantly lowered plasma MG levels in patients with type 2 diabetes, but the lower dosage of metformin (0.5-1 g/day, 3 months) had no effect (*196*). Chronic treatment with metformin both at low dose (50-65 mg/kg/day, 10 weeks) and high dose (500-650 mg/kg/day, 10 weeks) reduces AGEs formation in the lens, kidney and nerves in diabetic rats (*223*). Fructose-elevated MG and AGEs levels were significantly decreased when rats were co-fed with metformin (500 mg/kg/day in drinking water, 9 weeks) (*25*).

Metformin is also a non-specific MG scavenger. It can react with other reactive α-dicarbonyl compounds, such as glyoxal (*221*), and with ROS, such as superoxide anion and hydroxyl radical (*224*).

1.6.2 AGEs breakers

Alagebrium (also known as ALT-711) breaks the established AGE crosslinks (*205*). Alagebrium is a stable derivative of phenacylthiazolium bromide (PTB), the first AGE breaking compound reported in 1996 (*205*). Since PTB degrades rapidly, alagebrium, which is more stable, was developed. Previous studies with VSMCs showed that MG (30 μM)-increased AGEs levels were completely decreased by treatment with alagebrium (50 or 100 μM) (*66*). In STZ-diabetic rats, treatment with alagebrium after 1 week of STZ injection resulted in a significant reduction in diabetes-increased levels of AGEs in the serum, aorta and the kidney (*88, 225*). Administration of alagebrium in 3-, 7- or 12-month-old diabetic db/db mice for 12 weeks decreased diabetes-elevated CML levels in the serum, skin, and kidney, and increased urinary CML excretion (*226*). These studies suggest that alagebrium breaks the preexisting AGEs *in vitro* and *in vivo*.

The administration of alagebrium (1.0 mg/kg/day i.p, 1-3 weeks) in STZ-diabetic rats reduced collagen crosslinks, and reversed systemic arterial stiffness (*201*). In the STZ-diabetic rats or diabetic db/db mice, treatment with alagebrium restored diabetes-decreased collagen solubility and attenuated diabetes-increased renal collagen content and growth factor expression (*123, 225, 226*). Moreover, alagebrium has been found to improve endothelial dysfunction. Treatment with alagebrium (1 mg/kg i.p., 2 weeks) restored diabetes-decreased endothelium-dependent vasodilation in diabetic mice (*227*). When 60-week-old SHR were treated with alagebrium (oral gavage, 1 mg/kg/day, 8 weeks), systolic blood pressure was significantly decreased (*228*). Individuals (aged 65 ± 2 years) with isolated systolic hypertension displayed an improvement in endothelial NO production

and endothelial flow-mediated dilations after receiving alagebrium (oral gavage, 210 mg twice per day, 8 weeks) (*229*).

Recent work indicates that alagebrium has the ability to scavenge MG in the test tube at a concentration ten-fold higher than MG (*85*), but whether alagebrium can reduce MG levels and prevent MG toxicity in biological system has not yet been firmly established. The cytotoxic effects of MG are mainly through formation of AGEs and/or ROS. We found that application of alagebrium completely prevented AGEs formation in MG-treated VSMCs, but only partially reduced MG-increased mitochondrial superoxide generation and intracellular nitrotyrosine levels (*66*). Moreover, treatment with alagebrium in STZ-diabetic rats or mice only partially or slightly reduced the excess formation of superoxide and peroxynitrite in the kidney (*230*, *231*).

1.6.3 RAGE blockade

RAGE is a specific receptor expressed in a variety of cells, and the receptor-mediated effects significantly contribute to the cytotoxicity of AGEs. The anti-RAGE F(ab')2 [the blocking F(ab')2 fragments of RAGE antibodies] and soluble RAGE (sRAGE) are being considered to block AGEs-RAGE interaction (*232*). F(ab')2 fragments of RAGE antibodies were generated by pepsin digestion of the intact antibody. sRAGE is the extracellular ligand binding domain of RAGE. sRAGE may competitively react with various ligands of RAGE, such as AGEs, and block the ligand-RAGE interaction (*49*). Pretreatment of endothelial cells with anti-RAGE F(ab')2 inhibited the RAGE-mediated up-regulation of the inflammatory factor monocyte chemoattractant protein-1 (*232*). When the endothelial cells were treated

with anti-RAGE F(ab')2 or sRAGE, the AGEs-elevated expression of VCAM-1 and adhesivity of the monolayer for Molt-4 cells (a human acute lymphoblastic leukemia cell line) were inhibited (*233*). Moreover, *in vivo* usage of sRAGE improves diabetic vascular complications (*234*). For example, administration of sRAGE (2.25-5.15 mg/kg) blocked vascular permeability in the intestine, skin, and kidney of diabetic rats (*49*) and suppressed the hyperglycemia-induced atherosclerosis in STZ-treated apoE null mice (*235*).

RAGE was initially identified as a receptor for AGEs (*236*), but it has also been shown to be a multi-ligand receptor which can recognize amyloid-beta peptide, β-sheet fibrils, S100/calgranulins, and Mac-1 (*237*). The blockage of RAGE may adversely affect ligand-induced signal transduction. For example, a recent study found that knockout of RAGE causes hyperactivity and increased sensitivity to auditory stimuli in mice (*238*).

1.6.4 Over-expression of glyoxalase-I

The effects of excess MG formation in cells can be inhibited by over-production of glyoxalase-I which converts α-dicarbonyl compounds, such as MG and glyoxal, to D-lactate with assistance of glyoxalase II and GSH. Over-expression of glyoxalase-I promoted MG metabolism to D-lactate and prevented the accumulation of MG and AGEs in bovine endothelial cells exposed to high glucose concentration (*36*). In glyoxalase-I transgenic Wistar rats, glyoxalase-I activity was increased ten- to fifty-fold in tissues (i.e. heart, kidney, eye, brain, aorta and skeletal muscle), and the hyperglycemia-elevated plasma MG, glyoxal and AGEs levels in STZ-induced diabetes were prevented (*239*). Over-expression of glyoxalase-I in *Caenorhabditis elegans (C. elegans)* attenuated aging-related MG and AGEs

accumulation, and extended its lifespan (*81*). Recently, *C. elegans* has been identified as a suitable model organism to study glucose toxicity (*240*). Feeding *C. elegans* with 40 mM glucose increased MG modification of mitochondrial proteins, elevated formation of ROS, and reduced its mean and maximum life span, but all of the above effects of high glucose were attenuated in glyoxalase-1 transgenic *C. elegans* (*240*).

However, over-expression of glyoxalase-1 may lead to enhanced consumption or trapping of intracellular GSH, an important antioxidant in the body. Transfection of NIH-3T3 cells with glyoxalase-1 cDNA increased cellular protein levels and activity of glyoxalase-1, but significantly reduced cellular GSH concentration (*241*). Reduction of GSH due to over-expression of glyoxalase-1 may limit the antioxidant capacity of cells and affect the activities of enzymes that use GSH as a cofactor. For example, over-expression of glyoxalase-1 in STZ-diabetic rats only partially counteracted the elevated oxidative stress levels, such as urine MDA and 8-isoprostane and kidney nitrotyrosine, and partially reversed the decreased protein levels of muscle mitochondrial complex I, II and III (*239*).

1.6.5 Blockage of Aldolase A-glycolysis and Aldolase B-fructose pathway

GA3P and DHAP are considered the major sources for endogenous MG generation (*5, 6*). Glucose or fructose can be converted into GA3P and DHAP through the action of the enzyme aldolase A or/and aldolase B (*7*). SD rats fed with fructose increase MG formation in the serum and the aorta (*72*). Hyperglycemia activated the polyol pathway and increased production of sorbitol and fructose in the aorta, retina and kidney tissues of STZ-diabetic rats (*242*). Increased MG and AGEs production were observed in the blood, retina and kidney of

STZ-diabetic rats (*87*). However, whether blockage of aldolase A or aldolase B can prevent MG overproduction and related deleterious effects in different types of cells or in different animal models with metabolic syndrome has not been reported yet.

1.7 Rationale and hypothesis

Increased production of MG in vascular tissues is one of the causative factors for hypertension and vascular complications of diabetes. MG and MG-induced AGEs cause mitochondrial dysfunction, enhanced formation of ROS (superoxide and peroxynitrite), activation of NF-κB and increased Akt1-mediated proliferation in VSMCs and/or endothelial cells. High glucose is known to increase MG production in VSMCs and endothelial cells. MG production from VSMCs is also elevated in hypertension in the absence of hyperglycemia. Recently, MG has been found to impair the insulin signaling pathway in 3T3-L1 adipocytes, which is characterized by a reduction in insulin-mediated phosphoinositide 3-kinase (PI3K) pathway and glucose uptake (*147*). The underlying mechanisms for MG overproduction in insulin-insensitive VSMCs and insulin-sensitive adipose cells are unknown. Among the major pathways that lead to MG production is the glycolytic pathway in which glucose is metabolized to GA3P and DHAP through the involvement of aldolase A, and both GA3P and DHAP can spontaneously convert to MG. Fructose, either derived from the diet (e.g., table sugar) or converted from glucose, can be catalyzed by aldolase B, a rate-limiting enzyme in fructose metabolism, to yield GA3P and DHAP and subsequently MG.

Our working hypotheses are that the up-regulation of the fructose-AldoB pathway in VSMCs is a common mechanism for vascular MG overproduction in metabolic syndrome,

while the insulin-upregulated aldolase A-glycolysis pathway is responsible for enhanced MG production in adipose cells. Futhermore, it is hypothesized that inhibition of fructose-aldoB pathway suppresses MG-induced ROS and cellular dysfunction.

1.8 Objectives and experimental approaches

1.8.1 To evaluate the contribution of fructose and aldolase B to MG formation in cultured VSMCs and in the aorta of different rat models with metabolic syndrome.

Whether fructose levels and aldolase B expression are elevated with the MG increase in the aorta *in vivo* in different rat disease models with metabolic syndrome was studied first. Aorta of rats with obesity, hypertension or diabetes were isolated, fructose and MG concentrations and gene expression of fructose transporter GLUT5 and enzymes involved in fructose metabolism, including aldose reductase (converting glucose to fructose through the polyol pathway), fructokinase (phosphorylating fructose to F-1-P), and aldolase B were measured. Gene expression of aldolase A, SSAO and CYP 2E1 which account for MG formation during glycolysis, protein and fatty acids metabolism, respectively, was examined.

Thereafter, whether fructose levels and aldolase B expression are elevated by high glucose or fructose (25 mM) and responsible for excess MG production in cultured VSMCs was studied. Rat aortic smooth muscle cells (A-10 cells) were incubated with high glucose or fructose. Gene expression of aldolase A and aldolase B, cellular levels of G-6-P (the first metabolite of glycolysis), sorbitol (the first metabolite of polyol pathway), fructose, GA3P, DHAP and MG were measured. The inhibitors for aldose reductase, sorbitol dehydrogenase as well as shRNA targeting aldolase A and B were employed in VSMCs to compare the

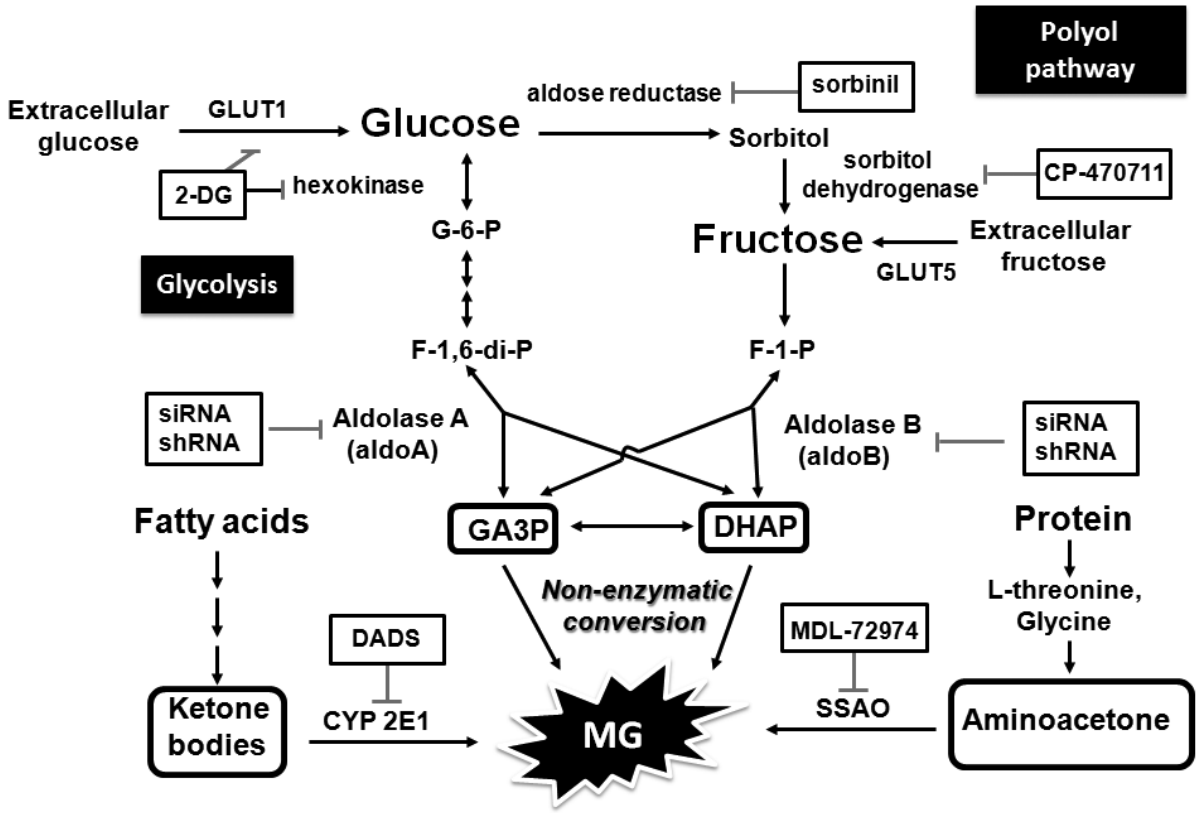

Figure 1-6 Experimental design. The relative contributions of different pathways or enzymes to MG formation were evaluated by using enzyme inhibitors or siRNAs/shRNAs targeting aldolase A or aldolase B. Sorbinil, CP-470711, diallyl disulfide (DADS) and (E)-2-(4-fluorophenethyl)-3-fluoroallylamine (MDL-72974) are specific inhibitors for aldose reductase, sorbitol dehydrogenase, cytochrome P450 2E1 (CYP 2E1) and semicarbazide-sensitive amine oxidase (SSAO), respectively. 2-Deoxy-D-glucose (2-DG) is a non-specific inhibitor for glucose uptake and hexokinase.

Abbreviations: DHAP – dihydroxacetone phosphate; F-1-P – fructose 1-phosphate; F-1,6-P2 – fructose-1,6-bisphosphate; G-6-P – glucose 6-phosphate; GA3P – glyceraldehyde 3-phosphate; GLUT1, GLUT5 – glucose transporter 1 and 5, respectively; MG – methylglyoxal; TIM – triosephosphate isomerase.

relative contributions of these enzymes to high fructose or glucose-induced MG overproduction (Figure 1-6).

Finally, the contribution of CYP 2E1 or SSAO to MG formation was evaluated. VSMCs were treated with acetone, glycine, or threonine (glycine and threonine are precursors of aminoacetone), and cellular MG levels were measured. The inhibitors for CYP 2E1 and SSAO were applied to evaluate contributions of these enzymes to high fructose or glucose-induced MG overproduction in VSMCs.

1.8.2 To investigate whether aldolase B knockdown prevents high glucose-induced MG overproduction and cellular dysfunction in endothelial cells.

Endothelial cells were treated with high glucose (25 mM), and gene expression of aldolase B and cellular levels of MG were measured. Aldolase B siRNA was transfected into endothelial cells to knock down aldolase B. Levels of MG, AGEs, oxidative stress markers (oxidized DCF, H_2O_2, protein carbonyls and 8-oxo-dG), O-GlcNAc modification of proteins (product of hexosamine pathway), membrane PKC activity and amounts of nuclear NF-κB in control or aldolase B siRNAs-transfected cells were measured under normal (5 mM) or high glucose (25 mM) conditions.

Whether MG can directly activate the metabolic and signaling pathways of glucose damage was investigated in endothelial cells treated with MG (30 or 100 μM). Moreover, whether aminoguanidine (a MG scavenger) or alagebrium (an AGEs breaker) prevents the high glucose-induced endothelial cell dysfunction was investigated.

1.8.3 To evaluate the contribution of insulin and aldolase A to MG formation in insulin-sensitive adipose cells

3T3-L1 cells (a mouse embryonic fibroblast-adipose like cell line) were differentiated into adipocytes (>90% differentiation). Thereafter, these adipocytes were treated with insulin (100 nM) or high glucose (25 mM) or their combination for 12 h. Gene expression of aldolase A and aldolase B, and cellular levels of G-6-P, sorbitol, fructose and MG were measured and compared with their control group (glucose 5 mM). The inhibitors for glycolysis, aldose reductase, SSAO and CYP2E1 as well as siRNA targeting aldolase A or B were employed in adipocytes to compare the relative contributions of different pathways or enzymes to MG formation induced by insulin or high glucose. MG levels were also measured in 3T3-L1 adipocytes treated with fructose, ketone bodies (acetone and acetol), glycerol (converting to DHAP during triglycerides degradation (*243*)), glycine and threonine (glycine and threonine are precursors of aminoacetone) at a concentration of 25 mM in the absence or presence of 100 nM insulin.

CHAPTER 2

GENERAL METHODOLOGY

2.1 Animals

All animal and experimental procedures were approved by the Animal Care Committee at The University of Saskatchewan, following guidelines of the Canadian Council on Animal Care. Male 4-week-old SD rats, 20-week-old WKY rats and SHR, and 16-week-old lean, obese and diabetic Zucker rats were purchased from Charles River Laboratories (Quebec, Canada). 4-week-old SD rats were treated with or without 60% fructose (w/w in chow) for another 16 weeks to induce hypertension which was confirmed by blood pressure measurement. After starving for 10 h, the rats were anaesthetized with sodium pentobarbital (60 mg/Kg, i.p.) or isoflurane (5%, inhalation). The depth of anesthesia was evaluated by limb withdrawal reflexes. A supplemental dose of pentobarbital (30 mg/Kg, i.p.) or a longer time of isoflurane inhalation was applied if nessary until the rats' reflexes disappeared. Blood was collected by cardiac puncture. Aorta from rats were collected and snap frozen in liquid nitrogen and stored at -80 ° C for further processing. Fasting serum glucose and insulin levels were measured using a glucose assay kit (Bioassay systems, Hayward, USA) and a rat-specific insulin ELISA kit (Mercodia AB, Sylveniusgatan, Uppsala, Sweden), respectively. Fasting serum fructose was measured by an enzymatic spectrophotometric assay (*166*).

2.2 Cell culture

Rat aortic smooth muscle cell line (A-10 cells) and mouse embryonic fibroblast-adipose like cell line (3T3-L1 fibroblast cells) were obtained from American Type Culture Collection. EA. hy926 cells, an endothelial cell line derived from the fusion of human

umbilical vein endothelial cells with A549 lung carcinoma cells (*244*), were a gift kindly provided by Dr. Cora-Jean Edgell, University of North Carolina at Chapel Hill. EA. hy926 cells well retain endothelial phenotype and functions, such as expression of eNOS, and grow rapidly in culture without requirement for special growth factors, and thus are very often used as an *in vitro* model for endothelial cells (*244-247*).

A-10 cells were cultured in low-glucose Dulbecco's Modified Eagle Medium (DMEM, 5 mM glucose, Sigma-Aldrich, Oakville, ON, Canada) containing 10% bovine serum (BS) and penicillin-streptomycin (PS, 1% v/v) at 37 °C in a humidified atmosphere of 5% CO_2 and 95% air, as described previously (*56*). Cells were starved in BS-free medium for 24 h before different treatments.

EA. hy926 cells were cultured in low-glucose DMEM supplemented with 10% fetal bovine serum (FBS) and PS (1% v/v) at 37 °C in a humidified atmosphere of 5% CO_2 and 95% air. EA. hy926 cells were starved in DMEM containing 0.5% FBS for 24 h before treatments.

3T3-L1 fibroblast cells (preadipocytes) were cultured in high-glucose DMEM (25 mM glucose, Sigma-Aldrich, Oakville, ON, Canada) containing 10% FBS and PS (1% v/v) at 37 °C in a humidified atmosphere of 5% CO_2 and 95% air. The differentiation of 3T3-L1 fibroblast cells to adipocytes was induced as described previously (*248*). At two days after confluence, cells were incubated with high-glucose DMEM (10 % FBS) containing 0.25 µM dexamethasone, 0.5 mM 3-isobutyl-1-methylxanthine, and 172 nM insulin for three days. The cell culture medium was changed every day. Thereafter, cells were cultured in high-glucose DMEM (10 % FBS) containing 172 nM insulin for 2 days and in high-glucose DMEM (10 % FBS) for 2-6 days till >90% of cells became adipocytes (the cell culture

medium was changed every two days). The differentiation was evaluated using Oil Red O staining. Cells were starved in FBS-free medium for 24 h before different treatments.

2.3 Gene knockdown in cells

Knockdown of aldolase A or B in A-10 cells was established by transfection with SureSilencing plasmid shRNAs purchased from Superarray (Frederick, MD, USA) according to manufacturer's instructions. The transfected cells were selected in low-glucose DMEM (10% BS) containing 600 μg/mL G418 for 2 weeks and the survivors were maintained in low-glucose DMEM (10% BS) containing 200 μg/mL G418. Gene knockdown was verified with real-time PCR assay.

Knockdown of aldolase A or B in EA. hy926 cells or in 3T3-L1 adipocytes was established by 24-h transfection of cells with a siRNA pool (a mixture of 4 different siRNA duplexes, purchased from Santa Cruz Biotechnology Inc., Santa Cruz, CA, USA) targeting aldolase A or B using DharmaFECT™ 4 Transfection Reagent (Thermo Fisher Scientific, Nepean, ON, Canada) or siRNA Transfection Reagent (Santa Cruz Biotechnology Inc., Santa Cruz, CA, USA), respectively. Gene knockdown was verified with real-time PCR assay.

2.4 MG measurement

MG levels were measured by derivatization of MG with o-phenylenediamine (o-PD), followed by quantification of the resulting quinoxaline, 2-methylquinoxaline (2-MQ), with high-performance liquid chromatography (HPLC).

MG levels in A-10 cells, 3T3-L1 adipocytes, and rat tissues were determined with the

o-PD-based assay established by Chaplen *et al*. (*249*). Briefly, tissues were ground to a fine powder using a mortar and pestle in liquid nitrogen. Cells and ground tissues were sonicated (5 seconds, 3 times, on ice) and centrifuged at 12,000 rpm (10 min, 4 ℃). 240 μL supernatant was mixed with 60 μL of perchloric acid (PCA, 1 N), kept on ice for 10 min, and deproteinized by centrifuging at 12,000 rpm (10 min, 4°C). 180 μL supernatant was mixed with 90 μL of o-PD (100 mM) and incubated at room temperature in the dark for 3 h, followed by centrifugation at 12,000 rpm (5 min, 4°C). 180 μL supernatant was mixed with 20 μL of 5-methylquinoxaline (5-MQ, internal standard) and analyzed by HPLC using a Hitachi D-7000 HPLC system (Hitachi, Ltd., Mississauga, ON, Canada). 100 μL of mixture was injected onto a HPLC column (Nova-Pak® C18 column, 3.9×150 mm, MA, USA) for analysis using a mobile phase buffer containing 17% acetonitrile, 8% 50 mM NaH_2PO_4 (pH 4.5), and 75% water at a flow rate of 1 ml/min.

It is well known that MG exists in a protein-bound form (99%), including reversibly and irreversibly bound forms, and in a free form (<1%) in biological samples (*2*). The irreversibly bound form of MG, such as AGEs, remains stable under the harsh assay conditions; however, the reversibly bound MG is in dynamic equilibrium with free MG and, therefore, it may release MG during sample treatment procedures and cause big variations in MG measurement (*2, 250*). To set up a standard protocol that yields consistent values of MG in a given biological sample, we modified Chaplen's protocol (*251*). We increased the incubation time of cell extracts or blood with o-PD under an acidic environment which forces more reversibly bound MG to release and react with o-PD. Briefly, cells or ground tissues were sonicated three times for 5 seconds each time and centrifuged at 12,000 rpm (10 min,

4 ℃). 180 μL of the supernatant was incubated with 180 μL of PCA (1 N) and 40 μL of o-PD (100 mM) for 24 h at room temperature in the dark. The mixture was centrifuged at 12,000 rpm (10 min, 4 ℃). 180 μL of the supernatant was mixed with 20 μL of 5-MQ, and analyzed by HPLC with a mobile phase buffer containing 17% acetonitrile, 8% 50 mM NaH_2PO_4 (pH 4.5), and 75% water. For the blood sample, 135 μL of serum was incubated with 135 μL of PCA (1 N) and 30 μL of o-PD (100 mM) for 24 h at room temperature in the dark. The mixture was centrifuged at 12,000 rpm (10 min, 4°C). 180 μL of the supernatant was mixed with 20 μL of 5-MQ and analyzed by HPLC. This modified method has been used in our lab since 2009 for MG measurement, including MG levels in rat blood and in cultured EA. hy926 cells.

2.5 Measurement of glucose metabolites

Cells or ground tissues were sonicated (5 seconds, 3 times, on ice) and centrifuged at 12,000 rpm (10 min, 4 ℃). Total protein levels were determined with a bicinchoninic acid protein assay kit (Sigma-Aldrich, Oakville, ON, Canada). Intracellular fructose levels were measured by a fructose assay kit (BioVision, Mountain View, USA). Aliquots of supernatant were deproteinized by ¼ volume of PCA (1N) and neutralized by 2.5 M K_2CO_3 to measure the levels of glucose 6-phosphate and sorbitol using enzymatic fluorometric methods (*252, 253*).

2.6 Measurement of oxidative stress level

Cells in 24 or 96-well plates were washed with phosphate buffered saline (PBS), and

the total intracellular ROS levels were stained with a non-specific ROS probe 2',7'-dichlorodihydrofluorescein diacetate (DCF-DA, D399, purchased from Invitrogen, Burlington, ON, Canada) for 30 min at 5 μM. Intracellular H_2O_2 levels were stained with a specific fluorogenic H_2O_2 probe (Calbiochem, San Diego, CA, USA) for 30 min at 1 μM. DCF-DA or H_2O_2 probe were dissolved in dimethyl sulfoxide (DMSO) as a stock solution and the solution was diluted in PBS to the final concentration. DCF-DA is non-fluorescent. It can react with multiple forms of ROS, such as superoxide, H_2O_2 and $ONOO^-$, to yield fluorescent DCF. The specific H_2O_2 probe is a monosulfonated non-fluorescent fluorescein ester compound which selectively reacts with H_2O_2 to produce fluorescein (*254*). The fluorescence intensities of each staining were analyzed with a Fluoroskan Ascent plate reader (Thermo LabSystem, Franklin, MA, USA). Protein oxidation was assessed by measuring total protein carbonyls with an immunoblot kit (Cell Biolabs Inc., San Diego, CA, USA). The DNA oxidation biomarker 8-oxo-dG was visualized by immunofluorescent staining and photographed under fluorescence microscopy, using a specific mouse monoclonal 8-oxo-dG antibody (Trevigen, Gaithersburg, MD, USA), following the manufacturer's instructions.

2.7 Real-time Quantitative PCR (RT-PCR)

Total RNA was isolated from A-10, EA. hy926 cells, and rat aorta using an RNeasy Mini Kit, and from 3T3-L1 adipose cells using an RNeasy Lipid Tissue Mini Kit (both kits were purchased from Qiagen sciences, Mississauga, ON, Canada). 1-2 μg of RNA are converted to cDNA with an iScript™ cDNA Synthesis Kit or iScript™ advanced cDNA Synthesis Kit (Bio-rad, Mississauga, ON, Canada). Real-time PCR was performed in an

iCycler iQ apparatus (Bio-Rad, Hercules, CA, USA) using SYBR Green PCR Master Mix (Bio-Rad) with primers listed in Table 2-1. All RT-PCRs were performed in triplicate in optical-grade PCR tubes or plates and running at 95℃ for 30 s, 55℃ for 1 min, and 72℃ for 30s for 45 cycles. Melting curves were acquired immediately after cycling.

Table 2-1 RT-PCR primers for different mRNAs

Gene	Forward primer	Reverse primer
Rat aldolase A	5'-CCAACTGCTGCTGACTG-3'	5'-GGGCACTACACCCTTATC-3'
Mouse aldolase A	5'-CAACGGTCACAGCACTTC-3'	5'-CTTCCTCACTCTGCCCTC-3'
Rat aldolase B	5'-ACAGCCTCCTACACCTACT-3'	5'-GCTCATACTCGCACTTCA-3'
Mouse aldolase B	5'-CCAGTTCCCTATGTTCCA-3'	5'-TTGCTGTGCCTCTTCTAT-3'
Human aldolase B	5'-AGCCTCGCTATCCAGGAAAACG-3',	5'-TGGCAGTGTTCCAGGTCATGGT-3'
Rat CYP 2E1	5'-GGGAAACAGGGTAA-3'	5'-GCTCAGCAGGTAGAA-3'
Rat β-actin	5'-CGTTGACATCCGTAAAGAC-3'	5'-TAGGAGCCAGGGCAGTA-3'
Human β-actin	5'-ACTTAGTTGCGTTACACCCTT-3',	5'-GTCACCTTCACCGTTCCA-3'
Primers of rat SSAO, GLUT5, aldose reductase, fructokinase and 18s rRNA, and mouse 18s rRNA were purchased from Qiagen Inc., Mississauga, ON, Canada		

2.8 Western blot

Cells or tissues were lysed for 1 h in an ice-cold radioimmunoprecipitation assay buffer (RIPA, purchased from Santa Cruz Biotechnology Inc., Santa Cruz, CA, USA) supplemented with 1% protease inhibitor cocktail solution (Santa Cruz Biotechnology Inc., Santa Cruz, CA, USA) and 1 mM phenylmethylsulfonyl fluoride (PMSF). After centrifugation at 12,000 rpm (10 min, 4℃), the supernatant was collected as total cell

proteins. Nuclear proteins were extracted as previously described (*255*). Total cell proteins (50 or 100 μg) or nuclear proteins (20 μg) were boiled with 2X SDS sample buffer (Bio-Rad, Mississauga, ON, Canada) for 5 min, resolved by 7.5-10 % SDS-PAGE, and transferred onto polyvinylidene fluoride (PVDF) membranes (Millipore Corp. Bedford, MA, USA). The membranes were blocked in 5% milk powder in PBST (PBS containing 0.1% Tween 20) for 30 min, and incubated for 3 h at room temperature or overnight at 4℃ with primary antibodies as follows: aldolase A (1:5000, Sigma-Aldrich, Oakville, ON, Canada), aldolase B (1:500, Epitomics Inc., Burlingame, CA, USA), O-GlcNAc (RL2) (1:1000, Thermo Fisher, Nepean, ON, Canada), aldose reductase (1:500, Santa Cruz), β-actin (1:5000, Santa Cruz), α-tubulin (1:500, Santa Cruz), NF-κB (p65) (1:500, Santa Cruz) and lamin B (1:1000, Santa Cruz Biotechnology Inc., Santa Cruz, CA, USA), respectively. Membranes were washed with PBST for 4-5 times and incubated with horse radish peroxidase conjugated secondary antibodies (1:2000-1:1000, Upstate, Waltham, MA, USA) for 3 h at room temperature. The protein bands were visualized with enhanced chemiluminescence reagents (Amersham Biosciences, Pistcataway, NJ, USA) and exposed to X-ray film (Santa Cruz Biotechnology Inc., Santa Cruz, CA, USA).

CHAPTER 3

UP-REGULATION OF ALDOLASE B AND OVERPRODUCTION OF METHYLGLYOXAL IN VASCULAR TISSUES FROM RATS WITHMETABOLIC SYNDROME

Jianghai Liu[1], Rui Wang[2], Kaushik Desai[1], and Lingyun Wu[1]

[1]Department of Pharmacology, University of Saskatchewan, Saskatoon, SK, S7N 5E5;

[2]Department of Biology, Lakehead University, Thunder Bay, ON, P7B 5E1, Canada

This chapter has been published as a paper in

Cardiovascular Research (2011) 92 (3): 494-503.

3.1 Abstract

Aims Methylglyoxal (MG) overproduction has been reported in metabolic syndrome with hyperglycemia (diabetes) or without hyperglycemia (hypertension), and the underlying mechanism was investigated.

Methods and results Contributions of different pathways or enzymes to MG formation were evaluated in aorta or cultured vascular smooth muscle cells (VSMCs). In all four animal models of metabolic syndrome, i.e. chronically fructose-fed hypertensive Sprague–Dawley rats, spontaneously hypertensive rats, obese non-diabetic Zucker rats, and diabetic Zucker rats, serum and aortic MG and fructose levels were increased, and the expression of GLUT5 (transporting fructose) and aldolase B (converting fructose to MG) in aorta were up-regulated. Aortic expressions of aldolase A, semicarbazide-sensitive amine oxidase (SSAO), and cytochrome P450 2E1 (CYP 2E1), accounting for MG formation during glycolysis, protein, and lipid metabolism, respectively, was unchanged/reduced. Fructose (25 mM) treatment of VSMCs up-regulated the expression of GLUT5 and aldolase B and accelerated MG formation. Insulin (100 nM) increased GLUT5 expression and augmented fructose-increased cellular fructose accumulation and MG formation. Glucose (25 mM) treatment activated the polyol pathway and enhanced fructose formation, leading to aldolase B up-regulation and MG overproduction. Inhibition of the polyol pathway reduced the glucose-increased aldolase B expression and MG generation. The excess formation of MG in under these conditions was eliminated by knock-down of aldolase B, but not by knock-down of aldolase A or inhibition of SSAO or CYP 2E1.

Conclusion Up-regulation of aldolase B by accumulated high fructose is a mechanism for

MG overproduction in VSMCs and aorta in different models of metabolic syndrome.

Key words Aldolase B, Fructose, Methylglyoxal, Metabolic syndrome

3.2 Introduction

Increased levels of methylglyoxal (MG) and MG-glycosylated proteins or advanced glycation endproducts (AGEs) are the key pathogenic event in the vascular dysfunction in diabetes and hypertension (*106, 131, 256*). MG induces mitochondrial dysfunction and increases production of superoxide and peroxynitrite in vascular smooth muscle cells (VSMCs) (*55, 66*). The interaction between MG and hydrogen sulfide, a natural vasorelaxant, in VSMCs has been also reported (*257*). However, the underlying mechanism for MG overproduction was unknown.

MG is generated through several metabolic pathways. Spontaneous non-enzymatic fragmentation of triosephosphates, glyceraldehyde 3-phosphate (GA3P) and dihydroxyacetone phosphate (DHAP), is a primary source for endogenous MG generation (*5*, *6*). Increased GA3P and DHAP generation, in turn, may occur due to increased availability of glucose and fructose. In the cytosol, glucose is metabolized enzymatically through the glycolytic pathway into fructose-1,6-bisphosphate (F-1,6-P_2), which subsequently forms GA3P and DHAP catalyzed by aldolase A (*7*). On the other hand, fructose, either derived from the diet (e.g., table sugar) or converted from glucose by aldose reductase and sorbitol dehydrogenase *via* the polyol pathway, can be phosphorylated by fructokinase to fructose 1-phosphate (F-1-P), which is cleaved by aldolase B to generate glyceraldehyde and DHAP (*7*). Other potential sources of MG include the oxidation of aminoacetone (generated during protein catabolism) by semicarbazide-

sensitive amine oxidase (SSAO) and the oxidation of acetone (generated from lipolysis) by cytochrome P450 2E1 (CYP 2E1) (*10*).

Most glucose is physiologically metabolized through glycolytic pathway to GA3P and DHAP, and, therefore, MG is traditionally considered an intrinsic metabolite of glycolysis (*258*). High levels of glucose with accumulation of endogenous MG have received much attention in diabetes research due to the potentially pathogenic roles of MG and AGEs in the development of diabetes and diabetic complications (*106*). However, the importance of glycolysis in MG overproduction during hyperglycemia is challenged because high levels of glucose did not change or even impair glycolysis, but it activated the polyol pathway and enhanced fructose production in diabetic states (*242, 259, 260*). Moreover, elevated MG levels are also present in the metabolic syndrome without hyperglycemia, such as hypertension (*131*). As spontaneously hypertensive rats (SHR) develop hypertension, MG levels in plasma and aorta increase in an age-dependent fashion (*131*), although no difference in blood glucose levels between SHR and control rats is apparent (*132*). When Sprague Dawley (SD) rats were fed with fructose for 16 weeks, elevated MG levels in the serum and the aorta with development of vascular remodeling and high blood pressure was evident (*25*), but plasma glucose levels were within physiological ranges (*147*). Indeed, fructose treatment directly increased levels of MG in cultured VSMCs (*73*). Aldolase B is a rate-limiting enzyme in fructose metabolism, and a deficiency of aldolase B results in fructose intolerance in humans (*157, 261, 262*). These observations raise an important question whether fructose and aldolase B are commonly and predominantly responsible for vascular MG overproduction in metabolic syndrome with normal blood glucose, such as hypertension and

obesity, and with hyperglycemia, such as diabetes.

In this study, different rat models including fructose-fed SD, SHR, obese and diabetic Zucker rats, and their respective controls, were used to investigate the involvement of fructose and aldolase B in MG formation *in vivo*. The gene expression of enzymes (aldose reductase, fructokinase, aldolase A, aldolase B, SSAO, and CYP 2E1) and glucose transporter 5 (GLUT5), a specific fructose transporter (*263*), was examined in the aorta from these rats and in cultured VSMCs (the major cellular constituent of aorta) after treatment with fructose or glucose. The inhibitors for aldose reductase, sorbitol dehydrogenase, SSAO, and CYP 2E1 as well as shRNA targeting aldolase A and B were employed in VSMCs to compare the relative contributions of these enzymes to fructose or glucose-induced MG overproduction.

3.3 Methods

3.3.1 Animal Studies

All animal and experimental procedures complied with the *Guide for the Care and Use of Laboratory Animals* published by the US National Institutes of Health (NIH Publication no. 85–23, revised 1996) as well as *the Directive 2010/63/EU of the European Parliamen*, and were approved by the Animal Care Committee at The University of Saskatchewan, following guidelines of the Canadian Council on Animal Care. Male 4-week-old SD rats, 20-week-old Wistar-Kyoto (WKY) and SHR, and 16-week-old lean, obese and diabetic Zucker rats were purchased from Charles River Laboratories. 4-week-old SD rats were treated with or without 60% fructose (in chow) for another 16 weeks. Rats were anaesthetized with sodium pentobarbital (60 mg/Kg, i.p.) or isoflurane (5%, inhalation). The

depth of anesthesia was evaluated by limb withdrawal reflexes. A supplemental dose of pentobarbital (30 mg/Kg, i.p.) or a longer time of isoflurane inhalation was applied until the rats' reflexes disappeared. Then the rats were euthanized by exsanguination, involving collection of blood from the heart, under deep anaesthesia, and their tissues were quickly collected. Serum glucose and insulin levels were measured using a glucose assay kit (Bioassay systems, Hayward, USA) and a rat-specific insulin ELISA kit (Mercodia AB, Sylveniusgatan, Uppsala, Sweden), respectively. Serum fructose was detected with a method based on fructose dehydrogenase (*166*), after deproteinization with ¼ volume of 1 N perchloric acid (PCA) and neutralization with 2.5 M K_2CO_3.

3.3.2 Cell culture

A-10 cells, a rat aortic smooth muscle cell line, were cultured in Dulbecco's modified Eagle medium containing 10% bovine serum. Sub-confluent (80%) VSMCs were starved for 24 h in bovine serum-free Dulbecco's modified Eagle medium before further treatments in Dulbecco's modified Eagle medium containing 10% bovine serum.

3.3.3 Plasmid small hairpin RNA (shRNA) knockdown of aldolase A or aldolase B

Knockdown of aldolase A or B was established by transfection of A-10 cells with SureSilencing plasmid shRNAs (aldolase A, CACTGCCAATAAACAGCTATT; aldolase B, CTAGAGCACTGCCAGTATGTT; and control, GGAATCTCATTC GATGCATAC). The transfected cells were selected in medium containing 600 μg/mL G418 for 2 weeks and the survivors were maintained in 200 μg/mL G418. Gene knockdown was verified with real-time

PCR and Western blotting according to manufacturer's instructions (SuperArray, Frederick, MD, USA).

3.3.4 MG Measurement

MG levels in the aorta and VSMCs were determined with a *o*-phenylenediamine (*o*-PD)-based assay (*249*). Briefly, samples were sonicated and centrifuged at 12,000 rpm (10 min, 4°C). 240 μL supernatant was mixed with 60 μL of PCA (1 N), kept on ice for 10 min, and deprotenized by centrifuging at 12,000 rpm (10 min, 4°C). Then 180 μL supernatant was incubated with 90 μL *o*-PD (100 mM) for 3 h at room temperature in the dark. The mixture was centrifuged at 12,000 rpm (5 min, 4°C). A portion of the supernatant (180 μL) was mixed with 20 μL of 5-methylquinoxaline (5-MQ, internal standard) and analyzed by high-performance liquid chromatography (HPLC) with a mobile phase buffer containing 17% acetonitrile, 8% NaH_2PO_4 (50 mM, pH 4.5), and 75% water.

MG levels in serum were determined using our recently modified method (*251*). Briefly, 135 μL serum was incubated with 135 μL PCA (1 N) and 30 μL *o*-PD (100 mM) for 24 h at room temperature in the dark. The mixture was centrifuged at 12,000 rpm (10 min, 4°C). 180 μL of the supernatant was mixed with 20 uL 5-MQ and analyzed by HPLC.

3.3.5 Biochemical assays

Cell or tissue samples were sonicated and centrifuged at 12,000 rpm (10 min, 4℃). Total protein levels were determined with a bicinchoninic acid protein assay kit (Sigma-Aldrich, Oakville, ON, Canada). Intracellular fructose levels were measured by a

fructose assay kit (BioVision, Mountain View, USA). Aliquots of supernatants were deproteinized by ¼ volume of PCA (1N) and neutralized by 2.5 M K_2CO_3 to measure the levels of glucose 6-phosphate, sorbitol, GA3P and DHAP using the enzymatic fluorometric methods (*252, 253*). Glyoxalase 1 or 2 activity was assayed by using a spectrophotometric method to monitor the increase and decrease of S-D-lactoylglutathione, respectively, as described (*264*).

3.3.6 Analysis of gene expression

Total RNA was isolated using an RNeasy Mini Kit (Qiagen Inc., Mississauga, ON, Canada) and converted to cDNA with an iScript™ cDNA Synthesis Kit (Bio-rad, Mississauga, ON, Canada). Real-time PCR was performed using SYBR Green PCR Master Mix (Bio-Rad) with the following primers: rat aldolase A forward 5'-CCAACTGCTGCTGACTG-3', reverse 5'-GGGCACTACACCCTTATC-3'; aldolase B forward 5'-ACAGCCTCCTACACCTACT-3', reverse 5'-GCTCATAC TCGCACTTCA-3'; CYP 2E1 forward 5-GGGAAACAGGGTAA-3, reverse 5-GCTCAGCAGGTAGAA-3; β-actin forward 5'-CGTTGACATCCGTAAAGAC-3', reverse 5'-TAGGAGCCAGGGCAGTA-3'. Primers of aldolase A and B to verify shRNA knockdown were provided by Superarray (Frederick, MD, USA). Primers of SSAO, GLUT5, aldose reductase, and fructokinase were purchase from Qiagen (Mississauga, ON, Canada). Protein levels were analyzed by Western blotting using antibodies as follows: aldolase A (1:5000, Sigma-Aldrich, Oakville, ON, Canada), aldolase B (1:500, Epitomics Inc., Burlingame, CA, USA), and β-actin (1:5000, Santa Cruz Biotechnology Inc., Santa Cruz, CA, USA).

3.3.7 Materials

Sorbinil and CP-470711 were generous gifts from Pfizer Inc. (Groton, CT). Diallyl disulfide (DADS) was purchased from Sigma-Aldrich (Oakville, ON, Canada). (E)-2-(4-fluorophenethyl)-3- fluoroallylamine (MDL-72974) was a generous gift from Dr. Peter Yu (Department of Pharmacology, University of Saskatchewan, Canada).

3.3.8 Statistics

Data are expressed as mean ± SEM from at least 4 mice ($n \geqslant 4$) or from at least five independent experiments in cell study ($n \geqslant 5$/each group). Statistical analyses were performed using by parametric Student's *t*-test (two-tailed) or one-way ANOVA followed by Tukey's post-hoc test.

3.4 Results

3.4.1 Up-regulation of aldolase B and increased MG levels in fructose-fed hypertensive SD rats

A previous study in our lab indicated that chronically fructose-fed SD rats displayed a normal fasting blood glucose but increased serum and aortic MG levels with the development of hypertension and insulin resistance (*25*, *147*). To determine why fructose resulted in MG overproduction, we focused on the fructose-related transport and metabolic pathway. We observed that in addition to increased MG and fructose levels in the aorta (Figure 3-1A), 16-week fructose feeding of SD rats raised mRNA levels of GLUT5, but had no effect on mRNA levels of aldose reductase (Figure 3-1B). Because our *in vitro* studies found that 95%

of GA3P or 26% of DHAP converted to MG non-enzymatically after 12-h incubation (Figure 3-S1), we investigated whether fructose feeding affects gene expression of aldolase B which cleaves F-1-P to generate glyceraldehyde and DHAP. As shown in Figure 3-1C, fructose feeding elevated mRNA levels of aldolase B in the aorta, but had no effect on the mRNA levels of aldolase A, SSAO and CYP 2E1. In addition, fructose feeding up-regulated aortic mRNA levels of fructokinase, an enzyme that phosphorylates fructose into F-1-P (Table 3-S1).

3.4.2 Increased fructose, aldolase B mRNA and MG levels in SHR

SHR and WKY rats at age of 20 weeks displayed similar levels of serum glucose; however, serum MG, fructose, and insulin levels were markedly increased in SHR (Table 3-1). Increased levels of MG and fructose, and up-regulated mRNA expression of GLUT5 and unaltered mRNA expression of aldose reductase, were observed in the aorta of SHR compared to WKY (Figures 3-1D, 3-1E). SHR had higher levels of fructokinase and aldolase B mRNA in the aorta than WKY rats (Table 3-S1, Figure 3-1F). Both SHR and WKY rats displayed similar mRNA levels of aldolase A and CYP 2E1 in the aorta, but SHR had lower levels of SSAO mRNA than WKY rats (Figure 3-1F).

3.4.3 Increased fructose, aldolase B mRNA and MG levels in obese, non-diabetic Zucker rats

When compared with lean rats, obese rats had similar levels of serum glucose but much higher levels of serum MG and insulin (Table 3-1). Serum fructose levels in obese rats

were increased (Table 3-1), although not significantly. Obese rats displayed higher levels of MG and fructose as well as up-regulated mRNA expression of GLUT5, fructokinase and aldolase B in the aorta (Figures 3-2A, 3-2B and 3-2D). However, aortic mRNA levels of aldose reductase, aldolase A, SSAO, and CYP 2E1 were not significantly different in obese and lean rats (Figures 3-2C, 3-2D).

3.4.4 Activation of polyol pathway and increased fructose, MG levels in diabetic Zucker rats

In comparison with obese rats, diabetic rats had similar but exacerbated alterations. Diabetic rats exhibited higher levels of fructose and MG in serum and the aorta as well as higher levels of aldolase B mRNA in the aorta than non-diabetic lean and obese rats (Table 3-1, Figs. 2A, 2D). Aortic mRNA levels of GLUT5 and fructokinase in diabetic rats were higher than those in lean rats but not significantly different than those in obese rats (Figure 3-2B). Unlike obese, hypertensive, and fructose-fed rats, diabetic rats displayed higher glucose and lower insulin levels in serum (Table 3-1). We also investigated whether the polyol pathway is involved in aortic fructose and MG overproduction in diabetic Zucker rats. As shown in Figure 3-2C, aortic levels of aldose reductase mRNA and sorbitol were higher in diabetic rats than non-diabetic lean and obese rats. In contrast, mRNA levels of aldolase A were decreased in diabetic rats (Figure 3-2D).

3.4.5 MG accumulation in VSMCs induced by fructose, fructose plus insulin, or glucose

To investigate whether fructose and aldolase B are primarily responsible for increased

MG levels in the aorta in the different rat models, cultured A-10 cells were used. We chose glucose at 25 mM to mimic the hyperglycemia of diabetics and chose fructose at 25 mM for comparative purposes. We observed that fructose (25 mM) induced time-dependent increases of cellular MG and fructose (Figures 3-3A, 3-3C). In the presence of insulin (100 nM), the cellular MG and fructose levels induced by fructose (25 mM, 6 and 12 h) were further augmented (Figures 3-3B, 3-3C). Insulin alone (100 nM) had no effect on cellular levels of MG and fructose (Figures 3-3B, 3-3C). Glucose (25 mM) also increased cellular MG and fructose levels in a time-dependent manner (Figures 3-3A, 3-3C). Application of insulin (100 nM) had no effect on cellular fructose levels induced by glucose (25 mM) (Figure 3-3C). In comparison with glucose (25 mM), fructose at the same concentration raised MG and fructose levels in a similar pattern but which started earlier (<3 h), reached the peak quicker, and stayed at elevated levels longer (~18 h).

We explored whether or not glucose or fructose induces a change of glyoxalase 1 and glyoxalase 2 activities because most of the cellular MG was degraded by these two enzymes into D-lactic acid (*264*). Glucose (25 mM), fructose (25 mM), or fructose plus insulin (100 nM) incubations of cultured A-10 cells increased the activity of glyoxalase 1 but not glyoxalase 2 after 12-h treatment, and increased the activity of both glyoxalase 1 and glyoxalase 2 after 24-h treatment (Figure 3-3D).

3.4.6 Fructose or fructose plus insulin-enhanced MG formation was totally prevented by aldolase B knockdown in VSMCs

After the cells were treated with fructose (25 mM) and insulin (100 nM), respectively,

we observed a similar rise in mRNA levels of GLUT5; with co-treatment of fructose and insulin, the GLUT5 mRNA was further elevated (Figure 3-4A). Fructose (25 mM) up-regulated the gene expression of fructokinase (mRNA) and aldolase B (mRNA and protein) but had no effect on aldolase A mRNA (Figures 3-4A - 3-4C). In the presence of insulin (100 nM), fructose-elevated fructokinase and aldolase B gene expression were further raised (Figures 3-4A - 3-4C). Insulin alone had no effect on fructokinase mRNA, aldolase A mRNA, and aldolase B mRNA and protein levels (Figures 3-4A - 3-4C). Transfection with shRNA targeting aldolase B successfully knocked-down aldolase B in A-10 cells, which reduced aldolase B mRNA by 75 % and protein by 84% compared to the transfection with control shRNA (Figure 3-4D). In these cells transfected with aldolase B shRNA, the increases in cellular MG production induced by fructose (25 mM) or fructose plus insulin (100 nM) were completely inhibited (Figure 3-4D).

3.4.7 Glucose-increased MG formation was reduced by inhibition of polyol pathway and totally prevented by knockdown of aldolase B in VSMCs

Treatment with glucose (25 mM, 12 h) elevated levels of polyol pathway metabolites sorbitol and fructose, as well as GA3P, DHAP and MG in A-10 cells, but unchanged levels of G-6-P (Figures 3-3C, 3-5A). The glucose-increased MG levels were reduced in the presence of sorbinil (a specific aldose reductase inhibitor) and CP-470711 (a specific sorbitol dehydrogenase inhibitor) (Figure 3-5B). Glucose (25 mM, 12 h) up-regulated aldolase B expression but down-regulated aldolase A expression in mRNA and protein levels (Figures 3-5C, 3-5D). The down-regulation of aldolase A and up-regulation of aldolase B evoked by

glucose (25 mM) were reduced in the presence of sorbinil, CP-470711, or their combination (Figures 3-5C, 3-5D). MG levels were raised in control shRNA cells treated with glucose (25 mM) *vs*. glucose (5 mM, 12 h). However, high glucose-increased MG levels were totally abolished by transfection with aldolase B shRNA (Figure 3-5E). Transfection with aldolase A shRNA reduced aldolase A mRNA (by 69%) and protein levels (by 86%) in A-10 cells (Figure 3-5E), but this aldolase A knockdown only partially inhibited glucose-induced MG overproduction (Figure 3-5E). Basal cellular MG levels in normal glucose (5 mM)-treated VSMCs were unchanged by application of sorbinil or CP-470711, or by knockdown of aldolase B, but reduced by knockdown of aldolase A (Figures 3-5A, 3-5E).

3.4.8 CYP 2E1 and SSAO are not implicated in MG formation in VSMCs

Treatment with acetone, glycine, or threonine (glycine and threonine are precursors of aminoacetone) at 25 mM for 3, 12, or 24 h did not alter MG levels in A-10 cells (Figure 3-S2). Co-application of DADS or MDL-72974, the specific inhibitor of CYP 2E1 and SSAO, respectively, for 12 h had no effect on basal MG formation induced by normal glucose (5 mM) and excess MG production induced by high glucose (25 mM), fructose (25 mM), or high fructose plus insulin (100 nM) (Figure 3-S2).

3.5 Discussion

The functional alterations induced by increased MG in the aorta *in vivo* or VSMCs *in vitro* have been shown in numerous studies from our lab. For example, we observed mitochondrial dysfunction, increased oxidative stress, and enhanced proliferation in cultured

VSMCs treated with MG (*38, 55, 66*). MG injection (iv/ip) induced endothelial dysfunction, such as decreases in eNOS activity, NO production, and endothelium-dependent relaxation, in the aorta of SD rats (*70*). Using MG scavengers, Dr Wu's group found that the over-produced MG contributed to the vascular remodeling in hypertensive rats (*25, 72*). With all these functional studies having been done, the focus and the novelty of the present study are to illustrate the molecular mechanisms for vascular MG overproduction and this study demonstrated that up-regulation of aldolase B by increased fructose is a common and primary mechanism for the increased MG production in vascular tissues, including both smooth muscle cells and endothelial cells, in different metabolic syndrome (obesity, hypertension, and diabetes), despite their varying blood glucose and insulin levels. Evidence supporting our hypothesis includes the observations that: 1) In all 4 rat models of metabolic syndrome, levels of fructose and MG in the serum and the aorta were increased; gene expression of aldolase B, but not aldolase A, SSAO and CYP 2E1, in the aorta were up-regulated; 2) in cultured VSMCs, glucose (25 mM), fructose (25 mM), or fructose plus insulin (100 nM) elevated cellular fructose accumulation, up-regulated aldolase B gene expression and increased MG formation; excess MG formation under these conditions was all completely inhibited by knockdown of aldolase B, but not by knockdown of aldolase A or inhibition of SSAO or CYP 2E1.

Because high-fructose diets impair vascular relaxation and increase blood pressure in arteries (*265, 266*), the role of fructose in cardiovascular diseases is gradually receiving more attention. We observed that rat models of hypertension or obesity showed normoglycemia but higher levels of fructose and MG in serum than their respective controls (Table 3-1).

Increased mRNA level of fructose transporter GLUT5 was found in VSMCs treated with fructose (25 mM) and in the aorta of fructose-fed rats, SHR, and obese Zucker rats (Figures 3-1, 3-2), which may, in turn, facilitate more fructose entering VSMCs. Fructose is well known as a precursor of MG in VSMCs and the aorta (*25, 73, 146*). Our data indicate that the increased circulating fructose levels in the serum and the subsequent fructose accumulation in the aorta could be the cause for aortic MG overproduction in metabolic-syndrome rats without hyperglycemia.

Insulin is likely to promote fructose-induced cellular fructose and MG accumulation in hypertension and obesity. High levels of insulin and fructose but normal glucose in serum were observed in obese (obese Zucker) and hypertensive (SHR) rats (Table 3-1), and, as previously reported, in rats fed with fructose (*266, 267*). Indeed, many clinical studies report a similar phenomenon in obese or hypertensive patients who have normal glucose (normoglycemia) but high insulin (hyperinsulinemia) (*188-190*). In VSMCs, we observed that fructose-elevated levels of cellular MG and gene expression of fructokinase (mRNA) and aldolase B (mRNA and protein) were further augmented in the presence of insulin (100 nM), although insulin alone had no effect on the expression of these enzymes, neither on cellular fructose and MG formation (Figures 3-3, 3-4). One possible reason for this increase in fructose-induced MG production induced by insulin is that insulin may up-regulate GLUT5 expression and by doing so, when extracellular fructose is increased, to enhance fructose transport and accumulation in cells. Our data showed that insulin alone up-regulated GLUT5 expression, and application of insulin augmented fructose-increased GLUT5 mRNA levels and cellular fructose accumulation in VSMCs (Figures 3-3, 3-4). Thus, hyperinsulinemia may

augment fructose-enhanced MG formation in obese and hypertensive rats through its up-regulation of GLUT5 rather than its effect on fructose catabolism.

A role for aldolase B in fructose accumulation-induced MG overproduction seems paramount. Aldolase B splits F-1-P, phosphorylated product of fructose, into MG precursors glyceraldehyde and DHAP, and plays a rate-limiting role in fructose metabolism (*261, 262*). Our data supported that elevated MG levels are associated with up-regulated fructose metabolism pathway, especially the key enzyme aldolase B in aorta of fructose-induced or genetic hypertensive, or obese non-diabetic rats (Figures 3-1, 3-2). Since GA3P and DHAP are considered direct sources for endogenous MG formation (*5, 6*) and showed high efficiencies of non-enzymatic conversion to MG (Figure 3-S1), our study suggests that up-regulation of aldolase B expression in metabolic syndrome is the triggering event for fructose accumulation-induced MG overproduction. However, aortic gene expression of aldolase A, SSAO and CYP 2E1, which are responsible for MG formation during glycolysis, protein and lipid metabolism, respectively, were unchanged or even reduced in these hypertensive or obese rats (Figures 3-1, 3-2). Our *in vitro* studies with cultured VSMCs treated with fructose or fructose plus insulin, a condition mimicking hypertension and obesity, also identify a major role of aldolase B in fructose-induced excess MG formation. High fructose (25 mM) concentration significantly increased mRNA and protein levels of aldolase B in VSMCs (Figure 3-4). As mentioned earlier, insulin (100 nM) can increase fructose transport and augment fructose-enhanced aldolase B expression, although insulin alone has no effects on aldolase B expression (Figure 3-4). In the VSMCs with aldolase B knockdown, the excess MG production induced by fructose or fructose plus insulin was totally prevented

(Figure 3-4). These observations *in vivo* and *in vitro* indicate that fructose accumulation and up-regulated aldolase B expression is mainly responsible for the aortic MG over-generation in obesity and hypertension without hyperglycemia.

Fructose and MG formation in diabetic rats seems more complicated. Diabetic Zucker rats had higher fructose and glucose (hyperglycemia), but lower insulin (hypoinsulinemia) levels in serum than both lean and obese rats (Table 3-1), similar to clinical observations in diabetic patients (*162, 268*). Glucose can metabolize to fructose *via* the polyol pathway (*106*). Diabetic rats displayed an up-regulation of GLUT5 and an activation of polyol pathway (evident by the elevated levels of aldose reductase mRNA and sorbitol) in the aorta when compared with non-diabetic lean and obese rats (Figure 3-2), indicating that both increased serum fructose and glucose contribute to aortic fructose formation. These diabetic rats showed exacerbated alterations in fructose accumulation, aldolase B expression and MG formation compared with non-diabetic obese and hypertensive rats (Figures 3-1, 3-2). However, mRNA levels of aldolase A, SSAO and CYP 2E1 were unchanged or even reduced in the aorta of diabetic rats. Our data suggest that fructose and aldolase B also predominantly contribute to MG overproduction in metabolic syndrome with hyperglycemia.

Most glucose is physiologically metabolized through the glycolytic pathway and the traditional view regards glucose-induced MG formation as a result of glycolysis (*258*). We indeed observed that the basal cellular MG levels in glucose (5 mM)-treated cells were reduced by shRNA knockdown of aldolase A, but not affected by knockdown of aldolase B or inhibition of polyol pathway, SSAO or CYP 2E1 (Figures 3-5, 3-S2), indicating a critical role for aldolase A and glycolysis in the maintenance of basal MG levels under normoglycemic

conditions, as shown in the aorta of untreated SD, WKY, and lean Zucker rats. However, hyperglycemia developing in diabetes is unlikely to increase metabolism through glycolysis in vascular cells (*259, 260*). In this work, we found that the levels of G-6-P, the first metabolite of glycolysis, in VSMCs treated with glucose at concentrations of 5 and 25 mM were not significantly affected (Figure 3-5). The gene expression of aldolase A was decreased in VSMCs treated with high glucose (Figure 3-5). In contrast, high glucose (25 mM) elevated cellular levels of polyol pathway metabolites sorbitol and fructose, up-regulated aldolase B expression, and increased GA3P, DHAP as well as MG formation (Figures 3-3, 3-5). High glucose induced a time-dependent increase of cellular MG and fructose but in a considerably delayed pattern compared to fructose treatment (Figure 3-3). Inhibition of aldose reductase and/or sorbitol dehydrogenase reduced glucose-elevated aldolase B expression and MG levels in VSMCs (Figure 3-5). More importantly, glucose-induced excess MG generation was completely prevented by shRNA knockdown of aldolase B in VMSCs, but only partially reduced by shRNA of aldolase A and not affected by inhibitor of SSAO or CYP 2E1 (Figures 3-5, 3-S2). These findings provide direct evidence that, in the hyperglycemic condition, the polyol pathway but not the glycolytic pathway was activated, and subsequently fructose is accumulated and aldolase B is up-regulated, resulting in excess MG formation in VSMCs.

In conclusion and as shown in Figure 3-6, with normoglycemia and normal levels of fructose and insulin, aortic glucose is metabolized through the glycolytic pathway, which results in basal levels of MG formation in lean Zucker, SD, and WKY rats. However, the situation changes with metabolic syndrome. With normoglycemia but increased serum fructose, aortic GLUT5 mRNA levels are up-regulated by fructose, and, as a consequence,

fructose levels in the aorta are elevated. Increased fructose up-regulates the gene expression of fructokinase and aldolase B, leading to increased fructose metabolism and excess MG generation in the aorta of obese Zucker, SHR, and fructose-fed SD rats. Serum insulin is also increased in obese or hypertensive rats, which may promote fructose transport and MG generation in the aorta by up-regulating GLUT5. When hyperglycemia with high levels of fructose but low levels of insulin in the serum are established in diabetes, much higher increases in fructose metabolism and MG formation are observed in the aorta of diabetic rats than in SHR or obese Zucker rats. The increased transport of serum fructose (resulting from raised GLUT5 mRNA levels in aorta) and the high glucose-activated polyol pathway metabolism (indicated by the elevated levels of aldose reductase mRNA and sorbitol in the aorta) both account for the higher levels of cellular fructose, fructose-induced fructokinase, and aldolase B expression and MG in the aorta of these diabetic rats. Unchanged levels of G-6-P and down-regulated aldolase A expression by high glucose suggests a lesser contribution of glycolysis to aortic MG overproduction in diabetic rats.

3.6 Acknowledgements

We are grateful to Mrs. Arlene Drimmie (Department of Pharmacology, University of Saskatchewan) for her excellent technical assistance. This work was supported by operating grants from Canadian Institutes of Health Research and the Heart and Stroke Foundation of Saskatchewan to L. Wu. J. Liu was supported by College of Medicine Graduate Scholarship, University of Saskatchewan.

Table 3-1 Basal parameters in serum of rat models.

Rat models	Age (wks)	n	MG (μM)	Fructose (mM)	Glucose (mM)	Insulin (ng/mL)
WKY	20	4	1.2 ±0.04	0.27 ±0.06	5.3 ±0.1	3.5 ±0.2
SHR	20	4	1.7 ±0.05**	0.46 ±0.04*	5.6 ±0.3	10.1 ±1.7**
Lean Zucker	16	5	1.1 ±0.05	0.25 ±0.05	4.9 ±0.06	2.4 ±0.2
Obese Zucker	16	5	1.4 ±0.04**	0.33 ±0.06	5.3 ±0.3	5.8 ±0.4**
Diabetic Zucker	16	5	2.3 ±0.1**$^{\#\#}$	0.53 ±0.05**$^{\#}$	19.2 ±0.6**$^{\#\#}$	1.1 ±0.1**$^{\#\#}$

$^{*}P$<0.05, $^{**}P$<0.01 *vs*. WKY or lean Zucker rats; $^{\#}P$< 0.05, $^{\#\#}P$< 0.01 *vs*. obese Zucker

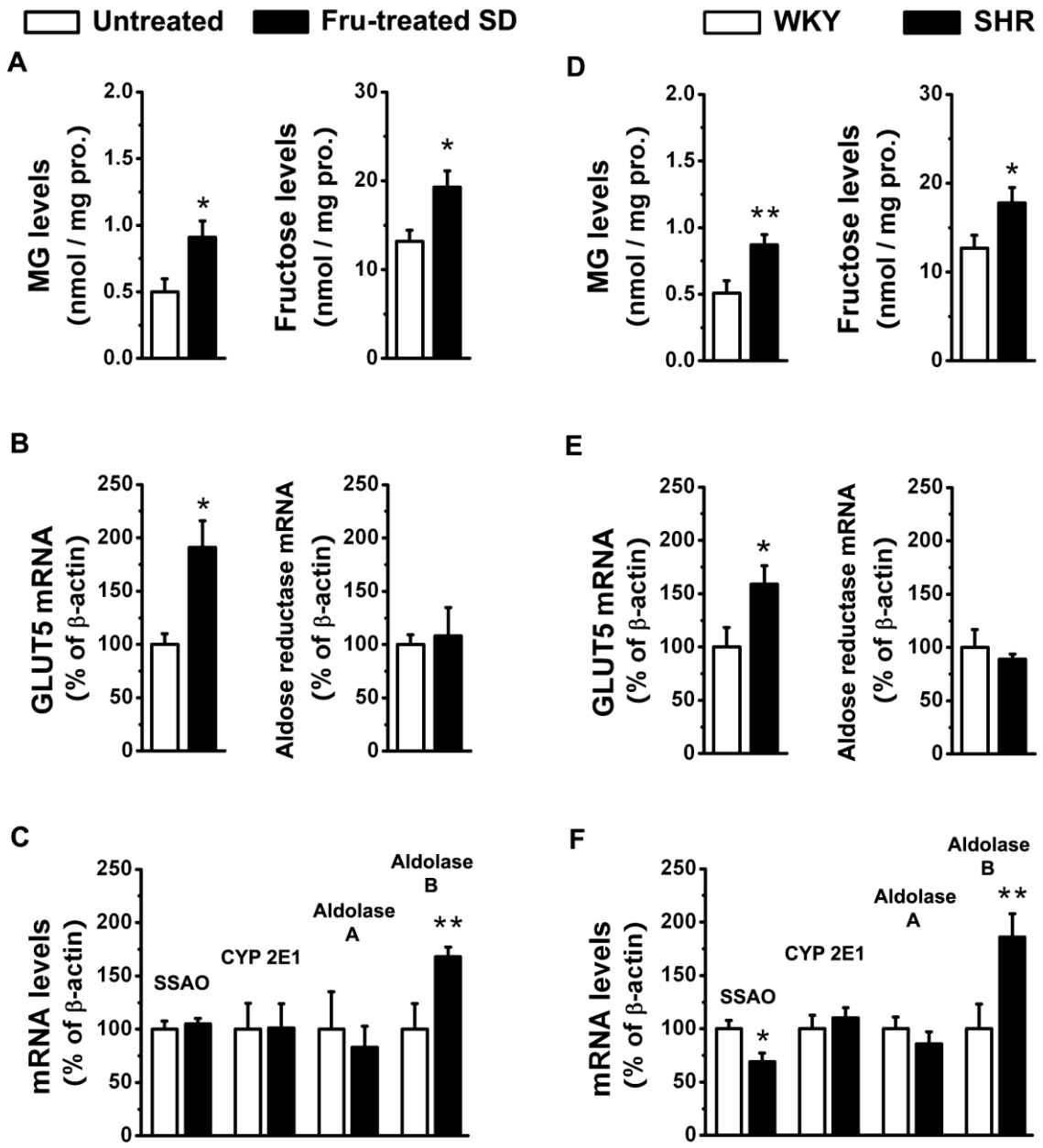

Figure 3-1 Fructose, aldolase B and MG in aorta of fructose-induced or genetic hypertensive rats. (A) Levels of MG and fructose, and mRNA levels of (B) glucose transporter 5 (GLUT5), aldose reductase, (C) semicarbazide-sensitive amine oxidase (SSAO), cytochrome P450 2E1 (CYP 2E1), aldolase A, and aldolase B in the aorta of 20-week-old Sprague Dawley (SD) rats treated or untreated with 60% fructose for 16 weeks. (D) Levels of MG and fructose, and (E, F) mRNA levels of different genes in the aorta of 20-week-old spontaneously hypertensive rats (SHR) and control Wistar-Kyoto (WKY) rats. $^{*}P<0.05$, $^{**}P<0.01$ *vs*. un-treated SD or WKY rats. $n = 4$ for each group in A-F.

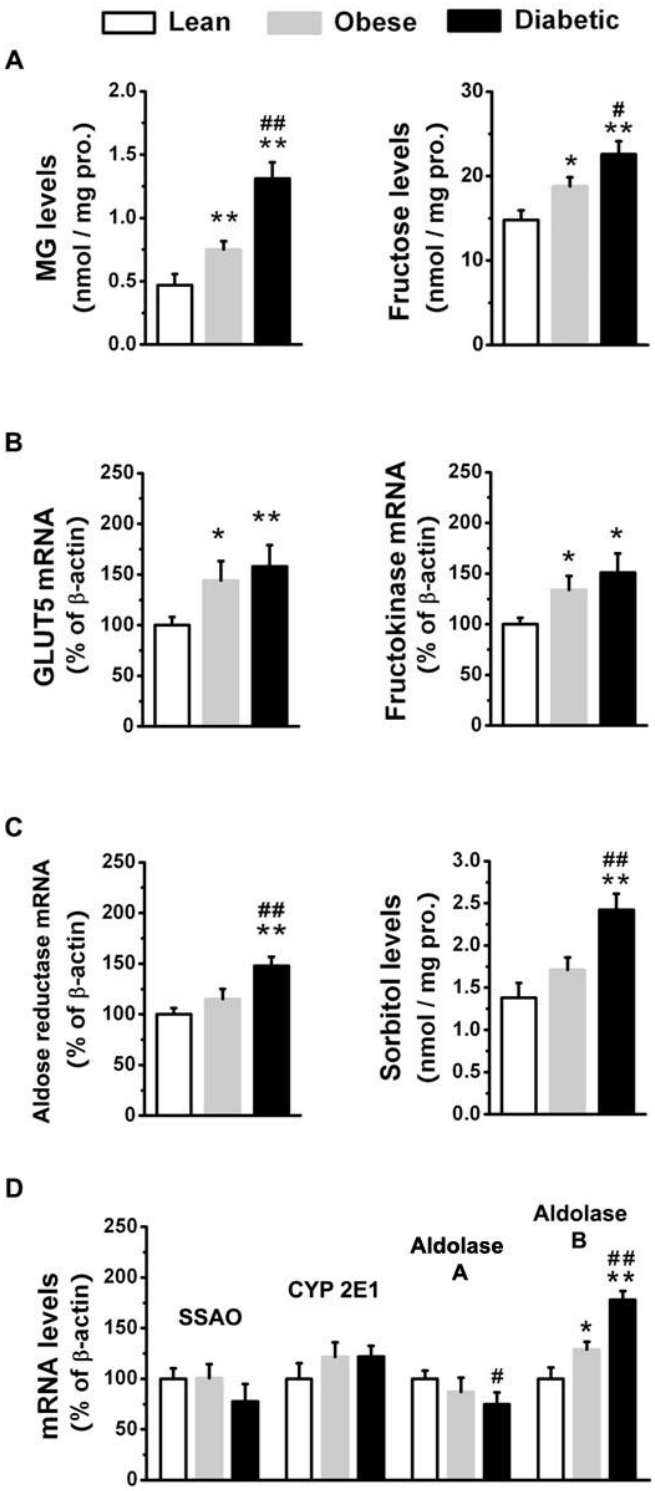

Figure 3-2 Fructose, aldolase B and MG in aorta of Zucker rats. (A) Levels of MG and fructose, (B) levels of glucose transporter 5 (GLUT5) and fructokinase mRNA, (C) levels of aldose reductase mRNA and sorbitol, and (D) levels of semicarbazide-sensitive amine oxidase (SSAO), cytochrome P450 2E1 (CYP 2E1), aldolase A, and aldolase B mRNA in the aorta of 16-week-old lean, obese, and diabetic Zucker rats. $^{*}P<0.05$, $^{**}P<0.01$ *vs*. lean rats and $^{\#}P< 0.05$, $^{\#\#}P< 0.01$ *vs*. obese rats. $n = 5$ for each group in A-D.

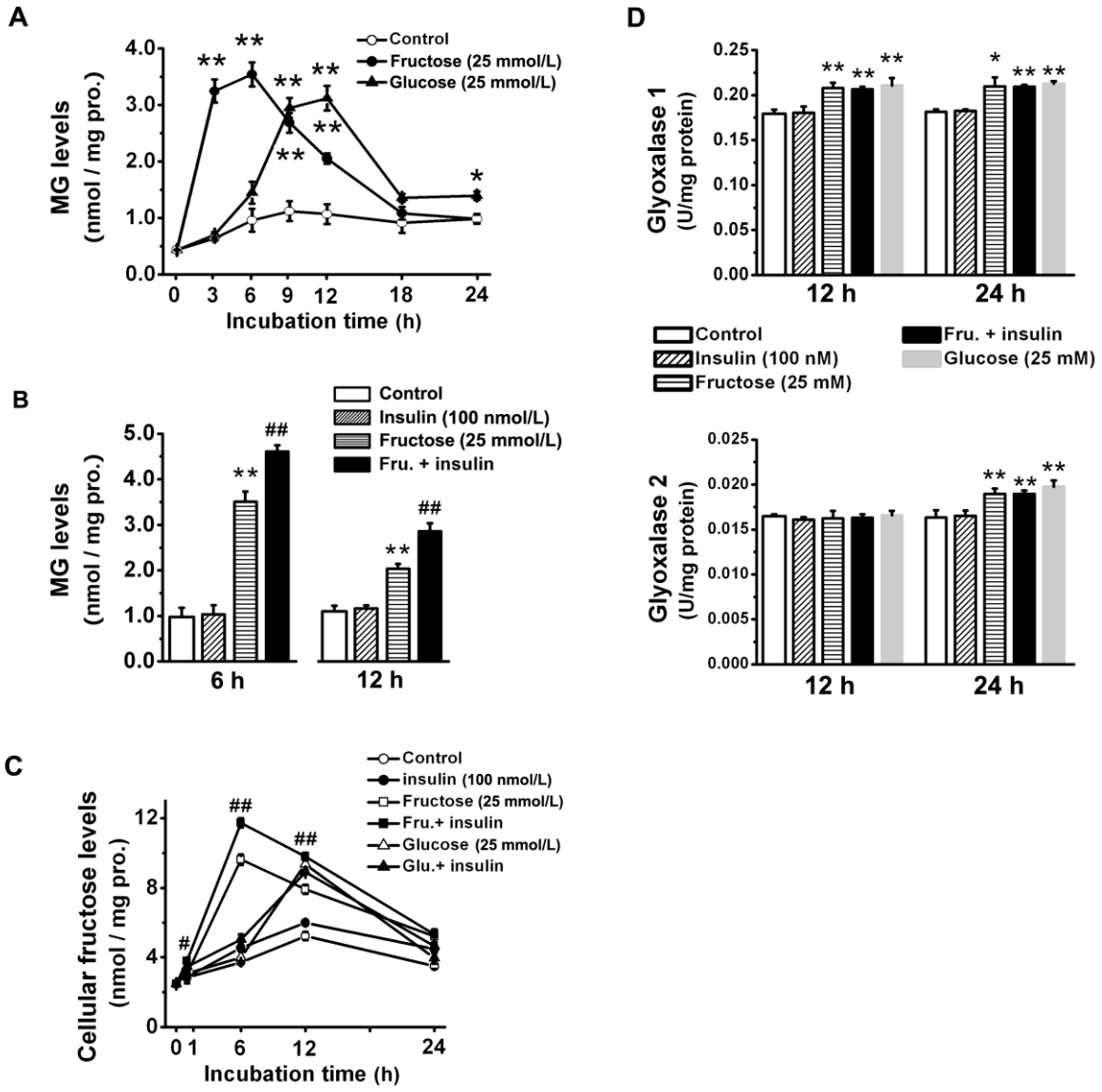

Figure 3-3 MG and fructose formation in A-10 cells. (A) Fructose or glucose (25 mM)-induced MG formation in A-10 cells. (B) MG levels in cells co-treated with fructose and insulin (100 nM) for 6 and 12 h. (C) Time-dependent increases in fructose levels in cells treated with fructose, glucose, and/or insulin. (D) Activity of glyoxalase 1 or glyoxalase 2 in cells after 12- or 24-h treatment. **P*<0.05, ***P*<0.01 *vs*. control (5 mM glucose) and $^{\#}P$< 0.05, $^{\#\#}P$< 0.01 *vs*. without insulin. *n* = 5 for each group in A-C and *n* = 6 for each group in D.

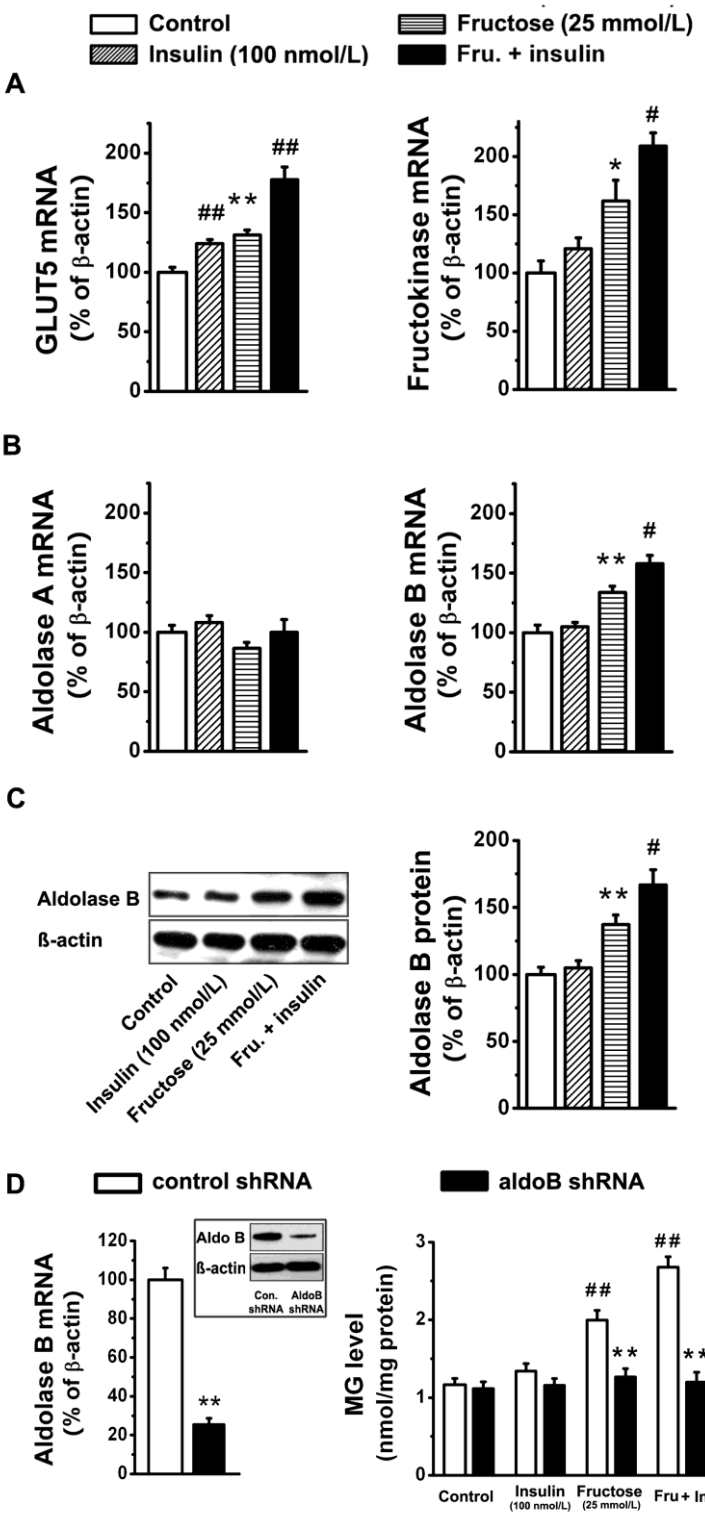

Figure 3-4 Fructose, aldolase B and MG in A-10 cells treated with fructose and/or insulin. mRNA levels of (A) glucose transporter 5 (GLUT5), fructokinase, (B) aldolase A and aldolase B, and (C) protein levels of aldolase B in cells treated with fructose (25 mM) and/or insulin (100 nM) for 12 h, **P*<0.05, ***P*<0.01 *vs*. control (5 mM glucose) and $^{\#}P<0.05$, $^{\#\#}P<0.01$ *vs*. without insulin. (D) Levels of aldolase B mRNA, protein (boxed inset) and MG in cells transfected with control or aldolase B shRNA, $^{**}P<0.01$ *vs*. control shRNA and $^{\#\#}P<0.01$ *vs*. control (5 mM glucose). *n* = 5 for each group in A-D.

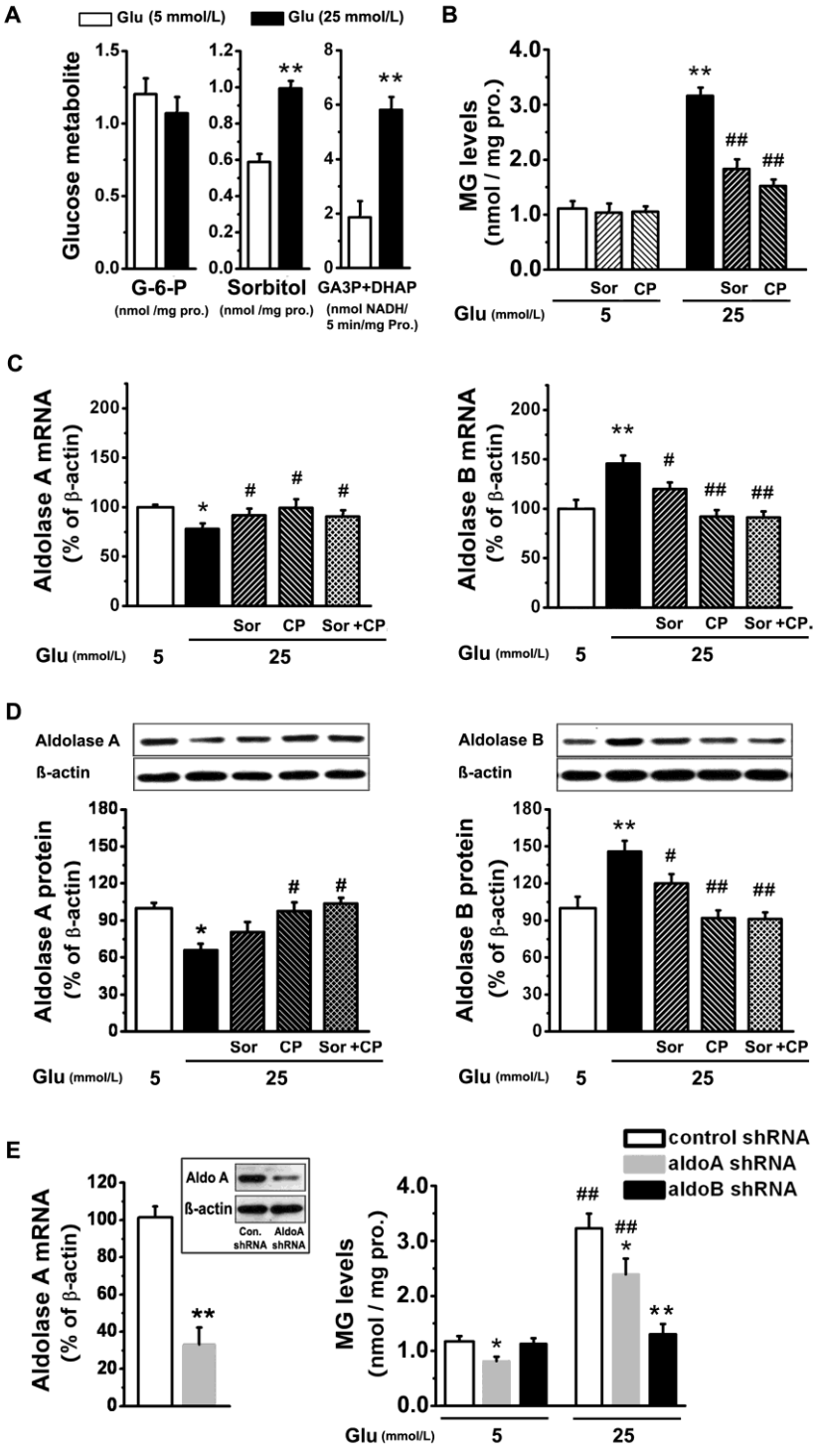

Figure 3-5 Fructose, aldolase B and MG in A-10 cells treated with glucose. (A) levels of glucose 6-phosphate (G-6-P), sorbitol, and GA3P + DHAP in cells treated with glucose for 12 h. (B) Levels of MG, (C) mRNA and (D) protein levels of aldolase A or aldolase B in cells treated with glucose in the presence or absence of sorbinil (Sor, 10 μM) and CP-470711 (CP, 1 μM) for 12 h, $^{*}P<0.05$, $^{**}P<0.01$ *vs*. 5 mM glucose, $^{\#}P<0.05$, $^{\#\#}P<0.01$ *vs*. 25 mM glucose. (E) Levels of aldolase A mRNA, protein (boxed inset) and MG in cells transfected with different shRNA, $^{*}P<0.05$, $^{**}P<0.01$ *vs*. control shRNA and $^{\#\#}P< 0.01$ *vs*. control (5 mM glucose). $n = 5$ for each group in A-E.

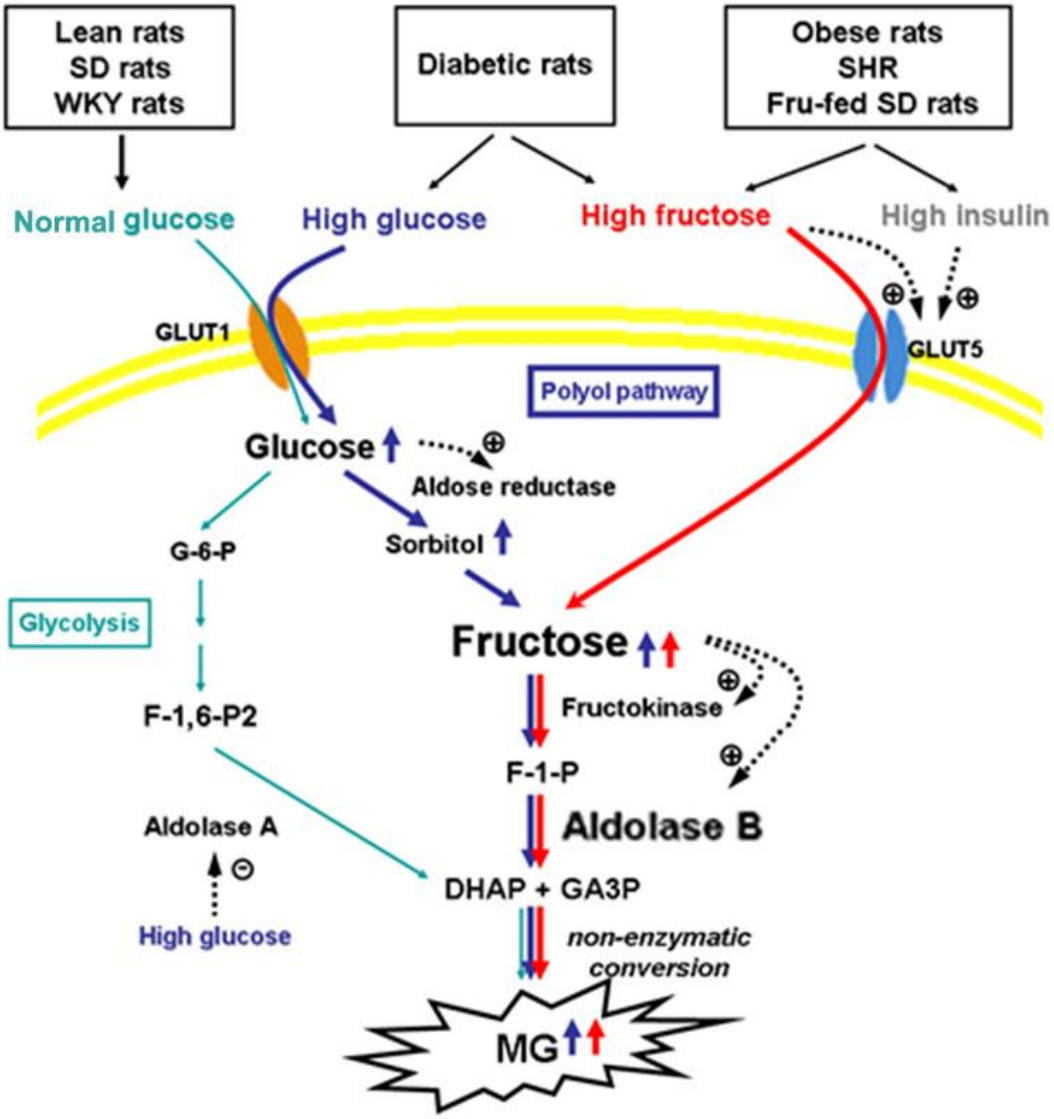

Figure 3-6 Summary of the mechanism for vascular MG overproduction in rat models with metabolic syndrome. Serum and aortic fructose levels are increased in fructose-fed SD, spontaneously hypertensive rats (SHR), and obesity rats, which up-regulate aldolase B expression and enhance MG generation in rat aorta. Hyperinsulinemia in these rats may promote aortic fructose accumulation and MG generation via up-regulating fructose transporter GLUT5. Hyperglycemia in diabetic rats down-regulates aldolase A, but activates polyol pathway and increases fructose generation in the aorta, leading to up-regulation of aldolase B and overproduction of MG. Moreover, serum fructose and aortic GLUT5 mRNA levels are increased in diabetic rats, indicating an important contribution of the elevated serum fructose to the MG overproduction.

Abbreviations: DHAP – dihydroxyacetone phosphate; F-1-P – fructose 1-phosphate; F-1,6-P_2 – fructose 1,6-bisphosphate; G-6-P – glucose 6-phosphate; GA3P – glyceraldehyde 3-phosphate; GLUT1, GLUT5 – glucose transporter 1 and 5, respectively; MG – methylglyoxal; SD – Sprague Dawley; WKY – Wistar-Kyoto.

3.7 Supplementary materials

Table 3-S1. mRNA levels of fructokinase in the aorta of rat models.

Rat models	Age (wks)	n	Fructokinase mRNA (%)
Un-treated SD	20	4	100 ±16
Fru.-treated SD	20	4	191 ±23 *
WKY	20	4	100 ±16
SHR	20	4	208 ±12 **

*P<0.05, **P<0.01 *vs*. Un-treated SD or WKY rats.

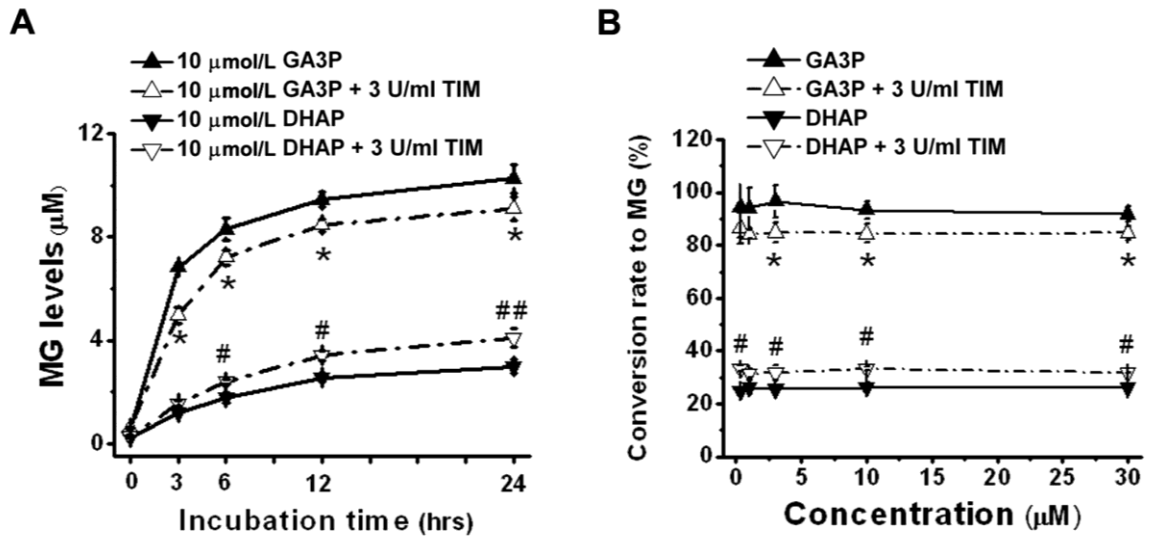

Figure 3-S1 Spontaneous MG production from GA3P or DHAP dissolved in PBS buffer, in the presence or absence of 3 U/mL triose phosphate isomerase (TIM), at 37℃ in the Eppendorf tubes, $^{*}P<0.05$, $^{**}P<0.01$ *vs*. GA3P alone and $^{\#}P< 0.05$, $^{\#\#}P< 0.01$ *vs*. DHAP alone. $n = 5$ for each group in A and B. Triose phosphate isomerase, an enzyme catalyzing the inter-conversion of GA3P and DHAP, was observed to change the conversion rate of each triose phosphate to MG but not to increase the total formation of MG.

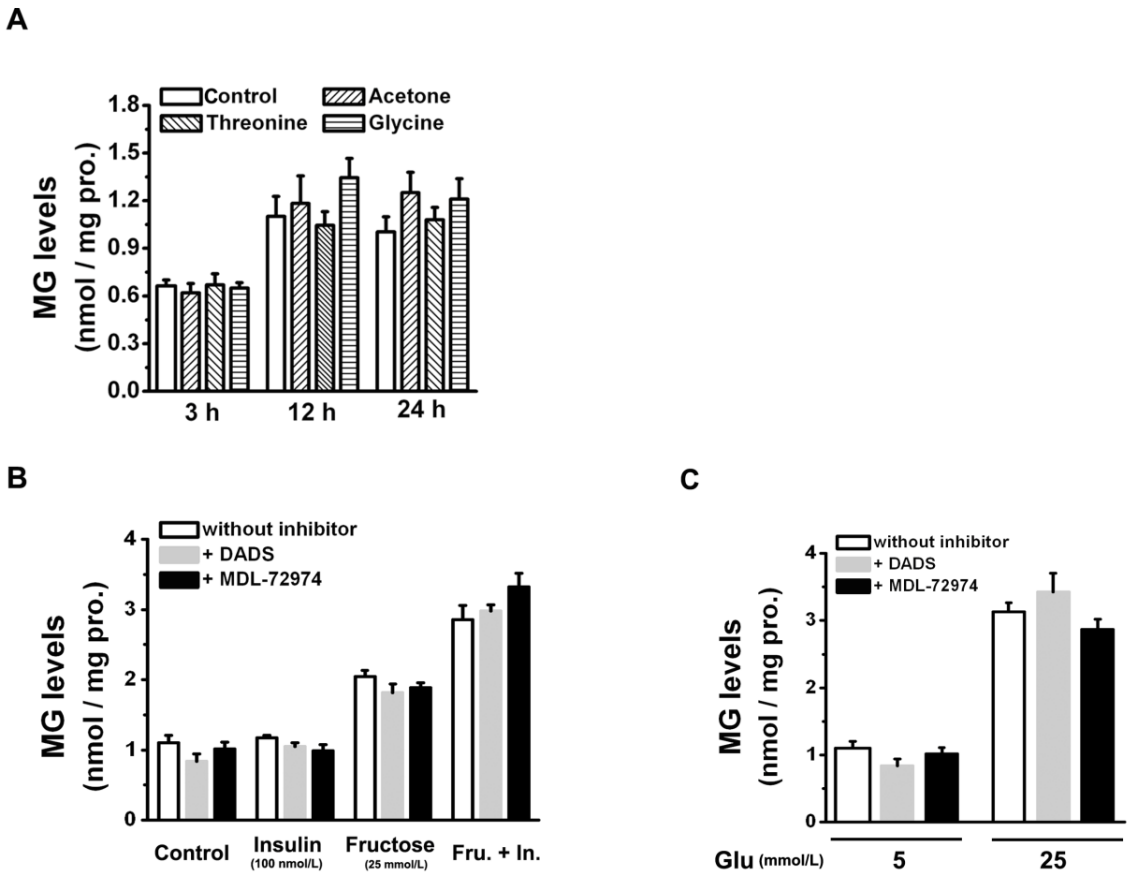

Figure 3-S2 Cytochrome P450 2E1 (CYP 2E1), semicarbazide-sensitive amine oxidase (SSAO) and MG in A-10 cells. (A) MG levels in A-10 cells treated with 25 mM acetone, glycine, or threonine (glycine and threonine are precursors of aminoacetone) for different times. (B, C) MG levels in A-10 cells cultured in different treatments for 12 h in the presence or absence of diallyl disulfide (DADS, 100 μM, a CYP 2E1 inhibitor) or (E)-2-(4-fluorophenethyl)-3-fluoroallylamine (MDL-72974, 5 μM, a SSAO inhibitor) (n = 5 for each group in A-C).

CHAPTER 4

ALDOLASE B KNOCKDOWN PREVENTED HIGH GLUCOSE-INDUCED METHYLGLYOXAL OVERPRODUCTION AND CELLULAR DYSFUNCTION IN ENDOTHELIAL CELLS

Jianghai Liu[1], Timothy Chun-Ping Mak[1], Ali Banigesh[1], Kaushik Desai[1], Rui Wang[2] and Lingyun Wu[1,3]

[1] Department of Pharmacology, College of Medicine, University of Saskatchewan, Saskatchewan; [2] Department of Biology and [3] Department of Health Sciences, Lakehead University and Thunder Bay Regional Research Institute, Canada

This chapter has been accepted by *PLOS one*

4.1 Abstract

We used the cultured endothelial EA. hy926 cell as a model to examine whether up-regulation of aldolase B and enhanced MG formation play an important role in high glucose-induced overproduction of advanced glycation endproducts (AGEs), oxidative stress and cellular dysfunction. High glucose (25 mM) incubation of EA. hy926 cells increased mRNA levels of aldose reductase (an enzyme converting glucose to fructose) and aldolase B (a key enzyme that catalyzes MG formation from fructose) and enhanced MG formation. High glucose-induced cellular MG overproduction was completely prevented by siRNA knockdown of aldolase B, but unaffected by siRNA knockdown of aldolase A, an enzyme responsible for MG formation during glycolysis, and by inhibition of cytochrome P450 2E1 and semicarbazide-sensitive amine oxidase, accounting for MG formation from metabolism of lipid and proteins, respectively. Both high glucose (25 mM) and MG (30, 100 μM) increased the formation of N(ε)-carboxyethyl-lysine (CEL, a MG-induced AGE), oxidative stress (determined by the generation of oxidized DCF, H_2O_2, protein carbonyls and 8-oxo-dG), *O*-GlcNAc modification (product of hexosamine pathway), membrane protein kinase C activity and nuclear translocation of NF-κB in EA. hy926 cells. However, the above metabolic and signaling alterations induced by high glucose were completely prevented by knockdown of aldolase B and partially by application of aminoguanidine (a MG scavenger) or alagebrium (an AGEs breaker). In conclusion, efficient inhibition of aldolase B can prevent high glucose-induced overproduction of MG and related cellular dysfunction in endothelial cells.

Key words: Aldolase B, Methylglyoxal, Glucose, Endothelial cell

4.2 Introduction

Hyperglycemia damages blood vessels and induces diabetic vascular complications in the retinal, renal, and cardiovascular tissues (*106, 269*). Vascular endothelial cell is the early and primary target of hyperglycemic damage in diabetes (*270, 271*). It has been reported that hyperglycemia increased endothelial permeability and inflammation, decreased nitric oxide (NO) bioavailability and endothelium-dependent relaxation, and vascular remodeling, thus hyperglycemia-triggered endothelial dysfunction is considered a key event in the pathogenesis of vascular complications of diabetes (*136*).

Methylglyoxal (MG) is a highly reactive metabolite of glucose (*146, 272*). Increased MG levels were observed in vascular endothelial cells cultured in high glucose-containing media and in the aorta, kidney and retina of diabetic rats (*36, 70, 87*). Accumulating evidence indicates that high glucose-increased MG production is an important molecular mechanism linking diabetes to endothelial damage. MG modifies lysine, arginine, and cysteine residues in peptides or proteins to yield irreversible advanced glycation end products (AGEs), leading to cross-linking and denaturation of proteins (*37, 38, 132*). MG also increases the generation of reactive oxygen species (ROS) and oxidative stress in endothelial cells (*70*). Studies on cultured vascular smooth muscle cells (VSMCs) showed that MG treatment induced the activation of NF-κB (*56*). Moreover, indirect evidence implicates MG in the high glucose-activated protein kinase C (PKC) and hexosamine pathway. For example, incubation with alagebrium, an AGEs breaker, reduced PKC activation in high glucose-treated VSMCs (*123*). Activation of hexosamine pathway by hyperglycemia leads to O-linked N-acetyl glucosamine (*O*-GlcNAc) modification of various proteins on serine or threonine residues

which impairs the normal functions of proteins (*106*). Overexpression of glyoxalase-1, an enzyme metabolizing MG, reduced high glucose-increased *O*-GlcNAc modification in endothelial cells (*111*). These data suggest that inhibition of MG production could be a strategy to prevent endothelial damage in diabetic vascular complications.

Several MG scavengers have been developed, but most of them, such as aminoguanidine, metformin and N-acetyl cysteine, are non-specific to MG and their utilization for scavenging MG and preventing diabetic damage are limited (*205*). We recently identified aldolase B, which converts glucose or fructose to MG, but not aldolase A, cytochrome P450 2E1 (CYP 2E1), and semicarbazide-sensitive amine oxidase (SSAO), as a primary enzyme responsible for MG overproduction in high glucose-treated VSMCs and in the aorta of diabetic rats (*272*). In this paper, the gene expression of aldolase B and its role in MG formation in high glucose-treated endothelial cells were evaluated and whether knockdown of aldolase B in endothelial cells prevented high glucose-induced MG overproduction and other metabolic and signaling abnormities was investigated.

4.3 Methods

4.3.1 Cell culture and treatment

EA. hy926 cells, a endothelial cell line derived from the fusion of human umbilical vein endothelial cells with A549 lung carcinoma cells (a gift kindly provided by Dr. Cora-Jean Edgell, University of North Carolina at Chapel Hill), were cultured in Dulbecco's modified Eagle medium (DMEM) supplemented with 10% fetal bovine serum (FBS). EA. hy926 cells were starved in DMEM containing 0.5% FBS for 24 h and then treated with

glucose (25 mM) or MG (30 or 100 μM) in DMEM containing 10% FBS for 3 days. Medium was not changed during the treatment. The control cells were EA. hy926 cells that were cultured in FBS (10%) - DMEM (5 mM glucose) without adding 25 mM glucose, MG or other agents into the medium.

4.3.2 Small interfering RNA (siRNA)

Knockdown of aldolase A or aldolase B was established by 24-h transfection of cells with a siRNA pool (a mixture of 3 or 4 different siRNA duplexes) targeting aldolase A or B (Santa Cruz Biotechnology Inc., Santa Cruz, CA, USA) in DharmaFECT™ 4 Transfection Reagent (Thermo Fisher, Nepean, ON, Canada). Briefly, transfection complexes were formed by incubating 100 μL siRNA pool (10 μM) with 25 μL of DharmaFECT 4 in 1 mL of serum-free DMEM for 20 min at room temperature. Transfection complexes were mixed with 4 mL of serum-free DMEM and added to the medium. After 6 h of incubation, 5 mL DMEM supplemented with 20% FBS was added for a final siRNA concentration at 100 nM. After another 18 h, the transfection medium was replaced by 10% FBS DMEM with or without MG or high glucose and incubated for 3 days. Aldolase B mRNA was determined by a real-time PCR assay using SYBR Green PCR Master Mix (Bio-Rad) with the primers for human aldolase B (forward 5'-AGCCTCGCTATCCAGGAAAACG-3', reverse 5'-TGGCAGTGTTC CAGGTCATGGT-3') and β-actin (forward 5'-ACTTAGTTGCGTTACACCCTT-3', reverse 5'-GTCACCTTCACCGTTCCA-3'). Primers for human aldolase A and aldose reductase were purchased from Qiagen (Mississauga, ON, Canada).

4.3.3 MG Measurement

MG levels were determined using our recently modified method (*251*). Briefly, cells were sonicated three times for 5 seconds each time and centrifuged at 12,000 rpm (10 min, 4℃). The supernatant of 180 μL was incubated with 180 μL of perchloric acid (PCA, 1 N) and 40 μL of *o*-phenylenediamine (*o*-PD, 100 mM) for 24 h at room temperature in the dark. The mixture was centrifuged at 12,000 rpm (10 min, 4°C). The supernatant of 180 μL was mixed with 20 μL of 5-methylquinoxaline (5-MQ, internal standard) and analyzed by high-performance liquid chromatography (HPLC) with a mobile phase buffer containing 17% acetonitrile, 8% 50 mM NaH_2PO_4 (pH 4.5), and 75% water.

4.3.4 Confocal imaging of AGEs

N(ε)-carboxyethyl-lysine (CEL) is a MG specific AGE formed by the reaction between MG and lysine residues in proteins (*273*). CEL formation in EA. hy926 cells was visualized by confocal microscopy after immunofluorescent staining. Cells were cultured on glass coverslips, fixed and permeabilized with pre-chilled methanol (20 min, -20℃), blocked with goat serum in phosphate-buffered saline (PBS) (1:30, 30 min), and then, incubated with mouse monoclonal CEL antibody (Cosmo Bio USA, Inc., Carlsbad, CA, USA, diluted 1:250 in blocking solution, 3 h at room temperature or overnight at 4℃). Subsequently, the processed cell preparations were washed with PBS, and incubated with Alexa 488-conjugated secondary antibodies (Invitrogen, Burlington, ON, Canada, diluted 1:300 in blocking solution, 2 h at room temperature). Finally, the prepared cells were washed again and mounted in mounting media with propidium iodide (Invitrogen, Burlington, ON, Canada). Thereafter, the

slides were examined under a confocal microscope with the appropriate filters. The fluorescence intensity was determined using Image J by analyzing at least 50 random cells per sample.

4.3.5 Measurement of oxidative stress

After different treatments, cells were washed with PBS, and then stained with a non-specific ROS probe (DCF-DA, Invitrogen, Burlington, ON, Canada) or a specific fluorogenic H_2O_2 probe (Calbiochem, San Diego, CA, USA). The fluorescence intensities of these probes were analyzed with a Fluoroskan Ascent plate reader (Thermo LabSystem, Franklin, MA, USA) as previously described (*55, 254*). Protein oxidation was assessed by measuring total protein carbonyls with an immunoblot kit (Cell Biolabs Inc., San Diego, CA, USA). DNA oxidation biomarker 8-oxo-dG was visualized by immunofluorescent staining and photographed under fluorescence microscopy, using a specific mouse monoclonal 8-oxo-dG antibody (Trevigen, Gaithersburg, MD, USA), following the manufacturer's instructions.

4.3.6 Western blot analysis

Cells were harvested and lysed in RIPA buffer (Santa Cruz Biotechnology Inc., Santa Cruz, CA, USA) supplemented with protease inhibitors. Total cellular proteins were fractionated by 10% SDS-PAGE and immunoblotted with antibodies as follows: *O*-GlcNAc (RL2) (1:1000, Thermo Fisher, Nepean, ON, Canada), and α-tubulin (1:500, Santa Cruz Biotechnology Inc., Santa Cruz, CA, USA). Nuclear proteins were extracted as previously

described (*255*) and level of nuclear NF-κB was measured with antibodies against NF-κB (p65) (1:500) and lamin B (1:1000) purchased from Santa Cruz Biotechnology Inc., Santa Cruz, CA, USA.

4.3.7 Membrane PKC activity

Cells cultured on 100-mm dish were washed, scrapped off, suspended in 1 mL of Tris-sucrose buffer (20 mM Tris-base, 2 mM EDTA, 0.5 mM EGTA and 0.3 M sucrose, pH 7.4), and then added with protease inhibitors and homogenized by being passed 15 times through a 27.5 gauge needle. After centrifugation at 2,500 g (10 min, 4℃) to remove nuclei and cell debris, cell membrane was fractionated by high speed ultra-centrifugation at 105,000 g (30 min, 4℃). Membrane pellets were washed with Tris buffer (20 mM Tris-base, 2 mM EDTA and 0.5 mM EGTA, pH 7.4), ultra-centrifuged (105,000 g, 30 min, 4℃) and re-suspended in 0.3 mL of Tris buffer with 0.5% Triton X-100 on ice for 1 h. The supernatant after ultra-centrifugation (105,000 g, 30 min, 4℃) was collected and membrane PKC proteins were purified through a DEAE cellulose (DE-52) column previously equilibrated with the Tris buffer. After washing the column with 3 mL of Tris buffer, the bound PKC was eluted with 0.5 ml Tris buffer containing 0.2 M NaCl. Membrane PKC activity was assessed by a PKC activity assay kit according to the manufacturer's instructions (Assay Designs, Ann Arbor, MI, USA).

4.3.8 Materials

(E)-2-(4-fluorophenethyl)-3-fluoroallylamine (MDL-72974) was a generous gift from

Dr. Peter Yu (Department of Pharmacology, University of Saskatchewan, Canada). Alagebrium was a generous gift from Synvista Therapeutics (Montvale, NJ). Diallyl disulfide (DADS) and aminoguanidine were purchased from Sigma-Aldrich, Oakville, ON, Canada

4.3.9 Statistics

Data are expressed as mean ± SEM from at least five independent experiments ($n \geqslant 5$ in each group). Statistical analyses were performed using parametric Student's t-test (two-tailed) or one-way ANOVA followed by posthoc Tukey's test.

4.4 Results

4.4.1 Knockdown of aldolase B prevented high glucose-increased MG formation

High glucose (25 mM) treatment up-regulated aldose reductase and aldolase B mRNA expression and accelerated MG formation in endothelial EA. hy926 cells (Figure 4-1A). Cellular MG overproduction induced by high glucose was partially reduced by aminoguanidine, and not reduced by alagebrium (Figure 4-1B). Transfection with aldolase B siRNA reduced cellular mRNA levels of aldolase B by 74%, and completely prevented high glucose-elevated formation of MG in endothelial cells (Figures 4-1C, 4-1D). Aldolase A, cytochrome P450 2E1 (CYP 2E1) and semicarbazide-sensitive amine oxidase (SSAO) are responsible for MG generation in glycolysis and in the metabolism of fatty acids and proteins, respectively (*272*). However, high glucose-increased cellular MG production was not affected by application of DADS (an inhibitor of CYP 2E1) or MDL-72974 (an inhibitor of SSAO), or by transfection with aldolase A siRNA which reduced cellular mRNA levels of aldolase A by

70% (Figures 4-1E, 4-1F and 4-1G).

4.4.2 Knockdown of aldolase B prevented high glucose-increased AGEs formation

Since incubation of EA. hy926 cells with MG (100 μM) or glucose (25 mM) induced a similar increase in cellular MG levels (Figure 4-2A), the direct effects of MG (30 or 100 μM) on endothelial cells were investigated. MG (30 or 100 μM) elevated CEL levels in EA. hy926 cells (Figure 4-2B). Glucose (25 mM) treatment increased cellular CEL levels, which was similar with that induced by MG (100 μM) (Figures 4-2B, 4-3C). High glucose-induced CEL overproduction in endothelial cells was partially reduced by aminoguanidine, but was completely reversed or prevented by alagebrium or knockdown of aldolase B (Figures 4-2C, 4-2D).

4.4.3 Knockdown of aldolase B prevented high glucose-induced ROS

High glucose-increased production of ROS is regarded as an important contributor to endothelial dysfunction in diabetic vascular complications (*274*). MG (30 or 100 μM,) elevated levels of oxidized DCF (an indicator of total cellular ROS) in EA. hy926 cells (Figure 4-3A). The increase in oxidized DCF levels induced by MG (100 μM) was similar with that induced by glucose (25 mM) (Figures 4-3A, 4-3B). High glucose-increased cellular formation of oxidized DCF was totally abolished by aminoguanidine or by transfection with aldolase B siRNA, and partially reduced by alagebrium (Figures 4-3B, 4-3C). Cellular levels of H_2O_2 were similarly elevated by MG (100 μM) and glucose (25 mM) (Figures 4-4A, 4-4B). Application of aminoguanidine or alagebrium, or transfection of aldolase B siRNA prevented

the formation of H_2O_2 in high glucose-treated endothelial cells (Figures 4-4B, 4-4C).

4.4.4 Knockdown of aldolase B prevented high glucose-induced protein and DNA oxidation

MG (100 μM) and glucose (25 mM) induced similar increases in levels of protein carbonyls (a marker of protein oxidation) in EA. hy926 cells (Figures 4-5A, 4-5B). Application of aminoguanidine or transfection of aldolase B siRNA totally abolished high glucose-increased levels of protein carbonyls (Figures 4-5B, 4-5C). Application of alagebrium partially reduced the formation of protein carbonyls in high glucose-treated cells (Figures 4-5B, 4-5C).

MG (30 or 100 μM, 3 days) elevated levels of 8-oxo-dG (a marker of DNA oxidation) in EA. hy926 cells (Figures 4-6A). The increase of 8-oxo-dG levels induced by MG (100 μM) was similar to that induced by glucose (25 mM) (Figures 4-6A, 4-6B). High glucose-increased 8-oxo-dG levels were prevented by aminoguanidine or by transfection with aldolase B siRNA, and partially reduced by alagebrium (Figures 4-6B, 4-6C).

4.4.5 Knockdown of aldolase B blocked high glucose-activated metabolic or signalling pathways

Activation of hexosamine pathway by high glucose causes an elevated *O*-GlcNAc modification of nuclear and cytosolic proteins (*106*). MG (30 or 100 μM) increased *O*-GlcNAc modification of proteins in EA. hy926 cells (Figure 4-7A). Glucose (25 mM)-elevated *O*-GlcNAc modification was similar to that induced by MG (100 μM), and

totally abolished by alagebrium or by transfection with aldolase B siRNA but only partially reversed by aminoguanidine (Figures 4-7B, 4-7C).

Activation of PKC leads to its translocation to the plasma membrane where it catalyzes the phosphorylation of various substrates and mediates a diverse variety of biological processes (*114*). MG (30 or 100 μM) elevated plasma membrane PKC activities in EA. hy926 cells (Figure 4-8A). High glucose (25 mM) incubation induced a similar elevation in the plasma membrane PKC activities as did 100 μM MG (Figures 4-8A, 4-8B). High glucose-elevated plasma membrane PKC activity was prevented by alagebrium or by knockdown of aldolase B, but only partially by aminoguanidine (Figures 4-8B, 4-8C).

Activated NF-κB (p50/p65 dimer) is translocated into the nucleus and regulates the expression of a large number of genes involved in immune and inflammatory responses, apoptosis, cell proliferation and differentiation (*125*). It was reported that MG or glucose triggered the nuclear translocation of NF-κB but unchanged its total protein levels in cells (*56, 275, 276*). Consistently, we found that MG (100 μM) and high glucose (25 mM) similarly increased nuclear p65 subunit of NF-κB in EA. hy926 cells (Figure 4-9A). High glucose-elevated nuclear amount of NF-κB p65 was blocked by alagebrium, aminoguanidine, and aldolase B knockdown (Figures 4-9B, 4-9C).

4.5 Discussion

Our present work demonstrated that siRNA knockdown of aldolase B blocked high glucose-activated metabolic and signaling pathways by the normalization of MG production in endothelial cells. This revelation was substantiated by the following observations: 1)

Treatment of EA. hy926 cells with MG (100 μM) and high glucose (25 mM) induced a similar increase in cellular MG levels and a similar activation of the major pathways involved in hyperglycemic damage; 2) Aldolase B is the major enzyme for high glucose-increased MG production in endothelial cells because aldolase B knockdown completely inhibited MG overproduction in high glucose-treated EA. hy926 cells; 3) Both knockdown of aldolase B and the application of aminoguanidine or alagebrium prevented high glucose-activated metabolic and signaling pathways in EA. hy926 cells.

Enhanced accumulation of MG is postulated to be one of the important molecular mechanisms leading to endothelial dysfunction and diabetic vascular complications (*70, 106, 136*). Our lab previously reported that incubation with MG (30 or 100 μM) and glucose (25 mM) similarly decreased NO synthase activity and NO production in cultured endothelial cells and reduced endothelium-dependent muscle relaxation in the rat aorta (*70*). Our present study further validates the role of MG as an upstream activator for hyperglycemia-induced metabolic and signaling changes. MG is the major precursor of AGEs in endothelial cells (*36*). MG treatment elevated AGEs (as estimated by intracellular CEL) levels in EA. hy926 cells (Figure 4-2). AGEs alter protein structures and functions. For example, MG-modified extracellular matrix molecules impaired matrix-matrix interactions and increased the stiffness of the vasculature (*42*). In addition, AGEs can activate their specific receptors on endothelial cells and cause cellular perturbation, such as increased permeability, oxidative stress, activation of NF-κB and vascular inflammation (*42*, *49*). MG is also a pro-oxidant (*54*, *55*). A possible reason is a MG-induced decrease in mitochondrial complex III and SOD activities (*66*). Here we found MG enhanced the formation of ROS and oxidation of protein and DNA

in EA. hy926 cells (Figures 4-3, 4-4, 4-5, and 4-6). Moreover, we provide the first evidence that treatment with MG can directly stimulate *O*-GlcNAc modification and plasma membrane PKC activation (Figures 4-7, 4-8). It is well known that abnormal activation of PKC by high glucose decreased NO production and increased vasoconstrictor endothelin-1 (ET-1) and ROS production in endothelial cells (*106*). Increased *O*-GlcNAc modification of proteins appears to be important in the pathogenesis of endothelial dysfunction. For example, high glucose-increased *O*-GlcNAc modification of endothelial NO synthase decreased its activity in endothelial cells (*108*). We also found that MG directly activated NF-κB by stimulating its nuclear translocation in endothelial cells (Figure 4-9). High glucose-activated NF-κB *via* AGEs, ROS or PKC increased expression of genes contributing to endothelial dysfunction, such as ET-1, adhesion molecules and inflammatory cytokines (*42, 97, 124*) .

Aldolase B is a major enzyme responsible for high glucose-induced MG overproduction in VSMCs and the aorta (*272*). GA3P and DHAP, which are produced by aldolase A or aldolase B during glucose metabolism, are considered major sources for endogenous MG formation and showed high efficiencies of non-enzymatic conversion to MG (*5, 6, 272*). Secondary sources of MG include the oxidation of aminoacetone by SSAO and the oxidation of acetone by CYP 2E1 (*59*). We have recently reported that aldolase B, but not aldolase A, SSAO or CYP 2E1, was up-regulated and MG was over-produced in the aorta of diabetic rats; knockdown of aldolase B prevented high glucose-elevated MG formation in VSMCs (*272*). In the present work, we observed that high glucose up-regulated aldolase B expression and increased MG formation in endothelial cells. siRNA knockdown of aldolase B completely inhibited the excess MG generation in glucose-treated endothelial cells (Figure

4-1). However, siRNA knockdown of aldolase A or inhibition of SSAO or CYP 2E1 had no effect on glucose-increased cellular MG overproduction (Figure 4-1). These data indicate that aldolase B is predominantly responsible for glucose-increased MG formation in endothelial cells and the inhibition of MG formation is solely responsible for the observed effects of aldolase B knockdown on high glucose-activated metabolic and signaling pathways.

Aminoguanidine and alagebrium are the most widely used MG scavenger and AGEs breaker, respectively (*205*). The inhibitory effects of aminoguanidine or alagebrium on high glucose-induced endothelial abnormalities confirm the role of MG as a mediator of high glucose-activated cellular pathways (Figures 4-2 - 4-9). However, our work also reveals limitations of aminoguanidine or alagebrium in accurately evaluating MG's contribution to endothelial dysfunction and diabetic complications, when compared with the knockdown of aldolase B which specifically prevents glucose-induced MG overproduction. Aminoguanidine is a non-specific MG scavenger. Its guanidine residue can react with the carbonyl in MG or in other carbonyl compounds, such as 3-deoxyglucosone and malondialdehyde (*205*). Moreover, aminoguanidine can react directly with ROS, such as H_2O_2, hydroxyl radical and peroxynitrite (*220*). We found that the application of aminoguanidine completely abolished oxidative stress, but only partially decreased MG and CEL production, *O*-GlcNAc modification and plasma membrane PKC activities in high glucose-treated cells (Figures 4-1 - 4-8). Alagebrium breaks the established AGE crosslinks (*205*). The application of alagebrium completely inhibited the formation of CEL, but it did not change MG levels in high glucose-treated EA. hy926 cells (Figures 4-1, 4-2). In addition to the formation of AGEs, MG also stimulates the formation of ROS (*66*). Our studies showed that alagebrium only

partially reduced the formation of oxidized DCF, protein carbonyls and 8-oxo-dG in high glucose-treated EA. hy926 cells (Figures 4-3, 4-5, and 4-6), although it can react with H_2O_2 in the test tube (*277*), and completely reduced the glucose-increased H_2O_2 formation in our test cells (Figure 4-4).

In conclusion, MG directly mediates high glucose-induced production of AGEs, oxidative stress, and increases in *O*-GlcNAc modification and protein levels or activities of protein kinase C and NF-κB in endothelial cells. More importantly, this study demonstrates that aldolase B is the major enzyme for glucose-increased MG production in endothelial cells. Knockdown of aldolase B prevents MG overproduction and, by doing so, blocks high glucose-induced activation of multiple metabolic and signaling pathways in endothelial cells.

4.6 Acknowledgements

We are grateful to Mrs. Arlene Drimmie (Department of Pharmacology, University of Saskatchewan) for her excellent technical assistance. This work was supported by operating grants from Canadian Institutes of Health Research and the Heart and Stroke Foundation of Saskatchewan to L. Wu. J. Liu was supported by a College of Medicine Graduate Scholarship, University of Saskatchewan.

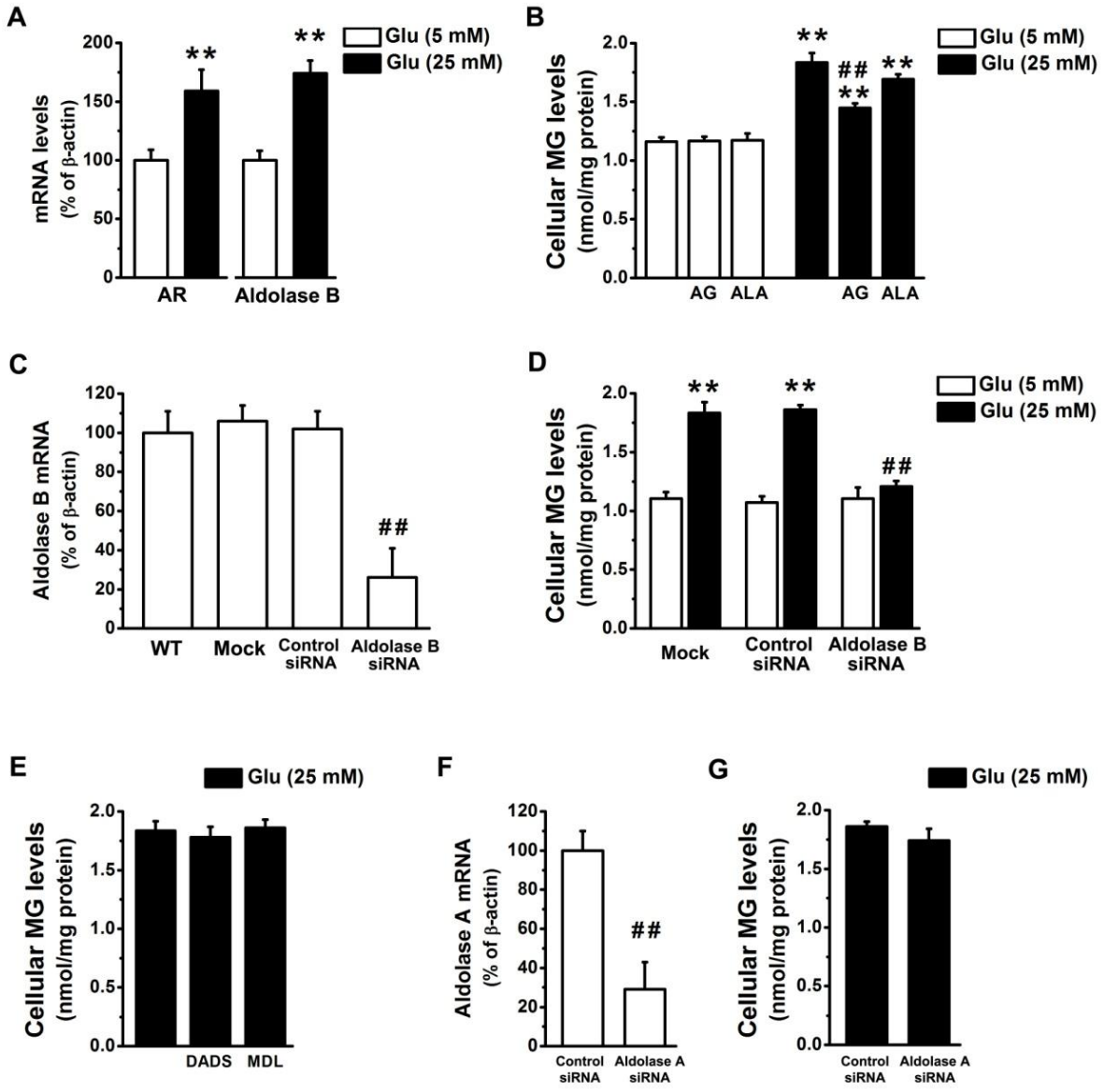

Figure 4-1 Knockdown of aldolase B prevented MG overproduction in high glucose-treated EA. hy926 cells. (A) Real-time PCR analysis of aldose reductase (AR) and aldolase B expression in cells treated with glucose (Glu) for 3 days. $^{**}P<0.01$ *vs*. 5 mM glucose; (B) MG levels in cells treated with glucose in the presence or absence of aminoguanidine (AG, 1 mM) and alagebrium (ALA, 100 μM) for 3 days. $^{**}P<0.01$ *vs*. 5 mM glucose; $^{\#\#}P<0.01$ *vs*. 25 mM glucose. (C) Levels of aldolase B mRNA and (D) levels of MG in wide-type cells (WT) and cells transfected with control or aldolase B siRNA, or only transfection agent (Mock). $^{**}P<0.01$ *vs*. 5 mM glucose; $^{\#\#}P<0.01$ *vs*. control siRNA. (E) MG levels in cells treated with 25 mM glucose in the presence or absence of (E)-2-(4-fluorophenethyl)-3- fluoroallylamine (MDL-72974, 5 μM) or diallyl disulfide (DADS, 100 μM) for 3 days. (F) Levels of aldolase A mRNA and (G) levels of MG in cells transfected with control or aldolase A siRNA. $^{\#\#}P<0.01$ *vs*. control siRNA.

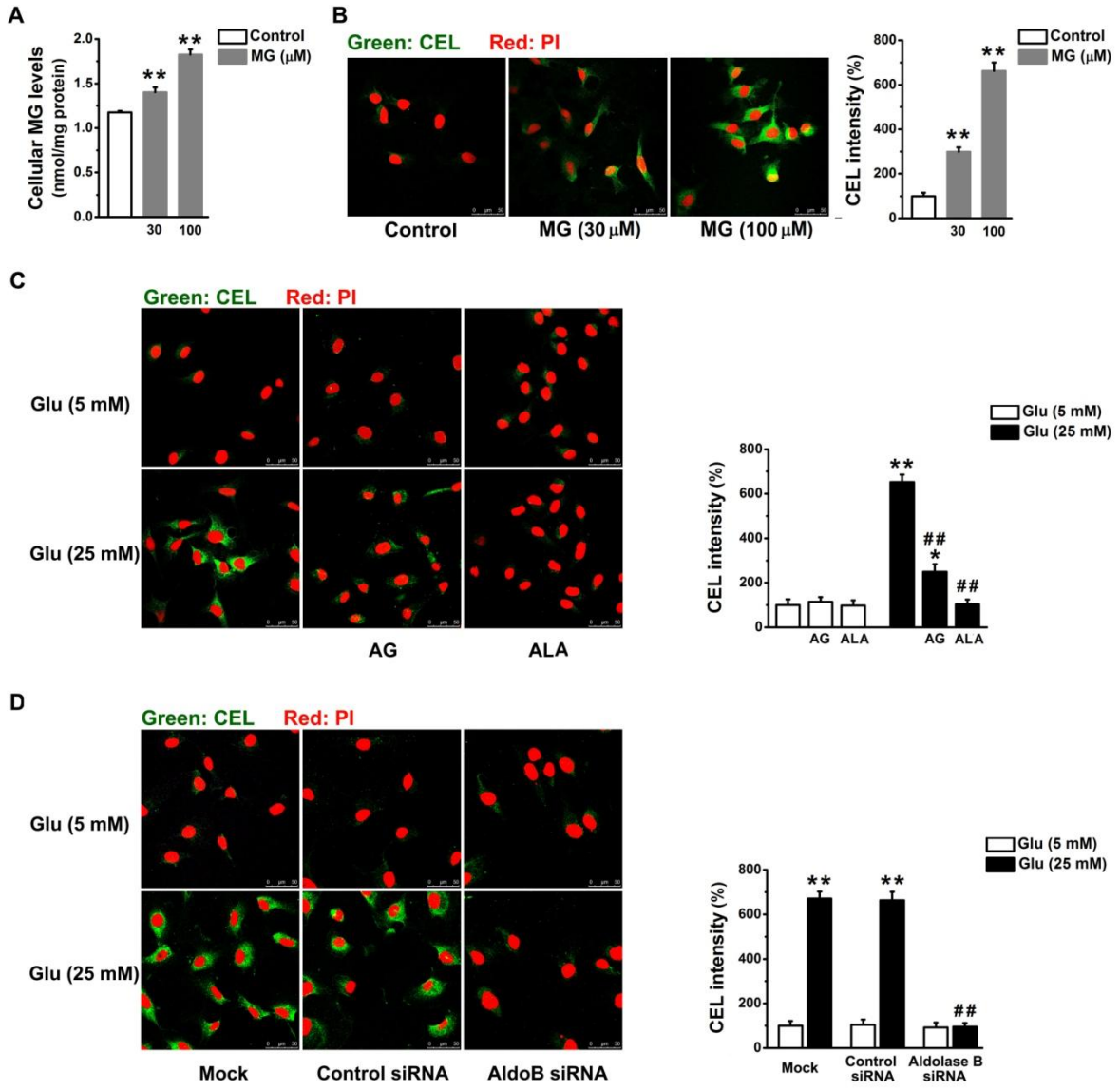

Figure 4-2 Knockdown of aldolase B prevented AGEs overproduction in high glucose-treated EA. hy926 cells. Levels of MG (A) and N(ε)-carboxyethyl-lysine (CEL) in green (B) in cells treated with exogenous MG for 3 days. $^{**}P<0.01$ *vs*. control (5 mM glucose). (C) CEL levels in cells treated with glucose (Glu) in the presence or absence of aminoguanidine (AG, 1 mM) and alagebrium (ALA, 100 μM) for 3 days. $^{**}P<0.01$ *vs*. 5 mM glucose; $^{\#\#}P<0.01$ *vs*. 25 mM glucose. (D) CEL levels in cells transfected with control or aldolase B siRNA, or only transfection agent (mock). $^{**}P<0.01$ *vs*. 5 mM glucose; $^{\#\#}P<0.01$ *vs*. control siRNA. Nuclear DNA (red) was stained with propidium iodide. The summary of fluorescence intensity of CEL was measured using Image J by analyzing at least 50 random cells in each group.

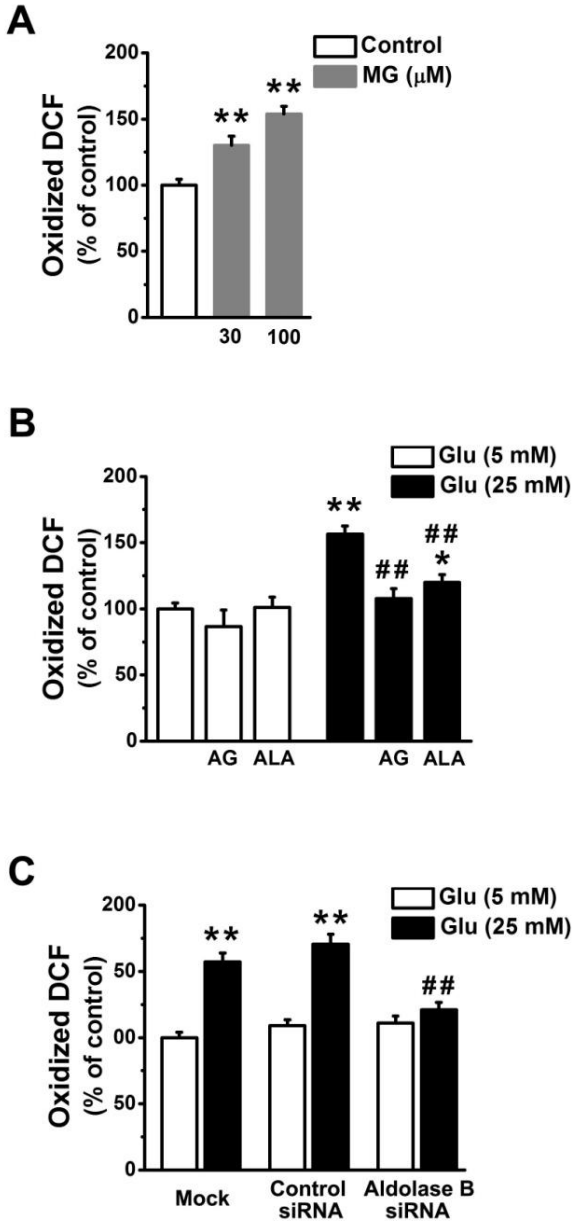

Figure 4-3 Knockdown of aldolase B prevented the increase of oxidized DCF levels in high glucose-treated EA. hy926 cells. (A) Levels of oxidized DCF in cells treated with exogenous MG for 3 days. $^{**}P<0.01$ *vs*. control (5 mM glucose). (B) Levels of oxidized DCF in cells treated with glucose (Glu) in the presence or absence of aminoguanidine (AG, 1 mM) and alagebrium (ALA, 100 μM). $^{*}P<0.05$, $^{**}P<0.01$ *vs*. 5 mM glucose; $^{\#\#}P<0.01$ *vs*. 25 mM glucose. (C) Levels of oxidized DCF in cells transfected with control or aldolase B siRNA, or only transfection agent (mock). $^{**}P<0.01$ *vs*. 5 mM glucose; $^{\#\#}P<0.01$ *vs*. control siRNA.

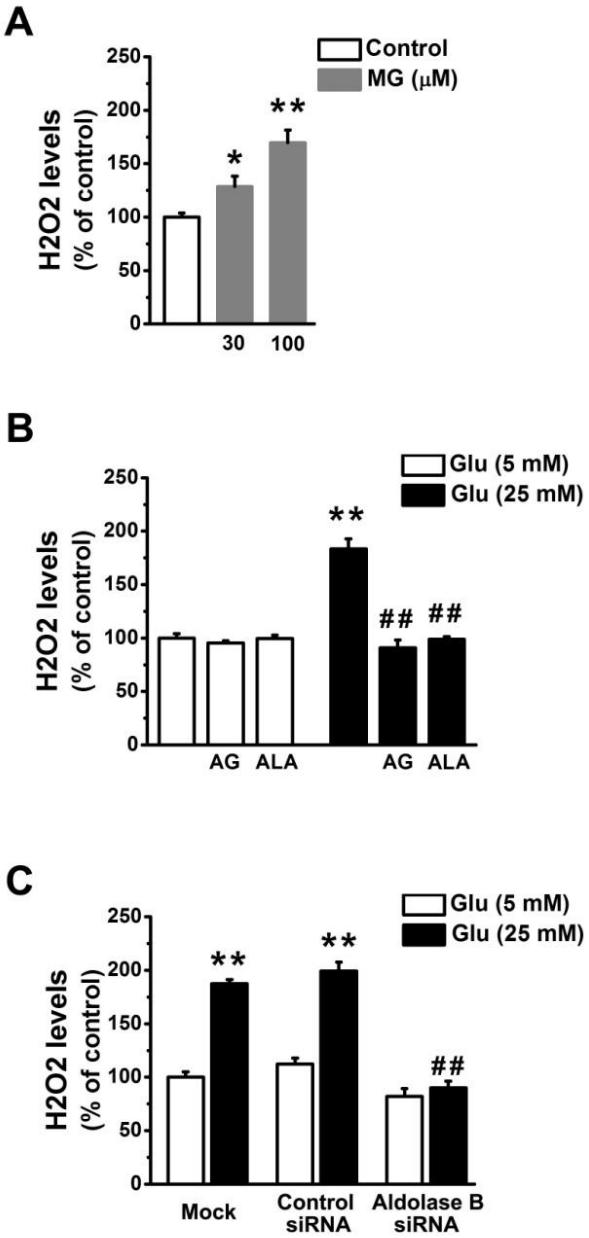

Figure 4-4 Knockdown of aldolase B prevented the generation of H_2O_2 in high glucose-treated EA. hy926 cells. (A) Levels of H_2O_2 in cells treated with exogenous MG for 3 days. $^{**}P<0.01$ *vs*. control (5 mM glucose). (B) Levels of H_2O_2 in cells treated with glucose (Glu) in the presence or absence of aminoguanidine (AG, 1 mM) and alagebrium (ALA, 100 μM). $^{*}P<0.05$, $^{**}P<0.01$ *vs*. 5 mM glucose; $^{\#\#}P<0.01$ *vs*. 25 mM glucose. (C) Levels of H_2O_2 in cells transfected with control or aldolase B siRNA, or only transfection agent (mock). $^{**}P<0.01$ *vs*. 5 mM glucose; $^{\#\#}P<0.01$ *vs*. control siRNA.

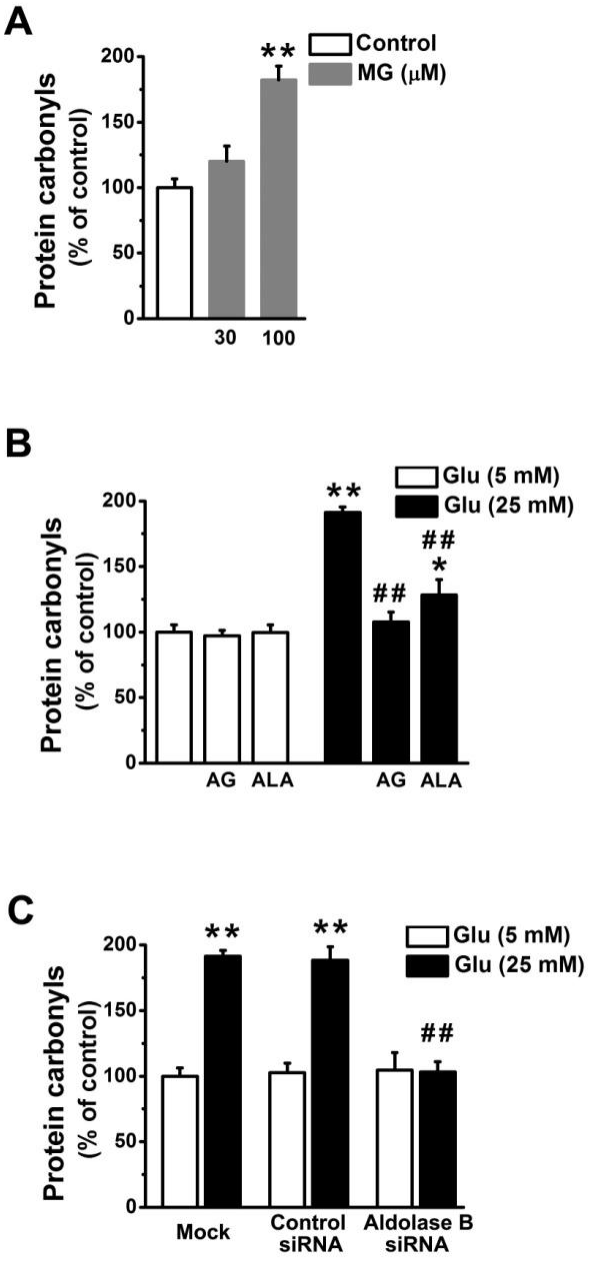

Figure 4-5 Knockdown of aldolase B prevented protein oxidation in high glucose-treated EA. hy926 cells. (A) Levels of protein carbonyls in cells treated with exogenous MG for 3 days. $^{**}P<0.01$ *vs*. control (5 mM glucose). (B) Levels of protein carbonyls in cells treated with glucose (Glu) in the presence or absence of aminoguanidine (AG, 1 mM) and alagebrium (ALA, 100 μM). $^{*}P<0.05$, $^{**}P<0.01$ *vs*. 5 mM glucose; $^{\#\#}P<0.01$ *vs*. 25 mM glucose. (C) Levels of protein carbonyls in cells transfected with control or aldolase B siRNA, or only transfection agent (mock). $^{**}P<0.01$ *vs*. 5 mM glucose; $^{\#\#}P<0.01$ *vs*. control siRNA.

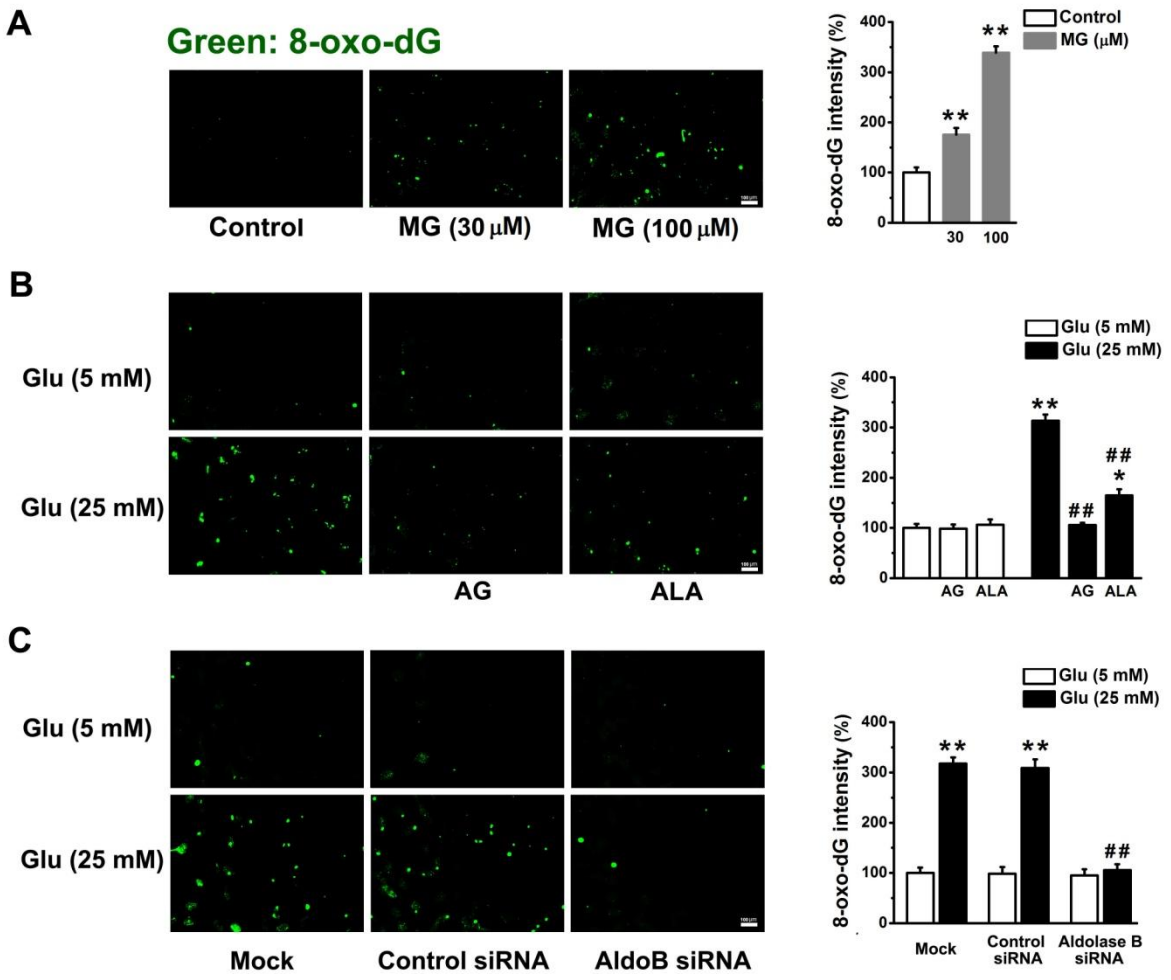

Figure 4-6 Knockdown of aldolase B prevented DNA oxidation in high glucose-treated EA. hy926 cells. (A) Levels of 8-oxo-dG in cells treated with exogenous MG for 3 days. $^{**}P<0.01$ *vs*. control (5 mM glucose). (B) Levels of 8-oxo-dG in cells treated with glucose (Glu) in the presence or absence of aminoguanidine (AG, 1 mM) and alagebrium (ALA, 100 μM). $^{*}P<0.05$, $^{**}P<0.01$ *vs*. 5 mM glucose; $^{\#\#}P<0.01$ *vs*. 25 mM glucose. (C) Levels of 8-oxo-dG in cells transfected with control or aldolase B siRNA, or only transfection agent (mock). $^{**}P<0.01$ *vs*. 5 mM glucose; $^{\#\#}P<0.01$ *vs*. control siRNA. The summary o f fluorescence intensity of 8-oxo-dG was measured using Image J by analyzing at least 50 random cells in each group.

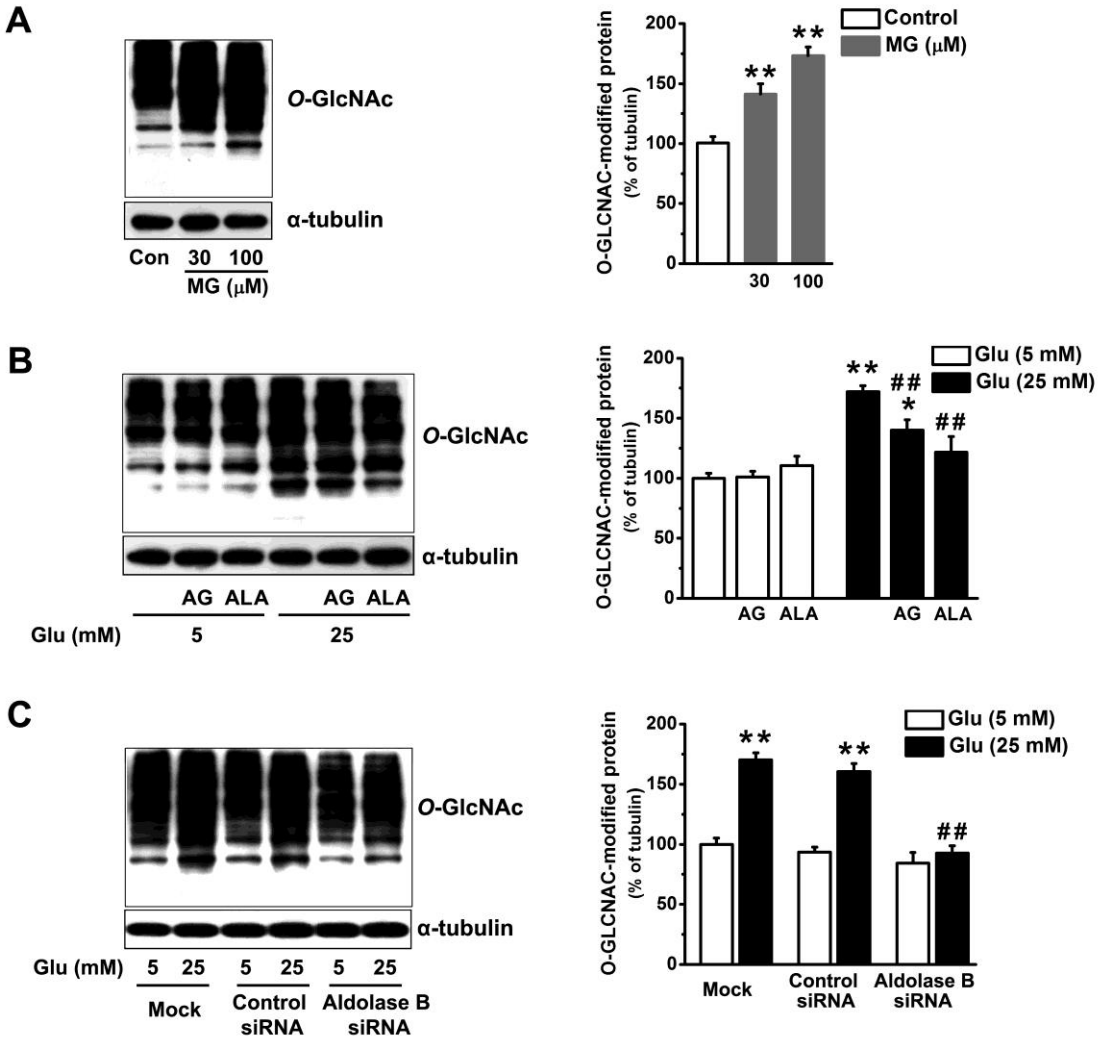

Figure 4-7 Knockdown of aldolase B prevented high glucose-increased *O*-GlcNAc modification in EA. hy926 cells. (A) *O*-GlcNAc modification of total cellular proteins in cells treated with exogenous MG for 3 days. $^{**}P<0.01$ *vs*. control (5 mM glucose). (B) *O*-GlcNAc modification of total cellular proteins in cells treated with glucose (Glu) in the presence or absence of aminoguanidine (AG, 1 mM) and alagebrium (ALA, 100 μM). $^{*}P<0.05$, $^{**}P<0.01$ *vs*. 5 mM glucose; $^{\#\#}P<0.01$ vs. 25 mM glucose. (C) *O*-GlcNAc modification of total cellular proteins in cells transfected with control or aldolase B siRNA, or only transfection agent (mock). $^{**}P<0.01$ *vs*. 5 mM glucose; $^{\#\#}P<0.01$ *vs*. control siRNA.

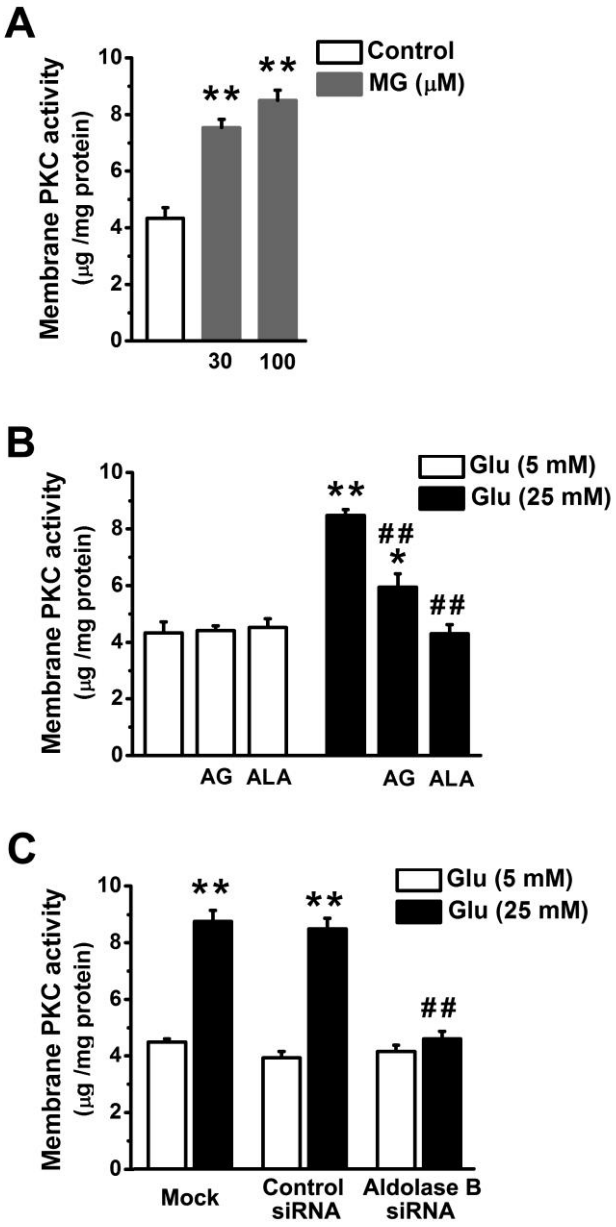

Figure 4-8 Knockdown of aldolase B prevented high glucose-increased membrane PKC activities in EA. hy926 cells. (A) Membrane PKC activities in cells treated with exogenous MG for 3 days. $^{**}P<0.01$ *vs*. control (5 mM glucose). (B) Membrane PKC activities in cells treated with glucose (Glu) in the presence or absence of aminoguanidine (AG, 1 mM) and alagebrium (ALA, 100 μM). $^{*}P<0.05$, $^{**}P<0.01$ *vs*. 5 mM glucose; $^{\#\#}P<0.01$ *vs*. 25 mM glucose. (C) Membrane PKC activities in cells transfected with control or aldolase B siRNA, or only transfection agent (mock). $^{**}P<0.01$ *vs*. 5 mM glucose; $^{\#\#}P<0.01$ *vs*. control siRNA.

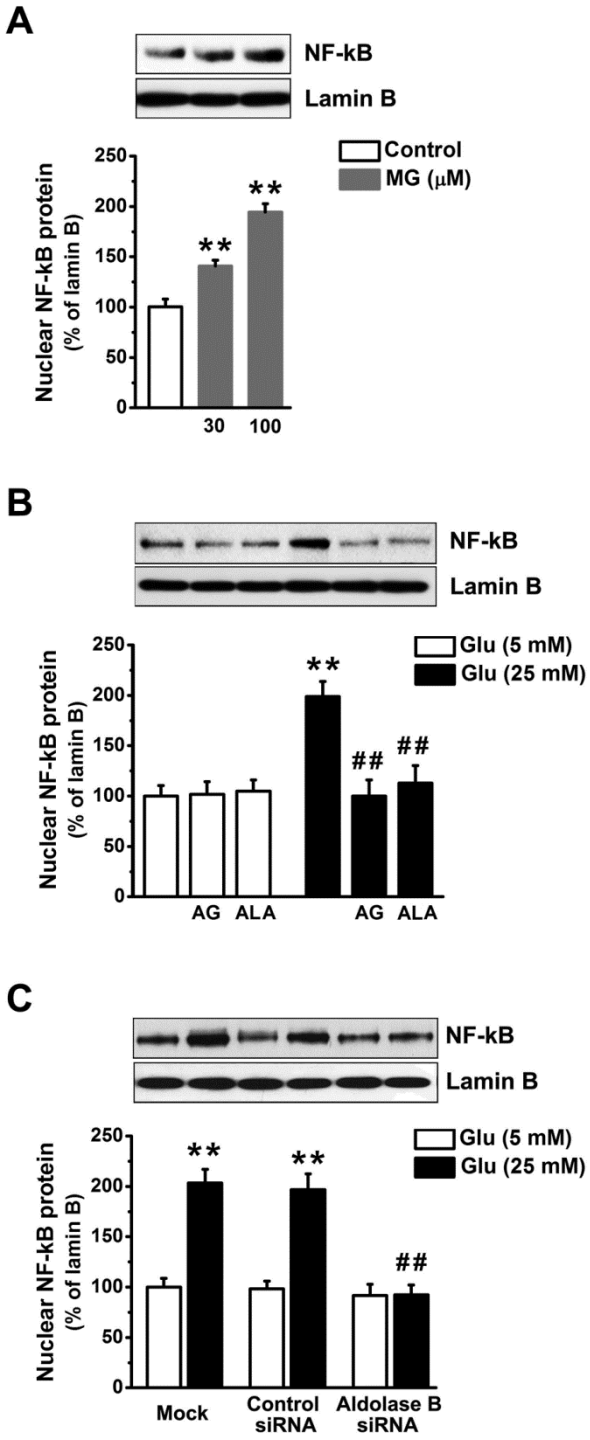

Figure 4-9 Knockdown of aldolase B prevented high glucose-increased NF-κB nuclear translocation in EA. hy926 cells. (A) Nuclear p65 subunit of NF-κB in cells treated with exogenous MG for 3 days. $^{**}P<0.01$ *vs*. control (5 mM glucose). (B) Nuclear p65 subunit of NF-κB in cells treated with glucose (Glu) in the presence or absence of aminoguanidine (AG, 1 mM) and alagebrium (ALA, 100 μM). $^{**}P<0.01$ *vs*. 5 mM glucose; $^{\#\#}P<0.01$ *vs*. 25 mM glucose. (C) Nuclear p65 subunit of NF-κB in cells transfected with control or aldolase B siRNA, or only transfection agent (mock). $^{**}P<0.01$ *vs*. 5 mM glucose; $^{\#\#}P<0.01$ *vs*. control siRNA.

CHAPTER 5

UP-REGULATION OF ALDOLASE A AND METHYLGLYOXAL OVERPRODUCTION IN ADIPOCYTES

Jianghai Liu[1], Kaushik Desai[1], Rui Wang[2], and Lingyun Wu[1,3]

[1]Department of Pharmacology, College of Medicine, University of Saskatchewan;

[2]Department of Biology and [3]Department of Health Sciences, Lakehead University and Thunder Bay Regional Research Institute, Canada

5.1 Abstract

We previously reported that up-regulation of aldolase B, a key enzyme in fructose metabolism, is mainly responsible for vascular methylglyoxal (MG) overproduction under different pathological conditions. Here we report that in insulin-sensitive adipocytes it is aldolase A, an enzyme of the glycolytic pathway, which causes MG overproduction. In cultured 3T3-L1 adipocytes, glucose (25 mM) had no effect on aldolase A gene expression, but insulin (100 nM) up-regulated aldolase A mRNA and protein levels in the absence or presence of 25 mM glucose. Treatment with insulin (100 nM) increased the levels of basal MG or glucose (25 mM)-induced MG and glucose 6-phosphate. However, insulin (100 nM), glucose (25 mM), or their combination had no effect on cellular levels of sorbitol and fructose, but down-regulated gene expression of aldolase B to a similar extent, when compared with the control group. Incubation of 3T3-L1 adipocytes with fructose, acetone, acetol, threonine or glycine (25 mM) in the absence or presence of insulin (100 nM) did not alter cellular MG levels. The elevated MG levels induced by insulin (100 nM), glucose (25 mM), or their combination in adipocytes was completely reduced by siRNA knockdown of aldolase A or application of 2-deoxy-D-glucose (a non-specific inhibitor of glucose uptake and glycolysis), but not by knockdown of aldolase B or by inhibition of aldose reductase, semicarbazide-sensitive amine oxidase or cytochrome P450 2E1. Our data indicate that insulin enhances MG overproduction in insulin-sensitive adipocytes by up-regulating aldolase A.

Key words: aldolase A, methylglyoxal, glucose, insulin, adipocytes

5.2 Introduction

Methylglyoxal (MG) is a highly reactive metabolite produced in mammalian cells. Glucose metabolites glyceraldehyde 3-phosphate (GA3P) and dihydroxyacetone phosphate (DHAP), which spontaneously and non-enzymatically degrade to MG, are considered major sources for endogenous MG formation (*6, 258, 272*). In the cytosol, glucose is physiologically metabolized through the glycolytic pathway into fructose 1,6-bisphosphate (F-1,6-P_2), which subsequently forms GA3P and DHAP catalyzed by aldolase A (*7*). Glucose can also metabolize through the aldose reductase pathway into sorbitol by aldose reductase and then to fructose by sorbitol dehydrogenase (*278*). In some cell types, such as vascular smooth muscle cells (VSMCs), the aldose reductase pathway becomes active when intracellular glucose is elevated (*272, 278, 279*). Fructose is phosphorylated to fructose 1-phosphate (F-1-P), which is cleaved by aldolase B to generate glyceraldehyde and DHAP (*7*). Secondary sources for MG formation include the degradation of aminoacetone generated from protein catabolism and ketone bodies (mainly acetone) from lipolysis by the action of semicarbazide-sensitive amine oxidase (SSAO) and cytochrome P450 2E1 (CYP 2E1), respectively (*11, 280*).

The occurrence of high levels of glucose coupled with the accumulation of endogenous MG has received much attention in diabetes research due to the potentially pathogenic roles of MG and MG-induced advanced glycation endproducts (AGEs) in the development of diabetes and diabetic complications (*106*). Glucose enters insulin-insensitive VSMCs and endothelial cells (ECs) mainly through an insulin-independent glucose transporter 1 (GLUT1) (*145, 281*). Higher MG levels were observed in VSMCs and ECs

treated with high glucose and in the aorta, kidney and retina of diabetic rats (*36, 70, 87, 272*). We have identified aldolase B, but not aldolase A, as a key enzyme responsible for high fructose and glucose-induced MG overproduction in VSMCs (*272*). Fructose up-regulates aldolase B expression while high glucose is converted into fructose, which results in MG overproduction in VSMCs (*272*). Recently, MG formation in insulin-sensitive cells has received much attention since high levels of MG have been found to disturb insulin signaling in 3T3-L1 adipocytes (*147*) and skeletal muscle L6 cells (*31*). Moreover, MG modifies the insulin molecule and impairs its biological functions, such as insulin-stimulated glucose transport in adipocytes (*37*). However, whether MG is over-produced in the insulin-sensitive cells under different pathological conditions is unknown. GLUT1 is expressed in adipocytes, but its intrinsic activity is >90% suppressed (*282*). An insulin-responsive GLUT4 is highly expressed in adipocytes but under conditions of low insulin, is sequestered in intracellular vesicles (*145*). Hyperinsulinemia is commonly observed in hypertension, obesity, and the early stage of type 2 diabetes (*272, 283, 284*). High levels of insulin promote membrane translocation of GLUT4 and stimulate glucose transport in adipocytes (*148*). Treatment with insulin (100 nM) elevated basal glucose levels in adipose cells by 3.6-fold (*187*). Insulin can also enhance glycolysis *via* up-regulating the transcription of glycolytic enzymes, such as hexokinase II, phosphofructokinase, and glyceraldehyde 3-phosphate dehydrogenase (GAPDH) (*149, 150*). We hypothesize that insulin up-regulates aldolase A expression and enhances glucose-induced MG formation in adipocytes.

In this study, cultured 3T3-L1 adipocytes were treated with insulin (100 nM), glucose (25 mM) or their combination. The relative contributions of different enzymes and pathways

to MG formation were evaluated by examining the gene expression of aldolase A and aldolase B and the glucose metabolism through glycolysis and the aldose reductase pathway, and by applying inhibitors for glycolysis, aldose reductase, SSAO, and CYP 2E1 as well as siRNA targeting aldolase A or B.

5.3 Methods

5.3.1 Cell culture

Mouse 3T3-L1 fibroblasts were cultured in Dulbecco's Modified Eagle Medium (DMEM, 25 mM glucose) containing 10% fetal bovine serum (FBS) and penicillin-streptomycin (1% v/v) at 37 ℃ in a humidified atmosphere of 5% CO_2 and 95% air. 3T3-L1 fibroblasts were differentiated into adipocytes in 100-mm culture dishes, as described previously (*248*). Two days after confluence, differentiation was initiated by incubation of cells for 3 days with DMEM (25 mM glucose, 10% FBS) supplemented with 0.25 µM dexamethasone, 0.5 mM 3-isobutyl-1-methylxanthine, and 172 nM insulin. The differentiation medium was changed every day. Thereafter, cells were grown in DMEM (25 mM glucose, 10% FBS) containing 172 nM insulin for 2 days and then in DMEM (25 mM glucose, 10% FBS) without insulin till >90% of cells differentiated into adipocytes. The insulin sensitivity of adipocytes was confirmed by measuring insulin (100 nM, 30 min)-stimulated uptake of [^{3}H]2-deoxy-D-glucose (data not shown). Adipocytes were starved in FBS-free DMEM (5 mM glucose) for 24 h before treatments. The untreated or control cells were 3T3 cells that were cultured in FBS (10%) - DMEM (5 mM glucose) without adding agents such as 100 nM insulin or 25 mM glucose into medium.

5.3.2 Small interference RNA (siRNA) knockdown

Knockdown of aldolase A or B was established by transfection of adipocytes with a siRNA pool (a mixture of 3 or 4 different siRNA duplexes) targeting aldolase A or B (Santa Cruz Biotechnology Inc., Santa Cruz, CA, USA) in siRNA Transfection Reagent (Santa Cruz). Briefly, transfection complexes were formed by incubating 30 μL siRNA pool (10 μM) with 30 μL of transfection reagent in 5 mL siRNA transfection medium (Santa Cruz) for 45 min at room temperature. Transfection complexes were added to cells grown in a 10-cm dish. After 6 h of incubation, 5 mL DMEM supplemented with 20% FBS was added for a final siRNA concentration at 30 nM and incubated for 18 h. After that, cells were starved in FBS-free DMEM (5 mM glucose) for 24 h and then treated with 10% FBS DMEM in the presence or absence of insulin or/and glucose for 12 h. >90% cells are viable at 60 h after transfection. Gene knockdown was verified by Semi-Quantitative Nested RT-PCR with primers designed by Santa Cruz according to manufacturer's instructions.

5.3.3 Biochemical assays

Cell were sonicated and centrifuged at 12,000 rpm (10 min, 4℃). Total protein levels were determined with a bicinchoninic acid protein assay kit (Sigma-Aldrich, Oakville, ON, Canada). Intracellular fructose levels were measured by a fructose assay kit (BioVision, Mountain View, USA). Aliquots of supernatants were deproteinized by ¼ volume of perchloric acid (PCA, 1N) and neutralized by 2.5 M K_2CO_3 to measure the levels of glucose 6-phosphate and sorbitol using the enzymatic fluorometric methods (*272*).

5.3.4 MG Measurement

MG levels in 3T3-L1 adipocytes were determined with an *o*-phenylenediamine (*o*-PD)-based assay (*56, 131, 132*). Briefly, cells were sonicated (three times for 5 seconds each) and centrifuged at 12,000 rpm (10 min, 4°C). 240 μL of supernatant was mixed with 60 μL of PCA (1 N), kept on ice for 10 min, and deproteinized by centrifuging at 12,000 rpm (10 min, 4°C). Then 180 μL of supernatant was incubated with 90 μL of *o*-PD (100 mM) for 3 h at room temperature in the dark. The mixture was centrifuged at 12,000 rpm (5 min, 4℃). A portion of the supernatant (180 μL) was mixed with 20 μL of 5-methylquinoxaline (5-MQ, internal standard) and analyzed by high-performance liquid chromatography (HPLC) with a mobile phase buffer containing 17% acetonitrile, 8% 50 mM NaH_2PO_4 (pH 4.5), and 75% water.

5.3.5 MG production in digitonin-permeabilized adipocytes

Adipocytes were permeabilized with digitonin as previously described (*285*). Cells were harvested by trypsin digestion, washed with phosphate buffered saline (PBS), and then incubated in PBS containing 40 μg/ml digitonin for 5 min. After centrifugation at 1,000 rpm for 5 min, the cell pellets were washed twice with buffer A (150 mM sucrose, 35 mM potassium acetate, 35 mM KCl, 5 mM $MgSO_4$, 5 mM NaH_2PO_4, and 40 mM Hepes, pH 7.55). Cell pellets were incubated at 37℃ for 3 h in buffer A supplemented with 2 mM ATP, 1 mM NAD^+ and different glucose metabolites. After centrifugation at 1,000 rpm for 5 min, the supernatant was collected for MG measurement.

5.3.6 Analysis of gene expression

Total RNA was isolated using an RNeasy Mini Kit (Qiagen Inc., Mississauga, ON, Canada) and converted to cDNA with an iScript™ cDNA Synthesis Kit (Bio-rad, Mississauga, ON, Canada). Real-time PCR was performed using SYBR Green PCR Master Mix (Bio-rad, Mississauga, ON, Canada) with the following primers: mouse aldolase A forward 5'-CAACGGTCACAGCACTTC-3', reverse 5'-CTTCCTCACTCTGCCCTC-3'; mouse aldolase B forward 5'-CCAGTTCCCTATG TTCCA-3', reverse 5'-TTGCTGTGCCTCTTCTAT-3'. Primers of mouse 18s rRNA were purchase from Qiagen (Mississauga, ON, Canada). Protein levels were analyzed by Western blotting using antibodies as follows: aldolase A (1:5000, Sigma-Aldrich, Oakville, ON, Canada), aldolase B (1:500, Epitomics Inc., Burlingame, CA, USA), and β-actin (1:5000, Santa Cruz Biotechnology Inc., Santa Cruz, CA, USA).

5.3.7 Materials

Sorbinil was a generous gift from Pfizer Inc. (Groton, CT). (E)-2-(4-fluorophenethyl) -3-fluoroallylamine (MDL-72974) was a generous gift from Dr. Peter Yu (Department of Pharmacology, University of Saskatchewan, Canada). 2-deoxy-D-glucose (2-DG) and diallyl disulfide (DADS) were purchased from Sigma-Aldrich, Oakville, ON, Canada.

5.3.8 Statistics

Data are expressed as mean ± SEM from five independent experiments. Statistical analyses were performed using by parametric Student's *t*-test (two-tailed) or one-way

ANOVA followed by posthoc Tukey's test.

5.4 Results

5.4.1 Insulin enhanced MG formation in adipocytes

Application of insulin (100 nM) increased basal MG production in 3T3-L1 adipocytes (Figure 5-1A). Glucose (25 mM) treatment elevated cellular MG levels, which was further augmented by co-treatment with insulin (Figure 5-1A). Glucose analog 2-DG competitively inhibits glucose uptake and glycolysis (*286*). Basal MG levels and the elevated MG levels induced by insulin (100 nM), glucose (25 mM) or their combination in adipocytes were reduced by application of 2-DG, but not affected by application of sorbinil, a specific aldose reductase inhibitor (Figure 5-1A). Incubation of 3T3-L1 adipocytes with fructose (25 mM) or fructose plus insulin (100 nM) did not increase MG levels (Figure 5-1B).

5.4.2 Insulin increased glycolysis in adipocytes

Glucose (25 mM) elevated levels of glucose 6-phosphate (G-6-P, the first metabolite of glycolysis) in 3T3-L1 adipocytes. Insulin (100 nM) increased basal and glucose (25 mM)-induced G-6-P formation (Figure 5-2A). However, insulin (100 nM), glucose (25 mM) or their combination had no effect on cellular levels of sorbitol and fructose (Figures 5-2B, 5-2C).

We compared the potency of glycolytic metabolites upstream of aldolase A (G-6-P and F-1,6-P2) or aldose reductase pathway metabolites upstream of aldolase B (sorbitol, fructose, and F-1-P) in generating MG in digitonin-permeabilized adipocytes, since most of these

metabolites are cell-impermeable. The amount of MG produced by G-6-P or F-1,6-P2 is 3.2- and 6.5-fold above the baseline levels of MG, respectively, and much higher than that produced by an equimolar concentration of F-1-P, which was 1.7-fold higher than control. Incubation with sorbitol or fructose did not elevate MG levels in digitonin-permeabilized adipocytes (Figure 5-2D).

5.4.3 Insulin up-regulated aldolase A gene expression in adipocytes

Insulin (100 nM) up-regulated mRNA and protein levels of aldolase A in 3T3-L1 adipocytes, but glucose (25 mM) had no effect on aldolase A gene expression in comparison with that from control cells (Figure 5-3A, 5-3B). Application of glucose (25 mM) had no effect on insulin (100 nM)-enhanced aldolase A mRNA and protein levels (Figures 5-3A, 5-3B). However, gene expression of aldolase B (in mRNA and protein levels) was suppressed by insulin (100 nM), glucose (25 mM) or their combination in the same adipocytes (Figures 5-3A, 5-3B).

5.4.4 Knockdown of aldolase A prevented MG formation in adipocytes

Transfection of 3T3-L1 adipocytes with single siRNA targeting aldolase A or aldolase B reduced mRNA levels of aldolase A by 70% and mRNA level of aldolase B by 78%, respectively (Figure 5-4A). Since single transfection with aldolase A siRNA elevated mRNA levels of aldolase B, we also used adipocytes cells double-transfected with aldolase A and aldolase B siRNAs in this study, which had 65% and 70% lower mRNA levels of aldolase A and aldolase B, respectively, in comparison to the transfection with control siRNA (Figure

5-4A). Basal MG levels were reduced in aldolase A siRNA-transfected cells and, although not significantly, in double siRNAs-transfected cells, but not in mock (transfected with only transfection agents), or control siRNA or aldolase B siRNA-transfected cells (Figure 5-4B). Excess MG production due to incubation with insulin (100 nM), glucose (25 mM) or their combination occurred in mock, control siRNA- or aldolase B siRNA-transfected cells, but was abolished in aldolase A siRNA- or double siRNAs-transfected cells (Figure 5-4B).

5.4.5 CYP 2E1 and SSAO are not implicated in MG formation in 3T3-L1 adipocytes

Incubation of 3T3-L1 adipocytes with acetone, acetol, glycerol [converting to DHAP during triglycerides degradation (*243*)], glycine and threonine (glycine and threonine are precursors of aminoacetone) at concentration of 25 mM, in the absence or presence of insulin (100 nM), did not alter cellular MG levels (Figure 5-5A). Application of DADS or MDL-72974, the specific inhibitor of CYP 2E1 and SSAO, respectively, had no effect on basal MG formation and excess MG formation induced by insulin (100 nM), glucose (25 mM) or their combination in 3T3-L1 adipocytes (Figure 5-5B).

5.5 Discussion

Our lab previously found that in insulin-insensitive VSMCs, fructose (25 mM) or glucose (25 mM) up-regulated aldolase B and promoted MG overproduction (*272*). In this study, we report a different mechanism for MG generation in insulin-sensitive adipocytes where fructose (25 mM) has no effect on MG production and glucose (25 mM) only slightly increases MG levels. However, insulin (100 nM) up-regulates aldolase A, an enzyme of the

glycolytic pathway, and significantly elevates basal and glucose (25 mM)-induced MG formation in adipocytes.

Insulin-insensitive cells (i.e. VSMCs and ECs) and insulin-sensitive cells (i.e. adipose and skeletal muscle cells) are traditionally distinguished by their sensitivity to insulin with respect to glucose transport. For example, glucose enters cells mainly through an insulin-independent GLUT1 in VSMCs while through an insulin-dependent GLUT4 in adipocytes (*145*). MG formation in VSMCs is likely insulin-independent, but here we found that insulin plays a crucial role in MG production in adipocytes. In VSMCs, glucose (25 mM) raised cellular MG levels by 3-fold, but insulin (100 nM) had no effect on gene expression of aldolase A and aldolase B and cellular MG levels when compared with the control group (5 mM glucose alone) (*272*). However, in 3T3-L1 adipocytes, we found that insulin (100 nM) treatment significantly increased basal MG formation and co-application of insulin and glucose (25 mM) significantly augmented glucose-increased MG levels (Figure 5-1).

Unlike VSMCs, adipocytes less rely on fructose and aldolase B for MG formation. Treatment of VSMCs with fructose (25 mM) up-regulated gene expression of GLUT5 and aldolase B and increased cellular MG production (*272*). Exogenous fructose is transported into cells through fructose transporter GLUT5 (*287*). Serum fructose levels are elevated and responsible for vascular MG overproduction in metabolic syndrome without hyperglycemia, such as obesity and hypertension (*272*). In addition, fructose-enhanced MG production in VSMCs was further augmented by insulin which up-regulated mRNA levels of GLUT5 and increased cellular fructose accumulation (*272*). However, treatment with fructose (25 mM) in the absence or presence of insulin (100 nM) did not alter MG generation in 3T3-L1

adipocytes (Figure 5-1). Fructose can be produced intracellularly from glucose through the aldose reductase pathway. Glucose (25 mM) treatment activated aldose reductase pathway and elevated sorbitol and fructose levels in VSMCs and ECs (*272, 288*), but not in 3T3-L1 adipocytes (Figure 5-2). Insulin seems not in favor of conversion of fructose from glucose (Figure 5-2). Previous studies have provided evidence that insulin did not alter glucose (5 or 25 mM)-induced sorbitol or fructose formation in erythrocytes, retina and kidney epithelial cells (*289, 290*). Here we also observed that insulin (100 nM) or insulin plus glucose (25 mM) did not affect sorbitol and fructose levels in 3T3-L1 adipocytes when compared with control cells treated with 5 mM glucose (Figure 5-2). More importantly, insulin (100 nM), glucose (25 mM) or their combination suppressed aldolase B expression in adipocytes (Figure 5-3). Inhibition of aldose reductase or knockdown of aldolase B did not reduce basal or excess MG formation in adipocytes under our tested conditions (Figures 5-1, 5-4).

Instead, aldolase A and glycolysis becomes the dominant contributor to MG generation in adipocytes. Aldolase A cleaves F-1,6-P_2 in the glycolytic pathway to yield GA3P and DHAP, which are considered as the direct precursors of MG (*6, 258, 272*). Knockdown of aldolase A or application of 2-DG reduced basal MG formation in normal glucose-treated 3T3-L1 adipocytes (Figures 5-1, 5-4), suggesting that aldolase A and glycolysis mainly account for basal MG formation in adipocytes. MG formation is increased with the increase of upstream metabolites (*146*). In the digitonin-permeabilized adipocytes, MG levels were significantly increased by G-6-P and, to a higher extent, by F-1,6-P_2 after a 3-h incubation (Figure 5-2). Glucose (25 mM) elevated G-6-P and MG levels in adipocytes although it had no effect on gene expression of aldolase A (Figures 5-1, 5-2 and 5-3). Insulin

was found to activate glycolysis in adipocytes (*149, 150, 291*). Moreover, insulin (100 nM) markedly increased aldolase A mRNA and protein levels in the absence or presence of 25 mM glucose (Figure 5-3), leading to an increased glycolysis and production of MG. Higher levels of G-6-P and MG were observed in insulin (100 nM)-treated adipocytes than those in glucose (25 mM)-treated adipocytes. In the presence of insulin, glucose (25 mM)-elevated G-6-P and MG levels were further increased (Figures 5-1, 5-2). When we blocked glycolysis with 2-DG or knocked down aldolase A expression in 3T3-L1 adipocytes, the insulin (100 nM), glucose (25 mM) or their combination-enhanced MG generation was completely prevented (Figures 5-1, 5-4). These data suggest that aldolase A is a key enzyme responsible for MG generation in 3T3-L1 adipocytes, and the basal or glucose (25 mM)-elevated MG formation was increased by insulin which up-regulated aldolase A.

Plasma or serum insulin levels are elevated in obesity, hypertension and the early stage of type 2 diabetes (*272, 283, 284*). Our work showing that treatment with insulin significantly elevated both basal and glucose (25 mM)-induced MG formation in adipocytes is of particular interest since it indicates that MG in adipose tissues may be over-produced by hyperinsulinemia in different metabolic syndrome, especially during the early stages when significant insulin resistance does not blunt insulin signaling. Thus, the possible overproduction of MG in the early stages of hyperinsulinemia may be implicated in the development of insulin resistance. Moreover, our recent studies on 3T3-L1 cells demonstrate that MG can enhance the mRNA expression of adipogenic markers, such as adiponectin, leptin, PPARγ and C/EBPα, and promote adipogenesis of preadipocyte cells (*292*). Data from the present study provides a possible mechanistic link between MG overproduction and

obesity development under hyperinsulinemic conditions where the insulin signaling has not deteriorated significantly.

In conclusion, the metabolic pathway for MG formation in insulin-sensitive cells is different than that in insulin-insensitive cells. Insulin up-regulates aldolase A and enhances MG formation in cultured 3T3-L1 adipocytes. Aldolase A would be a target to reduce excess MG generation in insulin-sensitive cells.

5.6 Acknowledgements

We are grateful to Mrs. Arlene Drimmie (Department of Pharmacology, University of Saskatchewan) for her excellent technical assistance. This work was supported by operating grants from Canadian Institutes of Health Research and the Heart and Stroke Foundation of Saskatchewan to L. Wu. J. Liu was supported by College of Medicine Graduate Scholarship, University of Saskatchewan.

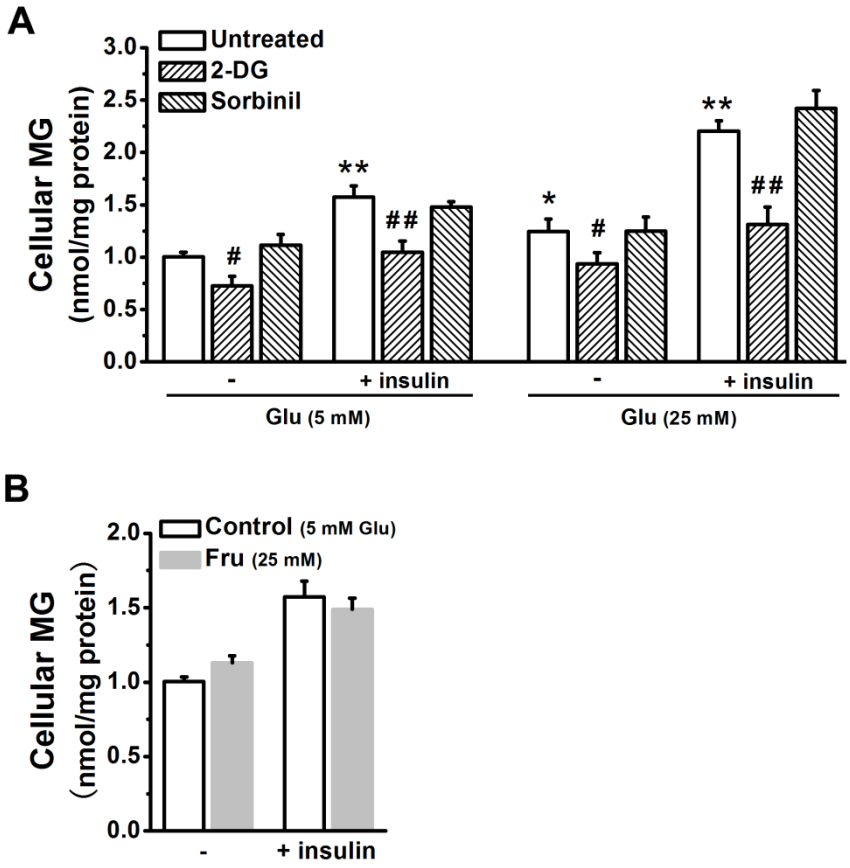

Figure 5-1 Insulin-enhanced MG formation in 3T3-L1 adipocytes. (A) Insulin (100 nM)-induced MG formation in adipocytes treated with or without 2-deoxy-D-glucose (2-DG, 5 mM) or sorbinil (10 μM) for 12 h. (B) MG levels in adipocytes after 12-h incubation with fructose alone or plus insulin (100 nM). n= 5 in each group in A and B, $^{*}P$<0.05, $^{**}P$<0.01*vs*. 5 mM glucose and $^{\#}P$< 0.05, $^{\#\#}P$< 0.01 *vs*. untreated.

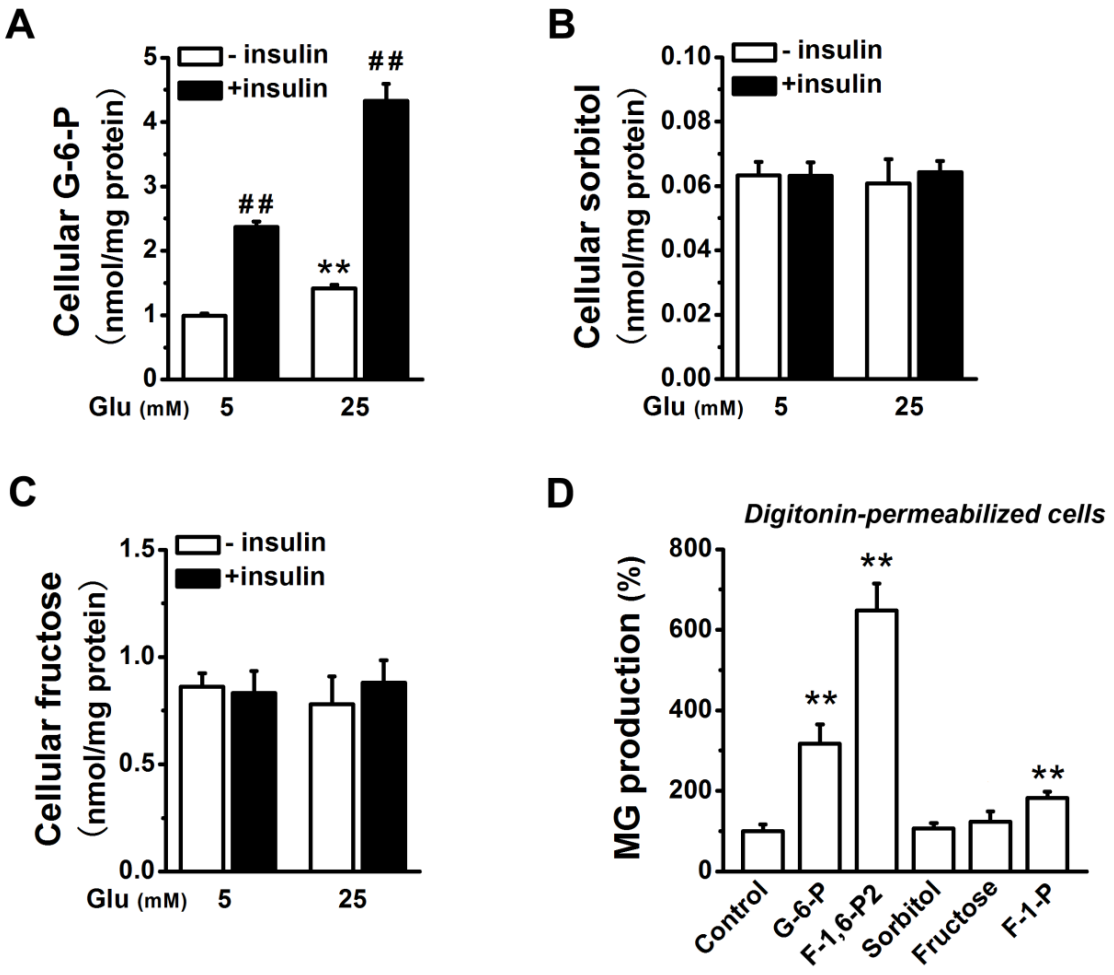

Figure 5-2 Glucose metabolism in 3T3-L1 adipocytes. (A) Levels of glucose 6-phosphate (G-6-P), (B) sorbitol and (C) fructose in adipocytes treated with or without insulin (100 nM) for 12 h. $^{**}P$<0.01 *vs*. 5 mM glucose and $^{\#\#}P$< 0.01 *vs*. glucose alone. (D) Relative MG production in digitonin-permeabilized adipocytes after treatment with glucose metabolites, G-6-P, fructose 1,6-bisphosphate (F-1,6-P_2), sorbitol, fructose, and fructose 1-phosphate (F-1-P), at same concentration of 1 mM for 3 h, respectively. *n*= 5 in each group in A-D, $^{**}P$<0.01 *vs*. control.

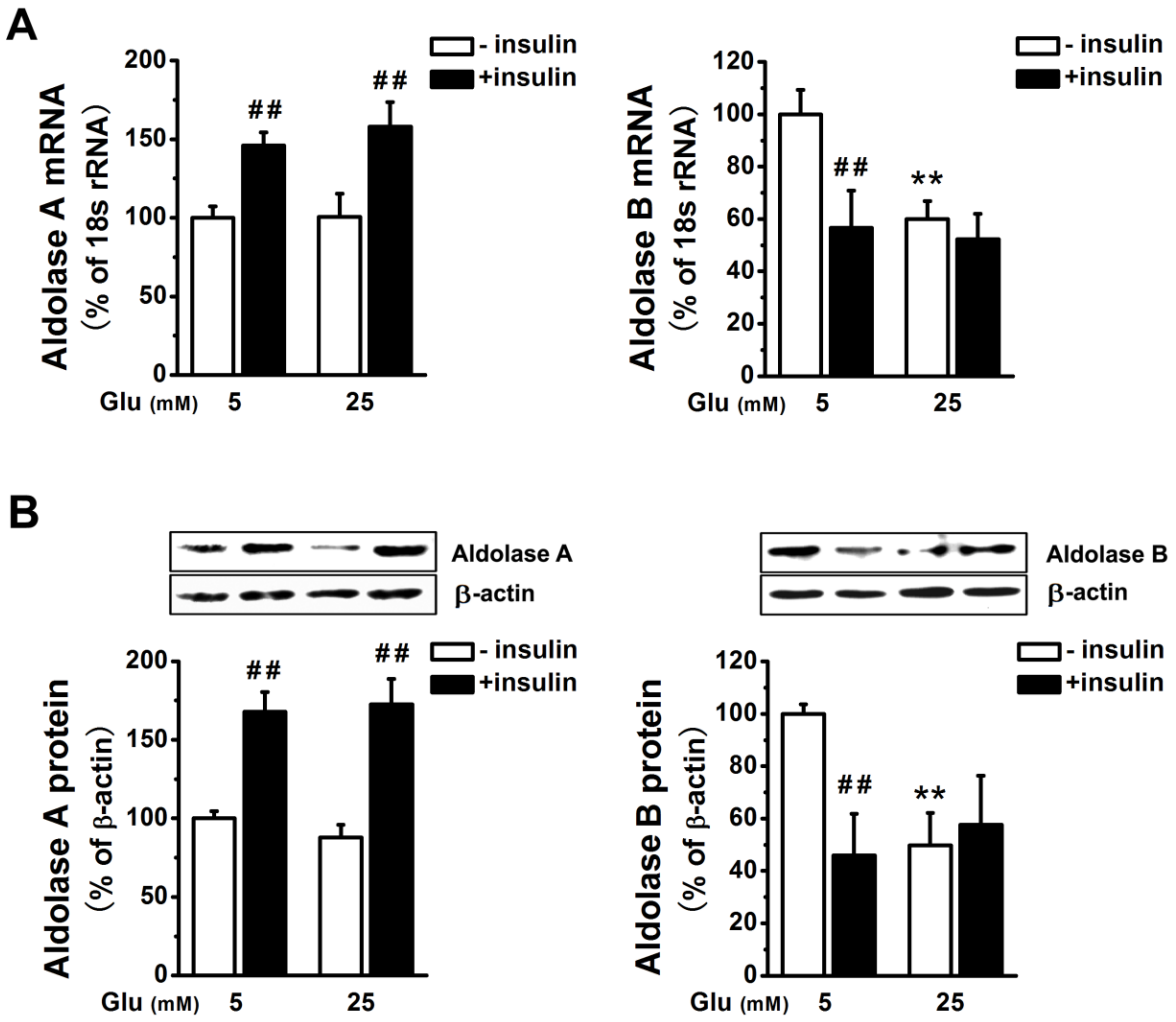

Figure 5-3 Gene expression of aldolase A and aldolase B in 3T3-L1 adipocytes. (A) Real-time PCR and (B) Western blot analysis of aldolase A and aldolase B gene expressions in adipocytes treated with or without insulin (100 nM) for 12 h. *n*= 5 in each group in A and B, $^{**}P<0.01$ *vs*. 5 mM glucose and $^{\#\#}P< 0.01$ *vs*. glucose alone.

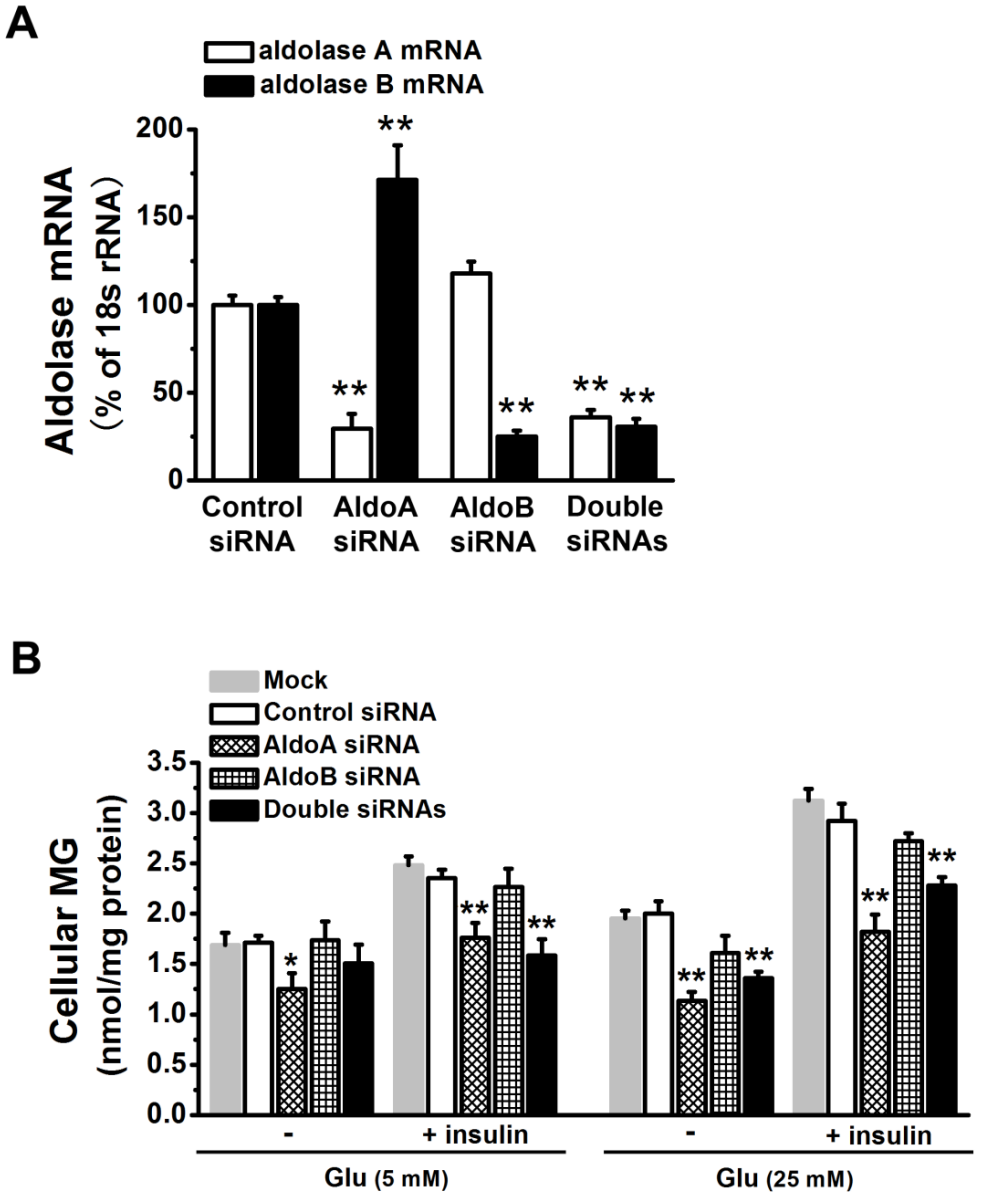

Figure 5-4 Knockdown of aldolase A prevented MG formation in 3T3-L1 adipocytes. (A) mRNA levels of aldolase A or aldolase B, and (B) levels of MG in adipocytes transfected with transfection agents (mock) or with control, aldolase A or aldolase B siRNA, or double siRNAs. After transfection, cells were grown in medium with or without insulin (100 nM) for 12 h. n= 4 in each group in A and n=6 in B. $^{*}P<0.05$, $^{**}P<0.01$ *vs*. respective control siRNA.

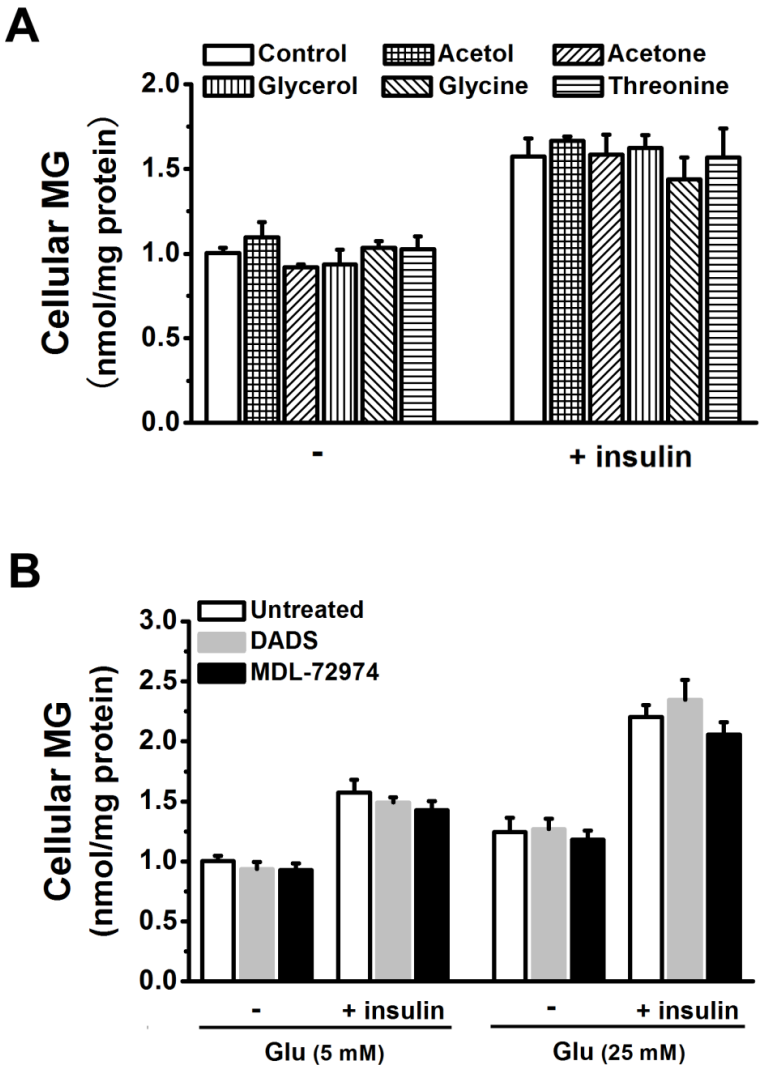

Figure 5-5 Effect of cytochrome P450 2E1 (CYP 2E1) and semicarbazide-sensitive amine oxidase (SSAO) on MG formation in 3T3-L1 adipocytes. (A) MG levels in 3T3-L1 adipocytes treated with acetone, acetol, glycerol, glycine or threonine at the same concentration of 25 mM for 12 h. (B) Insulin (100 nM)-induced MG formation in the presence or absence of diallyl disulfide (DADS, 100 μM, a CYP 2E1 inhibitor) or (E)-2-(4-fluorophenethyl)-3-fluoroallylamine (MDL-72974, 5 μM, a SSAO inhibitor) for 12 h. *n*= 5 for each group in A and B.

CHAPTER 6

DISCUSSION AND CONCLUSIONS

6.1 General discussion

Increased MG accumulation in vascular cells has been postulated as an important mechanism for diabetic vascular complications (*56, 106*). Moreover, Dr Wu's group has found that MG was over-produced in VSMCs, aorta and mesenteric arteries of rats with hypertension (*25, 56, 72, 131*). In SHR, MG levels in the plasma and the aorta increase in an age-dependent fashion, which is correlated with the increase of blood pressure (*131*). The elevation of MG levels in the aorta is obvious in the 8-week-old SHR when hypertension is not yet fully established (*131*). When SD rats were fed with fructose for 16 weeks, there were elevated MG levels in the serum and the aorta with the development of vascular remodeling and high blood pressure (*25*). However, the underlying mechanisms for vascular MG overproduction in metabolic syndrome, such as diabetes and hypertension, and the exact role of increased MG in the development of vascular complications, were not clear.

A traditional view regards MG as a product of glycolysis, since the GA3P and DHAP generated through glycolysis can spontaneously and non-enzymatically convert to MG (*5, 6, 258*). However, this view is challenged by the observation that MG is over-produced in VSMCs and the aorta in hypertensive rats which have normal blood glucose levels (*25, 56, 72, 131*). This view is also challenged by our finding in chapter 3 that high glucose did not change the levels of glucose 6-phosphate and caused a down-regulation of aldolase A gene expression in the cultured A-10 cells. Furthermore, we found a down-regulation of aldolase A and an overproduction of MG in the aorta of diabetic rats.

Interestingly, we observed that levels of serum and aortic fructose and MG and mRNA levels of aortic aldolase B were increased in different rat models of metabolic syndrome,

including fructose-fed SD rats, SHR, obese non-diabetic Zucker rats and diabetic Zucker rats. However, the mRNA levels of aortic aldolase A were unchanged or even down-regulated in these rat models. Fructose increased MG generation in VSMCs (*66*). Chronically feeding fructose increased serum and aortic MG levels and elevated blood pressure in SD rats, but the blood glucose remained within the normal range (*25, 147*). In this project, we found that fructose (25 mM) had no effect on aldolase A expression, but up-regulated aldolase B expression in VSMCs. Knockdown of aldolase B completely prevented fructose (25 mM)-elevated MG generation in A-10 cells. These data suggest that up-regulation of aldolase B by increased fructose is a reason for MG over-production in the aorta of hypertensive or obese rats with normoglycemia.

We found that insulin up-regulated GLUT5, leading to increased fructose uptake and MG generation in VSMCs. We also found that blood insulin levels and aortic GLUT5 mRNA levels are elevated in hypertensive or obese rats. However, in the hypertension or obesity, vascular tissues are insulin resistant (*298, 299*). Whether the high blood insulin contributes to the up-regulation of GLUT5 and overproduction of MG in aorta of fructose-fed SD rats, SHR, or obese Zucker rats requires further investigation. It is possible that in the early stages when hyperinsulinemia starts developing, the insulin signaling may not have deteriorated enough to blunt the response to hyperinsulinemia, in which case more MG can be produced.

It is well known that high glucose saturates hexokinase (the first enzyme in glycolysis) but elevates flux through the polyol pathway and produces fructose (*153, 154*). Does fructose and aldolase B contribute to vascular MG overproduction in diabetic rats? Here we found that high glucose activated the polyol pathway, increased fructose production and up-regulated

gene expression of aldolase B in the cultured A-10 cells. More importantly, the elevated MG generation produced by high glucose was prevented by blockage of polyol pathway or by knockdown of aldolase B, but only partially reduced by knockdown of aldolase A in VSMCs. The results suggest that the increased fructose production from glucose and up-regulated aldolase B mainly account for hyperglycemia-induced MG overproduction in vascular cells in diabetes. Our work identifies a common pathway, fructose-aldolase B pathway, for vascular MG generation in different rat models of metabolic syndrome with or without hyperglycemia. However, the basal MG levels in A-10 cells treated with 5 mM glucose was not reduced by knockdown of aldolase B but reduced by knockdown of aldolase A, suggesting that aldolase A plays a role for the basal MG formation in vascular cells under physiological conditions.

Endothelial dysfunction occurs at the early stage of many pathological conditions such as diabetes mellitus, hypertension and atherosclerosis, and is a major risk factor of cardiovascular complications in the metabolic syndrome (*136*). Increased MG accumulation is considered as an important molecular mechanism linking diabetes to endothelial damage (*36, 70, 87*). However, whether knockdown of aldolase B can prevent high glucose-induced MG overproduction and related endothelial cell dysfunction are largely unsettled. Our study in chapter 4 identified aldolase B as the major enzyme responsible for high glucose (25 mM)-increased MG overproduction in endothelial cells. We found that knockdown of aldolase B not only prevented high glucose-elevated MG overproduction but also prevented high glucose-induced activation of multiple metabolic and signaling pathways, including AGEs accumulation, oxidative stress, O-GlcNAc modification, membrane protein kinase C

activity and nuclear translocation of NF-κB. Our data indicate that normalizing MG generation by aldolase B knockdown prevented high glucose-induced cellular dysfunction in endothelial cells. This conclusion was supported by our findings that the application of aminoguanidine (a non-specific MG scavenger) or alagebrium (an AGEs breaker), to a lesser extent, attenuated these metabolic and signaling alterations induced by high glucose. On the other hand, we found that MG (100 μM) directly increased AGEs formation and oxidative stress, and activated the above metabolic and signaling pathways in endothelial cells to nearly the same extent as did high glucose (25 mM). These results indicate an exact role of MG in the toxicity of high glucose as an upstream activator for other metabolic and signaling pathways. Aldolase B is likely a promising and novel target in preventing glucose-induced overproduction of MG and related endothelial dysfunction in diabetes.

The last part of my PhD program was to study the MG formation in insulin-sensitive adipose cells. A recent study in our lab demonstrated that incubation of 3T3-L1 adipocytes with MG impaired insulin signaling pathways and insulin-stimulated glucose uptake (*147*). However, whether MG is over-produced in adipocytes in the metabolic syndrome and the underlying mechanism are unknown. Unlike those in insulin-insensitive VSMCs, glucose transport and metabolism in adipose cells are insulin-dependent (*291*). Insulin can stimulate glucose uptake through insulin-responsive GLUT4 (*148*) and enhance glycolysis in adipocytes (*149, 150*). It was reported that hyperinsulinemia associated with obesity significantly increased glucose uptake and glycolysis in adipose tissues (*293*). Our studies *in vitro* showed that the application of insulin (100 nM), high glucose (25 mM) or their combination up-regulated aldolase A expression and increased G-6-P and MG levels in

cultured 3T3-L1 adipocytes when compared with the control cells treated with 5 mM glucose. Knockdown of aldolase A expression or blockage of glycolysis decreased the basal level of MG and prevented MG overproduction induced by insulin, high glucose or their combination. In contrast, insulin (100 nM), high glucose (25 mM), or their combination had no effect on cellular levels of sorbitol and fructose, in comparison with that from the control group. Furthermore, insulin (100 nM), high glucose (25 mM), and insulin plus high glucose reduced the mRNA and protein of aldolase B to a similar lower level. Knockdown of aldolase B expression or blockage of the polyol pathway did not reduce MG overproduction induced by insulin, high glucose or their combination in 3T3-L1 adipocytes. This work indicates that insulin enhances glycolysis and aldolase A expression, leading to excess MG formation in adipocytes.

SSAO-catalyzed deamination of aminoacetone and CYP 2E1-catalyzed catabolism of acetone are considered as the important sources for cellular MG generation (*10*). The role of SSAO in MG overproduction received much attention due to the significantly raised plasma SSAO activity in diabetes and hypertension (*131, 294*). Acetone is considered as a potential source for MG overproduction since the plasma level of acetone is significantly increased in patients with diabetes, which can be up to 8.9 mM in diabetic ketoacidosis (*295*). However, in this project, we found that even incubation with aminoacetone or acetone at a concentration of 25 mM for 12 h did not alter MG levels in VSMCs or adipose cells. Application of the specific inhibitor of CYP 2E1 or SSAO unchanged either basal MG formation or excess MG formation induced by fructose, glucose and/or insulin in cultured VSMCs, endothelial cells and adipose cells, suggesting that CYP 2E1 and SSAO were not implicated with either

vascular or adipose MG formation. However, since our studies have been performed in cultured VSMCs, endothelial cells and adipose cells, we cannot rule out the role of CYP2E1 and SSAO in MG production *in vivo* in different disease conditions.

6.2 Conclusions

Fructose up-regulated aldolase B and enhanced MG generation in VSMCs. Levels of serum and aortic fructose were increased in the obese or hypertensive rats, leading to up-regulation of aldolase B and overproduction of MG in the aorta. High glucose activated the polyol pathway and increased fructose and MG production in VSMCs, endothelial cells, and in the aorta of diabetic rats. Knockdown of aldolase B completely prevented high fructose or glucose-induced MG overproduction in VSMCs and high glucose-induced MG overproduction in endothelial cells. Thus, local aortic smooth muscle MG production may be contributing to the development of increased vascular contractility, hypertension and atherosclerosis.

MG is an upstream mediator for high glucose-induced biochemical abnormalities and endothelial cell dysfunction. Knockdown of aldolase B prevented high glucose-increased AGEs formation, oxidative stress, and activation of the PKC, O-GlcNAc, and NFκB pathways. Endothelial overproduction of MG can contribute to endothelial dysfunction, and the development of reduced endothelium-dependent relaxation, increased vascular contractility, prothrombotic tendency and hypertension and atherosclerosis. In the capillary endothelial cells, such as those in the adipose tissue, it can also contribute to abnormalities in the function of lipoprotein lipase, triglyceride/fatty acid exchange and dyslipidemia. Thus,

more work needs to be done to substantiate these possibilities.

Insulin did not change the glucose metabolism through the polyol pathway and down-regulated aldolase B, but up-regulated aldolase A and increased MG generation in insulin-sensitive adipose cells. Blockage of glycolysis or knockdown of aldolase A prevented the excess MG generation induced by high insulin in adipose cells. An overproduction of MG in the adipose cells may be lipogenic leading to adipose tissue fat accumulation and contributing to central obesity in the metabolic syndrome.

The net *in vivo* contribution of elevated MG production in several different cell types may thus contribute to the different abnormalities that together make up the metabolic syndrome. In this regard we need to study MG production in other cell types such the hepatocytes, the kidney cells, skeletal muscle cells and the brain cells.

6.3 Significance of the study

The significance of the studies from my Ph.D. program is the identification of two key enzymes, aldolase A and aldolase B, that contribute to MG overproduction in different cell types. Inhibitors targeting these enzymes can be designed and investigated leading to the development of potential therapeutic agents. Thus, we have elucidated the important role of fructose-AldoB pathway in vascular MG overproduction and vascular function in different subtypes of metabolic syndrome. Increased MG accumulation in blood vessels has been implicated in the development of vascular complications in metabolic syndrome. We, for the first time, identify fructose-AldoB pathway as a common pathway for vascular MG overproduction in different metabolic syndrome. Aldolase B is a key enzyme for MG

overproduction in insulin-insensitive vascular smooth muscle cells and endothelial cells. Specifically targeting the aldolase B might represent a new avenue for the prevention and treatment of hypertension and vascular complications of diabetes. More importantly, we found that aldolase B knockdown has a greater inhibitory effect on high glucose-induced endothelial abnormalities than application of aminoguanidine and alagebrium (the most widely used MG scavenger and AGEs breaker, respectively).

We found, for the first time, that insulin can increase MG generation in insulin-sensitive adipose cells. Levels of blood insulin are increased in the hypertension and obesity (*272, 283, 284*). Our work suggests a linkage between hyperinsulinemia, MG, and development of insulin resistance and obesity with the understanding that the relation between hyperinsulinemia, insulin signaling sensitivity and defects, and MG production in the adipose tissue needs to be established in the pre-, early and late stages of obesity *in vivo*. However, we found it is aldolase A, but not aldolase B, that is up-regulated by high insulin and mainly responsible for MG overproduction in adipose cells, indicating aldolase A as a target to prevent adipose MG overproduction in metabolic syndrome.

6.4 Limitations of the study

Increased serum and urinary fructose concentrations were reported in patients with diabetes (*162*). Hyperglycemia-induced activation of the polyol pathway has been postulated to be an important mechanism, since the increases in gene expression and activities of aldose reductase and sorbitol dehydrogenase, and increases in cellular levels of the polyol pathway metabolites, sorbitol and fructose, have been widely observed in different tissues of diabetic

animals (*242, 296, 297*). Our studies in chapter 3 report that the serum fructose levels are elevated in obese or hypertensive rats and, to a higher extent, in diabetic rats. However, no study is available to clarify the reason for the fructose elevation in metabolic syndrome without hyperglycemia and the reason for the higher increase of serum fructose in diabetes than hypertension and obesity.

In Chapter 3, we incubated cultured VSMCs with glucose at concentration of 25 mM to mimic the hyperglycemia of diabetics and, for comparative purposes, we have to use the same concentration of 25 mM for fructose. Inevitably, this concentration of fructose used is much higher than the pathological serum levels of fructose (1-2 mM). However, we can argue that chronic elevations of serum fructose even in the 1-2 mM range over several years are likely to cause progressive cumulative metabolic changes and damage to the involved cells. The use of higher concentrations in acute studies ranging from 3 h to 5 days, is universally practiced and accepted and helps to reveal possible long-term consequences of lower concentrations encountered *in vivo*. From the current studies in Chapter 3, it is not clear whether the elevated serum MG is also caused by a release of excess MG from VSMCs and/or from endothelial cells. MG can cross the cell membrane to a limited extent and in one study about 10% of MG synthesized in cells was released into the surrounding environment (*34*). Moreover, increased MG accumulation has been also reported in the retina and the kidney (*87*), which contain several different types of cells. The contribution of MG formed in vascular cells to the MG accumulation in blood and organs need to be clarified *in vivo* in mice with cell-specific knockout of aldolase B.

In Chapter 4, we identify MG as a mediator for high glucose-induced changes in

different biochemical pathways, but the underlying mechanism of how MG activates these pathways were not addressed. MG increased oxidative stress through impairing mitochondrial function, up-regulating NADPH oxidase, and reducing cellular antioxidant defences (*66, 70*). The role of MG in the increase of O-GlcNAc modification, activation of PKC and NF-κB, and in their related deleterious actions requires extensive further studies. Moreover, generally speaking, endothelial dysfunction includes the impaired endothelium-dependent relaxation, vascular remodeling and other pathological changes in blood vessels. The relationship between MG and endothelial dysfunction needs further investigation in isolated blood vessels or *in vivo* in animals.

The last question for our studies is how insulin and carbohydrates regulate gene expression of aldolase A and aldolase B. Whether insulin or carbohydrates affect the mRNA and protein stability of aldolase A or aldolase B, or regulate the post-transcription of these enzymes is totally unknown. It is quite likely that insulin, glucose and fructose may be delaying or attenuating mRNA or protein degradation of aldolase A or aldolase B. We also observed that high glucose up-regulated aldolase B in VSMCs but down-regulated aldolase B in adipose cells. Insulin had no effect on aldolase A in VSMCs but up-regulated aldolase A in adipose cells. The cell-specific manner of gene regulation may be caused by the cell-specific distribution of nuclear transcription factors. For example, hepatocyte nuclear factor 1 (HNF-1), an important transactivator of the aldolase B gene promoter, is highly expressed in the liver and the kidney, but not in the spleen and the lungs (*300*).

REFERENCES

1. Creighton, D. J., Migliorini, M., Pourmotabbed, T., and Guha, M. K. (1988) Optimization of efficiency in the glyoxalase pathway, *Biochemistry 27*, 7376-7384.
2. Lo, T. W., Westwood, M. E., McLellan, A. C., Selwood, T., and Thornalley, P. J. (1994) Binding and modification of proteins by methylglyoxal under physiological conditions. A kinetic and mechanistic study with N alpha-acetylarginine, N alpha-acetylcysteine, and N alpha-acetyllysine, and bovine serum albumin, *J Biol Chem 269*, 32299-32305.
3. Shipar, M. A. H. (2006) Formation of methyl glyoxal in dihydroxyacetone and glycine Maillard reaction: A computational study, *Food Chemistry 98*, 395–402.
4. Mitsuo Namiki, T. H. (1983) *A new mechanism of the Maillard reaction involving sugar fragmentation and free radical formation, Am Chem Soc. 215,* 21-46.
5. Phillips, S. A., and Thornalley, P. J. (1993) The formation of methylglyoxal from triose phosphates. Investigation using a specific assay for methylglyoxal, *Eur J Biochem 212*, 101-105.
6. Richard, J. P. (1993) Mechanism for the formation of methylglyoxal from triosephosphates, *Biochem Soc Trans 21*, 549-553.
7. Cox, T. M. (1994) Aldolase B and fructose intolerance, *FASEB J 8*, 62-71.
8. Hopper, D. J., and Cooper, R. A. (1972) The purification and properties of Escherichia coli methylglyoxal synthase, *Biochem J 128*, 321-329.
9. Murata, K., Fukuda, Y., Watanabe, K., Saikusa, T., Shimosaka, M., and Kimura, A. (1985) Characterization of methylglyoxal synthase in Saccharomyces cerevisiae,

Biochem Biophys Res Commun 131, 190-198.

10. Chang, T., and Wu, L. (2006) Methylglyoxal, oxidative stress, and hypertension, *Can J Physiol Pharmacol 84*, 1229-1238.

11. Koop, D. R., and Casazza, J. P. (1985) Identification of ethanol-inducible P-450 isozyme 3a as the acetone and acetol monooxygenase of rabbit microsomes, *J Biol Chem 260*, 13607-13612.

12. Beisswenger, B. G., Delucia, E. M., Lapoint, N., Sanford, R. J., and Beisswenger, P. J. (2005) Ketosis leads to increased methylglyoxal production on the Atkins diet, *Ann N Y Acad Sci 1043*, 201-210.

13. Deng, Y., and Yu, P. H. (1999) Simultaneous determination of formaldehyde and methylglyoxal in urine: involvement of semicarbazide-sensitive amine oxidase-mediated deamination in diabetic complications, *J Chromatogr Sci 37*, 317-322.

14. Yu, P. H., Wright, S., Fan, E. H., Lun, Z. R., and Gubisne-Harberle, D. (2003) Physiological and pathological implications of semicarbazide-sensitive amine oxidase, *Biochim Biophys Acta 1647*, 193-199.

15. El Hadri, K., Moldes, M., Mercier, N., Andreani, M., Pairault, J., and Feve, B. (2002) Semicarbazide-sensitive amine oxidase in vascular smooth muscle cells: differentiation-dependent expression and role in glucose uptake, *Arterioscler Thromb Vasc Biol 22*, 89-94.

16. Enrique-Tarancon, G., Marti, L., Morin, N., Lizcano, J. M., Unzeta, M., Sevilla, L., Camps, M., Palacin, M., Testar, X., Carpene, C., and Zorzano, A. (1998) Role of

semicarbazide-sensitive amine oxidase on glucose transport and GLUT4 recruitment to the cell surface in adipose cells, *J Biol Chem 273*, 8025-8032.

17. Thornalley, P. J. (1990) The glyoxalase system: new developments towards functional characterization of a metabolic pathway fundamental to biological life, *Biochem J 269*, 1-11.

18. Vander Jagt, D. L., Robinson, B., Taylor, K. K., and Hunsaker, L. A. (1992) Reduction of trioses by NADPH-dependent aldo-keto reductases. Aldose reductase, methylglyoxal, and diabetic complications, *J Biol Chem 267*, 4364-4369.

19. Thornalley, P. J. (1996) Pharmacology of methylglyoxal: formation, modification of proteins and nucleic acids, and enzymatic detoxification--a role in pathogenesis and antiproliferative chemotherapy, *Gen Pharmacol 27*, 565-573.

20. Yadav, S. K., Singla-Pareek, S. L., Ray, M., Reddy, M. K., and Sopory, S. K. (2005) Methylglyoxal levels in plants under salinity stress are dependent on glyoxalase I and glutathione, *Biochem Biophys Res Commun 337*, 61-67.

21. Adams, C. J., Boult, C. H., Deadman, B. J., Farr, J. M., Grainger, M. N., Manley-Harris, M., and Snow, M. J. (2008) Isolation by HPLC and characterisation of the bioactive fraction of New Zealand manuka (Leptospermum scoparium) honey, *Carbohydr Res 343*, 651-659.

22. Nagao, M., Fujita, Y., Wakabayashi, K., Nukaya, H., Kosuge, T., and Sugimura, T. (1986) Mutagens in coffee and other beverages, *Environ Health Perspect 67*, 89-91.

23. Daglia, M., Papetti, A., Aceti, C., Sordelli, B., Spini, V., and Gazzani, G. (2007) Isolation and determination of alpha-dicarbonyl compounds by RP-HPLC-DAD in

green and roasted coffee, *J Agric Food Chem 55*, 8877-8882.

24. Adams, C. J., Manley-Harris, M., and Molan, P. C. (2009) The origin of methylglyoxal in New Zealand manuka (Leptospermum scoparium) honey, *Carbohydr Res 344*, 1050-1053.

25. Wang, X., Jia, X., Chang, T., Desai, K., and Wu, L. (2008) Attenuation of hypertension development by scavenging methylglyoxal in fructose-treated rats, *J Hypertens 26*, 765-772.

26. Dhar, A., Dhar, I., Jiang, B., Desai, K. M., and Wu, L. (2011) Chronic methylglyoxal infusion by minipump causes pancreatic beta-cell dysfunction and induces type 2 diabetes in Sprague-Dawley rats, *Diabetes 60*, 899-908.

27. Nemet, I., Varga-Defterdarovic, L., and Turk, Z. (2006) Methylglyoxal in food and living organisms, *Mol Nutr Food Res 50*, 1105-1117.

28. Thornalley, P. J., Langborg, A., and Minhas, H. S. (1999) Formation of glyoxal, methylglyoxal and 3-deoxyglucosone in the glycation of proteins by glucose, *Biochem J 344 Pt 1*, 109-116.

29. Fujioka, K., and Shibamoto, T. (2004) Formation of genotoxic dicarbonyl compounds in dietary oils upon oxidation, *Lipids 39*, 481-486.

30. Fatemeh Niyati-Shirkhodaee, T. S. (1993) Gas chromatographic analysis of glyoxal and methylglyoxal formed from lipids and related compounds upon ultraviolet irradiation, *JAgri Food Chem. 41* 227–230.

31. Riboulet-Chavey, A., Pierron, A., Durand, I., Murdaca, J., Giudicelli, J., and Van Obberghen, E. (2006) Methylglyoxal impairs the insulin signaling pathways

independently of the formation of intracellular reactive oxygen species, *Diabetes 55*, 1289-1299.

32. Che, W., Asahi, M., Takahashi, M., Kaneto, H., Okado, A., Higashiyama, S., and Taniguchi, N. (1997) Selective induction of heparin-binding epidermal growth factor-like growth factor by methylglyoxal and 3-deoxyglucosone in rat aortic smooth muscle cells. The involvement of reactive oxygen species formation and a possible implication for atherogenesis in diabetes, *J Biol Chem 272*, 18453-18459.

33. Fiory, F., Lombardi, A., Miele, C., Giudicelli, J., Beguinot, F., and Van Obberghen, E. (2011) Methylglyoxal impairs insulin signalling and insulin action on glucose-induced insulin secretion in the pancreatic beta cell line INS-1E, *Diabetologia 54*, 2941-2952.

34. Chaplen, F. W., Fahl, W. E., and Cameron, D. C. (1996) Method for determination of free intracellular and extracellular methylglyoxal in animal cells grown in culture, *Anal Biochem 238*, 171-178.

35. Figarella, K., Uzcategui, N. L., Zhou, Y., LeFurgey, A., Ouellette, M., Bhattacharjee, H., and Mukhopadhyay, R. (2007) Biochemical characterization of Leishmania major aquaglyceroporin LmAQP1: possible role in volume regulation and osmotaxis, *Mol Microbiol 65*, 1006-1017.

36. Shinohara, M., Thornalley, P. J., Giardino, I., Beisswenger, P., Thorpe, S. R., Onorato, J., and Brownlee, M. (1998) Overexpression of glyoxalase-I in bovine endothelial cells inhibits intracellular advanced glycation endproduct formation and prevents hyperglycemia-induced increases in macromolecular endocytosis, *J Clin Invest 101*, 1142-1147.

37. Jia, X., Olson, D. J., Ross, A. R., and Wu, L. (2006) Structural and functional changes in human insulin induced by methylglyoxal, *FASEB J 20*, 1555-1557.

38. Chang, T., Wang, R., Olson, D. J., Mousseau, D. D., Ross, A. R., and Wu, L. (2011) Modification of Akt1 by methylglyoxal promotes the proliferation of vascular smooth muscle cells, *FASEB J 25*, 1746-1757.

39. Bourajjaj, M., Stehouwer, C. D., van Hinsbergh, V. W., and Schalkwijk, C. G. (2003) Role of methylglyoxal adducts in the development of vascular complications in diabetes mellitus, *Biochem Soc Trans 31*, 1400-1402.

40. Frye, E. B., Degenhardt, T. P., Thorpe, S. R., and Baynes, J. W. (1998) Role of the Maillard reaction in aging of tissue proteins. Advanced glycation end product-dependent increase in imidazolium cross-links in human lens proteins, *J Biol Chem 273*, 18714-18719.

41. Mostafa, A. A., Randell, E. W., Vasdev, S. C., Gill, V. D., Han, Y., Gadag, V., Raouf, A. A., and El Said, H. (2007) Plasma protein advanced glycation end products, carboxymethyl cysteine, and carboxyethyl cysteine, are elevated and related to nephropathy in patients with diabetes, *Mol Cell Biochem 302*, 35-42.

42. Goldin, A., Beckman, J. A., Schmidt, A. M., and Creager, M. A. (2006) Advanced glycation end products: sparking the development of diabetic vascular injury, *Circulation 114*, 597-605.

43. Herbst, T. J., McCarthy, J. B., Tsilibary, E. C., and Furcht, L. T. (1988) Differential effects of laminin, intact type IV collagen, and specific domains of type IV collagen on endothelial cell adhesion and migration, *J Cell Biol 106*, 1365-1373.

44. Haitoglou, C. S., Tsilibary, E. C., Brownlee, M., and Charonis, A. S. (1992) Altered cellular interactions between endothelial cells and nonenzymatically glucosylated laminin/type IV collagen, *J Biol Chem 267*, 12404-12407.

45. Lee, H. J., Howell, S. K., Sanford, R. J., and Beisswenger, P. J. (2005) Methylglyoxal can modify GAPDH activity and structure, *Ann N Y Acad Sci 1043*, 135-145.

46. Morgan, P. E., Dean, R. T., and Davies, M. J. (2002) Inactivation of cellular enzymes by carbonyls and protein-bound glycation/glycoxidation products, *Arch Biochem Biophys 403*, 259-269.

47. Neeper, M., Schmidt, A. M., Brett, J., Yan, S. D., Wang, F., Pan, Y. C., Elliston, K., Stern, D., and Shaw, A. (1992) Cloning and expression of a cell surface receptor for advanced glycosylation end products of proteins, *J Biol Chem 267*, 14998-15004.

48. Thornalley, P. J. (1998) Cell activation by glycated proteins. AGE receptors, receptor recognition factors and functional classification of AGEs, *Cell Mol Biol (Noisy-le-grand) 44*, 1013-1023.

49. Wautier, J. L., Zoukourian, C., Chappey, O., Wautier, M. P., Guillausseau, P. J., Cao, R., Hori, O., Stern, D., and Schmidt, A. M. (1996) Receptor-mediated endothelial cell dysfunction in diabetic vasculopathy. Soluble receptor for advanced glycation end products blocks hyperpermeability in diabetic rats, *J Clin Invest 97*, 238-243.

50. Neumann, A., Schinzel, R., Palm, D., Riederer, P., and Munch, G. (1999) High molecular weight hyaluronic acid inhibits advanced glycation endproduct-induced NF-kappaB activation and cytokine expression, *FEBS Lett 453*, 283-287.

51. Basta, G., Schmidt, A. M., and De Caterina, R. (2004) Advanced glycation end

products and vascular inflammation: implications for accelerated atherosclerosis in diabetes, *Cardiovasc Res 63*, 582-592.

52. Schmidt, A. M., Hasu, M., Popov, D., Zhang, J. H., Chen, J., Yan, S. D., Brett, J., Cao, R., Kuwabara, K., Costache, G., and et al. (1994) Receptor for advanced glycation end products (AGEs) has a central role in vessel wall interactions and gene activation in response to circulating AGE proteins, *Proc Natl Acad Sci U S A 91*, 8807-8811.

53. Bierhaus, A., Illmer, T., Kasper, M., Luther, T., Quehenberger, P., Tritschler, H., Wahl, P., Ziegler, R., Muller, M., and Nawroth, P. P. (1997) Advanced glycation end product (AGE)-mediated induction of tissue factor in cultured endothelial cells is dependent on RAGE, *Circulation 96*, 2262-2271.

54. Wu, L. (2005) The pro-oxidant role of methylglyoxal in mesenteric artery smooth muscle cells, *Can J Physiol Pharmacol 83*, 63-68.

55. Chang, T., Wang, R., and Wu, L. (2005) Methylglyoxal-induced nitric oxide and peroxynitrite production in vascular smooth muscle cells, *Free Radic Biol Med 38*, 286-293.

56. Wu, L., and Juurlink, B. H. (2002) Increased methylglyoxal and oxidative stress in hypertensive rat vascular smooth muscle cells, *Hypertension 39*, 809-814.

57. Du, J., Suzuki, H., Nagase, F., Akhand, A. A., Ma, X. Y., Yokoyama, T., Miyata, T., and Nakashima, I. (2001) Superoxide-mediated early oxidation and activation of ASK1 are important for initiating methylglyoxal-induced apoptosis process, *Free Radic Biol Med 31*, 469-478.

58. Kalapos, M. P., Littauer, A., and de Groot, H. (1993) Has reactive oxygen a role in

methylglyoxal toxicity? A study on cultured rat hepatocytes, *Arch Toxicol 67*, 369-372.

59. Desai, K. M., Chang, T., Wang, H., Banigesh, A., Dhar, A., Liu, J., Untereiner, A., and Wu, L. (2010) Oxidative stress and aging: is methylglyoxal the hidden enemy?, *Can J Physiol Pharmacol 88*, 273-284.

60. Droge, W. (2002) Free radicals in the physiological control of cell function, *Physiol Rev 82*, 47-95.

61. Chance, B., Oshino, N., Sugano, T., and Mayevsky, A. (1973) Basic principles of tissue oxygen determination from mitochondrial signals, *Adv Exp Med Biol 37A*, 277-292.

62. Rosca, M. G., Monnier, V. M., Szweda, L. I., and Weiss, M. F. (2002) Alterations in renal mitochondrial respiration in response to the reactive oxoaldehyde methylglyoxal, *Am J Physiol Renal Physiol 283*, F52-59.

63. Grivennikova, V. G., and Vinogradov, A. D. (2006) Generation of superoxide by the mitochondrial Complex I, *Biochim Biophys Acta 1757*, 553-561.

64. Raha, S., McEachern, G. E., Myint, A. T., and Robinson, B. H. (2000) Superoxides from mitochondrial complex III: the role of manganese superoxide dismutase, *Free Radic Biol Med 29*, 170-180.

65. Kudin, A. P., Bimpong-Buta, N. Y., Vielhaber, S., Elger, C. E., and Kunz, W. S. (2004) Characterization of superoxide-producing sites in isolated brain mitochondria, *J Biol Chem 279*, 4127-4135.

66. Wang, H., Liu, J., and Wu, L. (2009) Methylglyoxal-induced mitochondrial

dysfunction in vascular smooth muscle cells, *Biochem Pharmacol 77*, 1709-1716.

67. Ushio-Fukai, M. (2006) Localizing NADPH oxidase-derived ROS, *Sci STKE 2006*, re8.

68. Gao, L., and Mann, G. E. (2009) Vascular NAD(P)H oxidase activation in diabetes: a double-edged sword in redox signalling, *Cardiovasc Res 82*, 9-20.

69. Ho, C., Lee, P. H., Huang, W. J., Hsu, Y. C., Lin, C. L., and Wang, J. Y. (2007) Methylglyoxal-induced fibronectin gene expression through Ras-mediated NADPH oxidase activation in renal mesangial cells, *Nephrology (Carlton) 12*, 348-356.

70. Dhar, A., Dhar, I., Desai, K. M., and Wu, L. (2010) Methylglyoxal scavengers attenuate endothelial dysfunction induced by methylglyoxal and high concentrations of glucose, *Br J Pharmacol 161*, 1843-1856.

71. Alderton, W. K., Cooper, C. E., and Knowles, R. G. (2001) Nitric oxide synthases: structure, function and inhibition, *Biochem J 357*, 593-615.

72. Wang, X., Chang, T., Jiang, B., Desai, K., and Wu, L. (2007) Attenuation of hypertension development by aminoguanidine in spontaneously hypertensive rats: role of methylglyoxal, *Am J Hypertens 20*, 629-636.

73. Wang, H., Meng, Q. H., Chang, T., and Wu, L. (2006) Fructose-induced peroxynitrite production is mediated by methylglyoxal in vascular smooth muscle cells, *Life Sci 79*, 2448-2454.

74. Chelikani, P., Fita, I., and Loewen, P. C. (2004) Diversity of structures and properties among catalases, *Cell Mol Life Sci 61*, 192-208.

75. Park, Y. S., Koh, Y. H., Takahashi, M., Miyamoto, Y., Suzuki, K., Dohmae, N., Takio,

K., Honke, K., and Taniguchi, N. (2003) Identification of the binding site of methylglyoxal on glutathione peroxidase: methylglyoxal inhibits glutathione peroxidase activity via binding to glutathione binding sites Arg 184 and 185, *Free Radic Res 37*, 205-211.

76. Kang, J. H. (2003) Modification and inactivation of human Cu,Zn-superoxide dismutase by methylglyoxal, *Mol Cells 15*, 194-199.

77. Choudhary, D., Chandra, D., and Kale, R. K. (1997) Influence of methylglyoxal on antioxidant enzymes and oxidative damage, *Toxicol Lett 93*, 141-152.

78. Wu, G., Fang, Y. Z., Yang, S., Lupton, J. R., and Turner, N. D. (2004) Glutathione metabolism and its implications for health, *J Nutr 134*, 489-492.

79. Vander Jagt, D. L., Hunsaker, L. A., Vander Jagt, T. J., Gomez, M. S., Gonzales, D. M., Deck, L. M., and Royer, R. E. (1997) Inactivation of glutathione reductase by 4-hydroxynonenal and other endogenous aldehydes, *Biochem Pharmacol 53*, 1133-1140.

80. Rosca, M. G., Mustata, T. G., Kinter, M. T., Ozdemir, A. M., Kern, T. S., Szweda, L. I., Brownlee, M., Monnier, V. M., and Weiss, M. F. (2005) Glycation of mitochondrial proteins from diabetic rat kidney is associated with excess superoxide formation, *Am J Physiol Renal Physiol 289*, F420-430.

81. Morcos, M., Du, X., Pfisterer, F., Hutter, H., Sayed, A. A., Thornalley, P., Ahmed, N., Baynes, J., Thorpe, S., Kukudov, G., Schlotterer, A., Bozorgmehr, F., El Baki, R. A., Stern, D., Moehrlen, F., Ibrahim, Y., Oikonomou, D., Hamann, A., Becker, C., Zeier, M., Schwenger, V., Miftari, N., Humpert, P., Hammes, H. P., Buechler, M., Bierhaus,

A., Brownlee, M., and Nawroth, P. P. (2008) Glyoxalase-1 prevents mitochondrial protein modification and enhances lifespan in Caenorhabditis elegans, *Aging Cell 7*, 260-269.

82. Yamagishi, S., Nakamura, K., Matsui, T., Ueda, S., Fukami, K., and Okuda, S. (2008) Agents that block advanced glycation end product (AGE)-RAGE (receptor for AGEs)-oxidative stress system: a novel therapeutic strategy for diabetic vascular complications, *Expert Opin Investig Drugs 17*, 983-996.

83. Eckel, R. H., Grundy, S. M., and Zimmet, P. Z. (2005) The metabolic syndrome, *Lancet 365*, 1415-1428.

84. Thornalley, P. J., Hooper, N. I., Jennings, P. E., Florkowski, C. M., Jones, A. F., Lunec, J., and Barnett, A. H. (1989) The human red blood cell glyoxalase system in diabetes mellitus, *Diabetes Res Clin Pract 7*, 115-120.

85. Dhar, A., Desai, K. M., and Wu, L. (2010) Alagebrium attenuates acute methylglyoxal-induced glucose intolerance in Sprague-Dawley rats, *Br J Pharmacol 159*, 166-175.

86. McLellan, A. C., Thornalley, P. J., Benn, J., and Sonksen, P. H. (1994) Glyoxalase system in clinical diabetes mellitus and correlation with diabetic complications, *Clin Sci (Lond) 87*, 21-29.

87. Phillips, S. A., Mirrlees, D., and Thornalley, P. J. (1993) Modification of the glyoxalase system in streptozotocin-induced diabetic rats. Effect of the aldose reductase inhibitor Statil, *Biochem Pharmacol 46*, 805-811.

88. Forbes, J. M., Yee, L. T., Thallas, V., Lassila, M., Candido, R., Jandeleit-Dahm, K. A.,

Thomas, M. C., Burns, W. C., Deemer, E. K., Thorpe, S. R., Cooper, M. E., and Allen, T. J. (2004) Advanced glycation end product interventions reduce diabetes-accelerated atherosclerosis, *Diabetes 53*, 1813-1823.

89. Rumble, J. R., Cooper, M. E., Soulis, T., Cox, A., Wu, L., Youssef, S., Jasik, M., Jerums, G., and Gilbert, R. E. (1997) Vascular hypertrophy in experimental diabetes. Role of advanced glycation end products, *J Clin Invest 99*, 1016-1027.

90. Stitt, A. W., Li, Y. M., Gardiner, T. A., Bucala, R., Archer, D. B., and Vlassara, H. (1997) Advanced glycation end products (AGEs) co-localize with AGE receptors in the retinal vasculature of diabetic and of AGE-infused rats, *Am J Pathol 150*, 523-531.

91. Beisswenger, P. J., Makita, Z., Curphey, T. J., Moore, L. L., Jean, S., Brinck-Johnsen, T., Bucala, R., and Vlassara, H. (1995) Formation of immunochemical advanced glycosylation end products precedes and correlates with early manifestations of renal and retinal disease in diabetes, *Diabetes 44*, 824-829.

92. Oldfield, M. D., Bach, L. A., Forbes, J. M., Nikolic-Paterson, D., McRobert, A., Thallas, V., Atkins, R. C., Osicka, T., Jerums, G., and Cooper, M. E. (2001) Advanced glycation end products cause epithelial-myofibroblast transdifferentiation via the receptor for advanced glycation end products (RAGE), *J Clin Invest 108*, 1853-1863.

93. Hammes, H. P., Martin, S., Federlin, K., Geisen, K., and Brownlee, M. (1991) Aminoguanidine treatment inhibits the development of experimental diabetic retinopathy, *Proc Natl Acad Sci U S A 88*, 11555-11558.

94. Tan, K. C., Chow, W. S., Ai, V. H., Metz, C., Bucala, R., and Lam, K. S. (2002) Advanced glycation end products and endothelial dysfunction in type 2 diabetes,

Diabetes Care 25, 1055-1059.

95. Ogawa, S., Nakayama, K., Nakayama, M., Mori, T., Matsushima, M., Okamura, M., Senda, M., Nako, K., Miyata, T., and Ito, S. (2010) Methylglyoxal is a predictor in type 2 diabetic patients of intima-media thickening and elevation of blood pressure, *Hypertension 56*, 471-476.

96. Inoguchi, T., Li, P., Umeda, F., Yu, H. Y., Kakimoto, M., Imamura, M., Aoki, T., Etoh, T., Hashimoto, T., Naruse, M., Sano, H., Utsumi, H., and Nawata, H. (2000) High glucose level and free fatty acid stimulate reactive oxygen species production through protein kinase C--dependent activation of NAD(P)H oxidase in cultured vascular cells, *Diabetes 49*, 1939-1945.

97. Nishikawa, T., Edelstein, D., Du, X. L., Yamagishi, S., Matsumura, T., Kaneda, Y., Yorek, M. A., Beebe, D., Oates, P. J., Hammes, H. P., Giardino, I., and Brownlee, M. (2000) Normalizing mitochondrial superoxide production blocks three pathways of hyperglycaemic damage, *Nature 404*, 787-790.

98. Evans, J. L., Goldfine, I. D., Maddux, B. A., and Grodsky, G. M. (2002) Oxidative stress and stress-activated signaling pathways: a unifying hypothesis of type 2 diabetes, *Endocr Rev 23*, 599-622.

99. Cosentino, F., Hishikawa, K., Katusic, Z. S., and Luscher, T. F. (1997) High glucose increases nitric oxide synthase expression and superoxide anion generation in human aortic endothelial cells, *Circulation 96*, 25-28.

100. Pacher, P., Obrosova, I. G., Mabley, J. G., and Szabo, C. (2005) Role of nitrosative stress and peroxynitrite in the pathogenesis of diabetic complications. Emerging new

therapeutical strategies, *Curr Med Chem 12*, 267-275.

101. Giugliano, D., Marfella, R., Coppola, L., Verrazzo, G., Acampora, R., Giunta, R., Nappo, F., Lucarelli, C., and D'Onofrio, F. (1997) Vascular effects of acute hyperglycemia in humans are reversed by L-arginine. Evidence for reduced availability of nitric oxide during hyperglycemia, *Circulation 95*, 1783-1790.

102. Spitaler, M. M., and Graier, W. F. (2002) Vascular targets of redox signalling in diabetes mellitus, *Diabetologia 45*, 476-494.

103. Mendez, J. I., Nicholson, W. J., and Taylor, W. R. (2005) SOD isoforms and signaling in blood vessels: evidence for the importance of ROS compartmentalization, *Arterioscler Thromb Vasc Biol 25*, 887-888.

104. Ho, F. M., Liu, S. H., Liau, C. S., Huang, P. J., and Lin-Shiau, S. Y. (2000) High glucose-induced apoptosis in human endothelial cells is mediated by sequential activations of c-Jun NH(2)-terminal kinase and caspase-3, *Circulation 101*, 2618-2624.

105. Srinivasan, S., Hatley, M. E., Bolick, D. T., Palmer, L. A., Edelstein, D., Brownlee, M., and Hedrick, C. C. (2004) Hyperglycaemia-induced superoxide production decreases eNOS expression via AP-1 activation in aortic endothelial cells, *Diabetologia 47*, 1727-1734.

106. Brownlee, M. (2001) Biochemistry and molecular cell biology of diabetic complications, *Nature 414*, 813-820.

107. Du, X. L., Edelstein, D., Rossetti, L., Fantus, I. G., Goldberg, H., Ziyadeh, F., Wu, J., and Brownlee, M. (2000) Hyperglycemia-induced mitochondrial superoxide

overproduction activates the hexosamine pathway and induces plasminogen activator inhibitor-1 expression by increasing Sp1 glycosylation, *Proc Natl Acad Sci U S A 97*, 12222-12226.

108. Du, X. L., Edelstein, D., Dimmeler, S., Ju, Q., Sui, C., and Brownlee, M. (2001) Hyperglycemia inhibits endothelial nitric oxide synthase activity by posttranslational modification at the Akt site, *J Clin Invest 108*, 1341-1348.

109. Kolm-Litty, V., Sauer, U., Nerlich, A., Lehmann, R., and Schleicher, E. D. (1998) High glucose-induced transforming growth factor beta1 production is mediated by the hexosamine pathway in porcine glomerular mesangial cells, *J Clin Invest 101*, 160-169.

110. Queisser, M. A., Yao, D., Geisler, S., Hammes, H. P., Lochnit, G., Schleicher, E. D., Brownlee, M., and Preissner, K. T. (2010) Hyperglycemia impairs proteasome function by methylglyoxal, *Diabetes 59*, 670-678.

111. Yao, D., Taguchi, T., Matsumura, T., Pestell, R., Edelstein, D., Giardino, I., Suske, G., Rabbani, N., Thornalley, P. J., Sarthy, V. P., Hammes, H. P., and Brownlee, M. (2007) High glucose increases angiopoietin-2 transcription in microvascular endothelial cells through methylglyoxal modification of mSin3A, *J Biol Chem 282*, 31038-31045.

112. Nishizuka, Y. (1988) The molecular heterogeneity of protein kinase C and its implications for cellular regulation, *Nature 334*, 661-665.

113. Geraldes, P., and King, G. L. (2010) Activation of protein kinase C isoforms and its impact on diabetic complications, *Circ Res 106*, 1319-1331.

114. Nishizuka, Y. (1992) Intracellular signaling by hydrolysis of phospholipids and

activation of protein kinase C, *Science 258*, 607-614.

115. Williams, B. (1995) Glucose-induced vascular smooth muscle dysfunction: the role of protein kinase C, *J Hypertens 13*, 477-486.

116. Porte, D., Jr., and Schwartz, M. W. (1996) Diabetes complications: why is glucose potentially toxic?, *Science 272*, 699-700.

117. Yasunari, K., Kohno, M., Kano, H., Yokokawa, K., Minami, M., and Yoshikawa, J. (1997) Mechanisms of action of troglitazone in the prevention of high glucose-induced migration and proliferation of cultured coronary smooth muscle cells, *Circ Res 81*, 953-962.

118. Koya, D., Jirousek, M. R., Lin, Y. W., Ishii, H., Kuboki, K., and King, G. L. (1997) Characterization of protein kinase C beta isoform activation on the gene expression of transforming growth factor-beta, extracellular matrix components, and prostanoids in the glomeruli of diabetic rats, *J Clin Invest 100*, 115-126.

119. Beckman, J. A., Goldfine, A. B., Gordon, M. B., Garrett, L. A., and Creager, M. A. (2002) Inhibition of protein kinase Cbeta prevents impaired endothelium-dependent vasodilation caused by hyperglycemia in humans, *Circ Res 90*, 107-111.

120. Aiello, L. P., Davis, M. D., Girach, A., Kles, K. A., Milton, R. C., Sheetz, M. J., Vignati, L., and Zhi, X. E. (2006) Effect of ruboxistaurin on visual loss in patients with diabetic retinopathy, *Ophthalmology 113*, 2221-2230.

121. Scivittaro, V., Ganz, M. B., and Weiss, M. F. (2000) AGEs induce oxidative stress and activate protein kinase C-beta(II) in neonatal mesangial cells, *Am J Physiol Renal Physiol 278*, F676-683.

122. Forbes, J. M., Cooper, M. E., Oldfield, M. D., and Thomas, M. C. (2003) Role of advanced glycation end products in diabetic nephropathy, *J Am Soc Nephrol 14*, S254-258.

123. Thallas-Bonke, V., Lindschau, C., Rizkalla, B., Bach, L. A., Boner, G., Meier, M., Haller, H., Cooper, M. E., and Forbes, J. M. (2004) Attenuation of extracellular matrix accumulation in diabetic nephropathy by the advanced glycation end product cross-link breaker ALT-711 via a protein kinase C-alpha-dependent pathway, *Diabetes 53*, 2921-2930.

124. Pieper, G. M., and Riaz ul, H. (1997) Activation of nuclear factor-kappaB in cultured endothelial cells by increased glucose concentration: prevention by calphostin C, *J Cardiovasc Pharmacol 30*, 528-532.

125. Barnes, P. J., and Karin, M. (1997) Nuclear factor-kappaB: a pivotal transcription factor in chronic inflammatory diseases, *N Engl J Med 336*, 1066-1071.

126. Hattori, Y., Hattori, S., Sato, N., and Kasai, K. (2000) High-glucose-induced nuclear factor kappaB activation in vascular smooth muscle cells, *Cardiovasc Res 46*, 188-197.

127. Patel, S., and Santani, D. (2009) Role of NF-kappa B in the pathogenesis of diabetes and its associated complications, *Pharmacol Rep 61*, 595-603.

128. Chen, S., Khan, Z. A., Cukiernik, M., and Chakrabarti, S. (2003) Differential activation of NF-kappa B and AP-1 in increased fibronectin synthesis in target organs of diabetic complications, *Am J Physiol Endocrinol Metab 284*, E1089-1097.

129. Kim, J., Son, J. W., Lee, J. A., Oh, Y. S., and Shinn, S. H. (2004) Methylglyoxal

induces apoptosis mediated by reactive oxygen species in bovine retinal pericytes, *J Korean Med Sci 19*, 95-100.

130. Okamoto, T., Yamagishi, S., Inagaki, Y., Amano, S., Koga, K., Abe, R., Takeuchi, M., Ohno, S., Yoshimura, A., and Makita, Z. (2002) Angiogenesis induced by advanced glycation end products and its prevention by cerivastatin, *FASEB J 16*, 1928-1930.

131. Wang, X., Desai, K., Chang, T., and Wu, L. (2005) Vascular methylglyoxal metabolism and the development of hypertension, *J Hypertens 23*, 1565-1573.

132. Wang, X., Desai, K., Clausen, J. T., and Wu, L. (2004) Increased methylglyoxal and advanced glycation end products in kidney from spontaneously hypertensive rats, *Kidney Int 66*, 2315-2321.

133. McNulty, M., Mahmud, A., and Feely, J. (2007) Advanced glycation end-products and arterial stiffness in hypertension, *Am J Hypertens 20*, 242-247.

134. Berlanga, J., Cibrian, D., Guillen, I., Freyre, F., Alba, J. S., Lopez-Saura, P., Merino, N., Aldama, A., Quintela, A. M., Triana, M. E., Montequin, J. F., Ajamieh, H., Urquiza, D., Ahmed, N., and Thornalley, P. J. (2005) Methylglyoxal administration induces diabetes-like microvascular changes and perturbs the healing process of cutaneous wounds, *Clin Sci (Lond) 109*, 83-95.

135. Golej, J., Hoeger, H., Radner, W., Unfried, G., and Lubec, G. (1998) Oral administration of methylglyoxal leads to kidney collagen accumulation in the mouse, *Life Sci 63*, 801-807.

136. Schalkwijk, C. G., and Stehouwer, C. D. (2005) Vascular complications in diabetes mellitus: the role of endothelial dysfunction, *Clin Sci (Lond) 109*, 143-159.

137. De Vriese, A. S., Verbeuren, T. J., Van de Voorde, J., Lameire, N. H., and Vanhoutte, P. M. (2000) Endothelial dysfunction in diabetes, *Br J Pharmacol 130*, 963-974.

138. Montagnani, M., Chen, H., Barr, V. A., and Quon, M. J. (2001) Insulin-stimulated activation of eNOS is independent of Ca2+ but requires phosphorylation by Akt at Ser(1179), *J Biol Chem 276*, 30392-30398.

139. Gornik, H. L., and Creager, M. A. (2004) Arginine and endothelial and vascular health, *J Nutr 134*, 2880S-2887S.

140. Vasdev, S., Ford, C. A., Longerich, L., Parai, S., Gadag, V., and Wadhawan, S. (1998) Aldehyde induced hypertension in rats: prevention by N-acetyl cysteine, *Artery 23*, 10-36.

141. Vasdev, S., Ford, C. A., Longerich, L., Gadag, V., and Wadhawan, S. (1998) Role of aldehydes in fructose induced hypertension, *Mol Cell Biochem 181*, 1-9.

142. Brouwers, O., Niessen, P. M., Haenen, G., Miyata, T., Brownlee, M., Stehouwer, C. D., De Mey, J. G., and Schalkwijk, C. G. (2010) Hyperglycaemia-induced impairment of endothelium-dependent vasorelaxation in rat mesenteric arteries is mediated by intracellular methylglyoxal levels in a pathway dependent on oxidative stress, *Diabetologia 53*, 989-1000.

143. Chang, T., Untereiner, A., Liu, J., and Wu, L. (2010) Interaction of methylglyoxal and hydrogen sulfide in rat vascular smooth muscle cells, *Antioxid Redox Signal 12*, 1093-1100.

144. Randell, E. W., Vasdev, S., and Gill, V. (2005) Measurement of methylglyoxal in rat tissues by electrospray ionization mass spectrometry and liquid chromatography, *J*

Pharmacol Toxicol Methods 51, 153-157.

145. Shepherd, P. R., and Kahn, B. B. (1999) Glucose transporters and insulin action--implications for insulin resistance and diabetes mellitus, *N Engl J Med 341*, 248-257.

146. Dhar, A., Desai, K., Kazachmov, M., Yu, P., and Wu, L. (2008) Methylglyoxal production in vascular smooth muscle cells from different metabolic precursors, *Metabolism 57*, 1211-1220.

147. Jia, X., and Wu, L. (2007) Accumulation of endogenous methylglyoxal impaired insulin signaling in adipose tissue of fructose-fed rats, *Mol Cell Biochem 306*, 133-139.

148. Slot, J. W., Geuze, H. J., Gigengack, S., Lienhard, G. E., and James, D. E. (1991) Immuno-localization of the insulin regulatable glucose transporter in brown adipose tissue of the rat, *J Cell Biol 113*, 123-135.

149. Ducluzeau, P. H., Perretti, N., Laville, M., Andreelli, F., Vega, N., Riou, J. P., and Vidal, H. (2001) Regulation by insulin of gene expression in human skeletal muscle and adipose tissue. Evidence for specific defects in type 2 diabetes, *Diabetes 50*, 1134-1142.

150. Alexander, M., Curtis, G., Avruch, J., and Goodman, H. M. (1985) Insulin regulation of protein biosynthesis in differentiated 3T3 adipocytes. Regulation of glyceraldehyde-3-phosphate dehydrogenase, *J Biol Chem 260*, 11978-11985.

151. Pfleiderer, G., Thoner, M., and Wachsmuth, E. D. (1975) Histological examination of the aldolase monomer composition of cells from human kidney and hypernephroid

carcinoma, *Beitrage zur Pathologie 156*, 266-279.

152. Kador, P. F. (1988) The role of aldose reductase in the development of diabetic complications, *Med Res Rev 8*, 325-352.

153. Cheng, H. M., and Gonzalez, R. G. (1986) The effect of high glucose and oxidative stress on lens metabolism, aldose reductase, and senile cataractogenesis, *Metabolism 35*, 10-14.

154. Ghahary, A., Luo, J. M., Gong, Y. W., Chakrabarti, S., Sima, A. A., and Murphy, L. J. (1989) Increased renal aldose reductase activity, immunoreactivity, and mRNA in streptozocin-induced diabetic rats, *Diabetes 38*, 1067-1071.

155. Munnich, A., Besmond, C., Darquy, S., Reach, G., Vaulont, S., Dreyfus, J. C., and Kahn, A. (1985) Dietary and hormonal regulation of aldolase B gene expression, *J Clin Invest 75*, 1045-1052.

156. Cross, N. C., de Franchis, R., Sebastio, G., Dazzo, C., Tolan, D. R., Gregori, C., Odievre, M., Vidailhet, M., Romano, V., Mascali, G., and et al. (1990) Molecular analysis of aldolase B genes in hereditary fructose intolerance, *Lancet 335*, 306-309.

157. Cross, N. C., Tolan, D. R., and Cox, T. M. (1988) Catalytic deficiency of human aldolase B in hereditary fructose intolerance caused by a common missense mutation, *Cell 53*, 881-885.

158. Johnson, R. J., Segal, M. S., Sautin, Y., Nakagawa, T., Feig, D. I., Kang, D. H., Gersch, M. S., Benner, S., and Sanchez-Lozada, L. G. (2007) Potential role of sugar (fructose) in the epidemic of hypertension, obesity and the metabolic syndrome, diabetes, kidney disease, and cardiovascular disease, *Am J Clin Nutr 86*, 899-906.

159. Basciano, H., Federico, L., and Adeli, K. (2005) Fructose, insulin resistance, and metabolic dyslipidemia, *Nutr Metab (Lond) 2*, 5.

160. Ferder, L., Ferder, M. D., and Inserra, F. (2010) The role of high-fructose corn syrup in metabolic syndrome and hypertension, *Curr Hypertens Rep 12*, 105-112.

161. Tappy, L., and Le, K. A. (2010) Metabolic effects of fructose and the worldwide increase in obesity, *Physiol Rev 90*, 23-46.

162. Kawasaki, T., Akanuma, H., and Yamanouchi, T. (2002) Increased fructose concentrations in blood and urine in patients with diabetes, *Diabetes Care 25*, 353-357.

163. Kawasaki, T., Igarashi, K., Ogata, N., Oka, Y., Ichiyanagi, K., and Yamanouchi, T. (2012) Markedly increased serum and urinary fructose concentrations in diabetic patients with ketoacidosis or ketosis, *Acta Diabetol* 49, 119-123.

164. Shiota, M., Galassetti, P., Monohan, M., Neal, D. W., and Cherrington, A. D. (1998) Small amounts of fructose markedly augment net hepatic glucose uptake in the conscious dog, *Diabetes 47*, 867-873.

165. Beutler, H. (1984) *D-Fructose. In Methods of Enzymatic Analysis.*, Vol. 4, Verlag Chemie, Weinheim, Germany.

166. Hui, H., Huang, D., McArthur, D., Nissen, N., Boros, L. G., and Heaney, A. P. (2009) Direct spectrophotometric determination of serum fructose in pancreatic cancer patients, *Pancreas 38*, 706-712.

167. Richthoff, J., Spano, M., Giwercman, Y. L., Frohm, B., Jepson, K., Malm, J., Elzanaty, S., Stridsberg, M., and Giwercman, A. (2002) The impact of testicular and accessory

sex gland function on sperm chromatin integrity as assessed by the sperm chromatin structure assay (SCSA), *Hum Reprod 17*, 3162-3169.

168. Sucha, R., Ulcova-Gallova, Z., Pavelkova-Seifertova, P., Krizanovska, K., Bouse, V., Svabek, L., Rokyta, P., Balvin, M., Pecen, L., and Rokyta, Z. (2002) [Fructose and glucose in follicular fluid and serum of women undergoing stimulation in an in vitro fertilization program], *Ceska Gynekol 67*, 144-148.

169. Kim, H. S., Paik, H. Y., Lee, K. U., Lee, H. K., and Min, H. K. (1988) Effects of several simple sugars on serum glucose and serum fructose levels in normal and diabetic subjects, *Diabetes Res Clin Pract 4*, 281-287.

170. Mayes, P. A. (1993) Intermediary metabolism of fructose, *Am J Clin Nutr 58*, 754S-765S.

171. Barone, S., Fussell, S. L., Singh, A. K., Lucas, F., Xu, J., Kim, C., Wu, X., Yu, Y., Amlal, H., Seidler, U., Zuo, J., and Soleimani, M. (2009) Slc2a5 (Glut5) is essential for the absorption of fructose in the intestine and generation of fructose-induced hypertension, *J Biol Chem 284*, 5056-5066.

172. Mendeloff, A. I., and Weichselbaum, T. E. (1953) Role of the human liver in the assimilation of intravenously administered fructose, *Metabolism 2*, 450-458.

173. Bode, C., Durr, H. K., and Bode, J. C. (1981) Effect of fructose feeding on the activity of enzymes of glycolysis, gluconeogenesis, and the pentose phosphate shunt in the liver and jejunal mucosa of rats, *Horm Metab Res 13*, 379-383.

174. Bar-On, H., and Stein, Y. (1968) Effect of glucose and fructose administration on lipid metabolism in the rat, *J Nutr 94*, 95-105.

175. Darakhshan, F., Hajduch, E., Kristiansen, S., Richter, E. A., and Hundal, H. S. (1998) Biochemical and functional characterization of the GLUT5 fructose transporter in rat skeletal muscle, *Biochem J 336 (Pt 2)*, 361-366.

176. Hallfrisch, J., Ellwood, K. C., Michaelis, O. E. t., Reiser, S., O'Dorisio, T. M., and Prather, E. S. (1983) Effects of dietary fructose on plasma glucose and hormone responses in normal and hyperinsulinemic men, *J Nutr 113*, 1819-1826.

177. Israel, K. D., Michaelis, O. E. t., Reiser, S., and Keeney, M. (1983) Serum uric acid, inorganic phosphorus, and glutamic-oxalacetic transaminase and blood pressure in carbohydrate-sensitive adults consuming three different levels of sucrose, *Ann Nutr Metab 27*, 425-435.

178. Reaven, G. M. (1991) Abnormalities of carbohydrate and lipoprotein metabolism in patients with hypertension. Relationship to obesity, *Ann Epidemiol 1*, 305-311.

179. Reiser, S., Powell, A. S., Scholfield, D. J., Panda, P., Ellwood, K. C., and Canary, J. J. (1989) Blood lipids, lipoproteins, apoproteins, and uric acid in men fed diets containing fructose or high-amylose cornstarch, *Am J Clin Nutr 49*, 832-839.

180. Yudkin, J. (1972) Sugar and disease, *Nature 239*, 197-199.

181. Schalkwijk, C. G., Stehouwer, C. D., and van Hinsbergh, V. W. (2004) Fructose-mediated non-enzymatic glycation: sweet coupling or bad modification, *Diabetes Metab Res Rev 20*, 369-382.

182. Sanchez-Lozada, L. G., Tapia, E., Jimenez, A., Bautista, P., Cristobal, M., Nepomuceno, T., Soto, V., Avila-Casado, C., Nakagawa, T., Johnson, R. J., Herrera-Acosta, J., and Franco, M. (2007) Fructose-induced metabolic syndrome is

associated with glomerular hypertension and renal microvascular damage in rats, *Am J Physiol Renal Physiol 292*, F423-429.

183. Kang, D. H., Park, S. K., Lee, I. K., and Johnson, R. J. (2005) Uric acid-induced C-reactive protein expression: implication on cell proliferation and nitric oxide production of human vascular cells, *J Am Soc Nephrol 16*, 3553-3562.

184. Sautin, Y. Y., Nakagawa, T., Zharikov, S., and Johnson, R. J. (2007) Adverse effects of the classic antioxidant uric acid in adipocytes: NADPH oxidase-mediated oxidative/nitrosative stress, *Am J Physiol Cell Physiol 293*, C584-596.

185. Raben, A., Vasilaras, T. H., Moller, A. C., and Astrup, A. (2002) Sucrose compared with artificial sweeteners: different effects on ad libitum food intake and body weight after 10 wk of supplementation in overweight subjects, *Am J Clin Nutr 76*, 721-729.

186. Nakagawa, T., Hu, H., Zharikov, S., Tuttle, K. R., Short, R. A., Glushakova, O., Ouyang, X., Feig, D. I., Block, E. R., Herrera-Acosta, J., Patel, J. M., and Johnson, R. J. (2006) A causal role for uric acid in fructose-induced metabolic syndrome, *Am J Physiol Renal Physiol 290*, F625-631.

187. Kovacic, P. B., Chowdhury, H. H., Velebit, J., Kreft, M., Jensen, J., and Zorec, R. (2011) New insights into cytosolic glucose levels during differentiation of 3T3-L1 fibroblasts into adipocytes, *J Biol Chem 286*, 13370-13381.

188. Singer, P., Godicke, W., Voigt, S., Hajdu, I., and Weiss, M. (1985) Postprandial hyperinsulinemia in patients with mild essential hypertension, *Hypertension 7*, 182-186.

189. Salonen, J. T., Lakka, T. A., Lakka, H. M., Valkonen, V. P., Everson, S. A., and Kaplan,

G. A. (1998) Hyperinsulinemia is associated with the incidence of hypertension and dyslipidemia in middle-aged men, *Diabetes 47*, 270-275.

190. Kreisberg, R. A., Boshell, B. R., DiPlacido, J., and Roddam, R. F. (1967) Insulin secretion in obesity, *N Engl J Med 276*, 314-319.

191. Yalow, R. S., Glick, S. M., Roth, J., and Berson, S. A. (1965) Plasma insulin and growth hormone levels in obesity and diabetes, *Ann N Y Acad Sci 131*, 357-373.

192. Penicaud, L., Ferre, P., Terretaz, J., Kinebanyan, M. F., Leturque, A., Dore, E., Girard, J., Jeanrenaud, B., and Picon, L. (1987) Development of obesity in Zucker rats. Early insulin resistance in muscles but normal sensitivity in white adipose tissue, *Diabetes 36*, 626-631.

193. Litherland, G. J., Hajduch, E., Gould, G. W., and Hundal, H. S. (2004) Fructose transport and metabolism in adipose tissue of Zucker rats: diminished GLUT5 activity during obesity and insulin resistance, *Mol Cell Biochem 261*, 23-33.

194. Hajduch, E., Litherland, G. J., Turban, S., Brot-Laroche, E., and Hundal, H. S. (2003) Insulin regulates the expression of the GLUT5 transporter in L6 skeletal muscle cells, *FEBS Lett 549*, 77-82.

195. Zeng, J., and Davies, M. J. (2005) Evidence for the formation of adducts and S-(carboxymethyl)cysteine on reaction of alpha-dicarbonyl compounds with thiol groups on amino acids, peptides, and proteins, *Chem Res Toxicol 18*, 1232-1241.

196. Beisswenger, P. J., Howell, S. K., Touchette, A. D., Lal, S., and Szwergold, B. S. (1999) Metformin reduces systemic methylglyoxal levels in type 2 diabetes, *Diabetes 48*, 198-202.

197. Freedman, B. I., Wuerth, J. P., Cartwright, K., Bain, R. P., Dippe, S., Hershon, K., Mooradian, A. D., and Spinowitz, B. S. (1999) Design and baseline characteristics for the aminoguanidine Clinical Trial in Overt Type 2 Diabetic Nephropathy (ACTION II), *Control Clin Trials 20*, 493-510.

198. Desai, K., and Wu, L. (2007) Methylglyoxal and advanced glycation endproducts: new therapeutic horizons?, *Recent Patents Cardiovasc Drug Discov 2*, 89-99.

199. Candido, R., Forbes, J. M., Thomas, M. C., Thallas, V., Dean, R. G., Burns, W. C., Tikellis, C., Ritchie, R. H., Twigg, S. M., Cooper, M. E., and Burrell, L. M. (2003) A breaker of advanced glycation end products attenuates diabetes-induced myocardial structural changes, *Circ Res 92*, 785-792.

200. Vaitkevicius, P. V., Lane, M., Spurgeon, H., Ingram, D. K., Roth, G. S., Egan, J. J., Vasan, S., Wagle, D. R., Ulrich, P., Brines, M., Wuerth, J. P., Cerami, A., and Lakatta, E. G. (2001) A cross-link breaker has sustained effects on arterial and ventricular properties in older rhesus monkeys, *Proc Natl Acad Sci U S A 98*, 1171-1175.

201. Wolffenbuttel, B. H., Boulanger, C. M., Crijns, F. R., Huijberts, M. S., Poitevin, P., Swennen, G. N., Vasan, S., Egan, J. J., Ulrich, P., Cerami, A., and Levy, B. I. (1998) Breakers of advanced glycation end products restore large artery properties in experimental diabetes, *Proc Natl Acad Sci U S A 95*, 4630-4634.

202. Vasan, S., Foiles, P., and Founds, H. (2003) Therapeutic potential of breakers of advanced glycation end product-protein crosslinks, *Arch Biochem Biophys 419*, 89-96.

203. Kass, D. A., Shapiro, E. P., Kawaguchi, M., Capriotti, A. R., Scuteri, A., deGroof, R.

C., and Lakatta, E. G. (2001) Improved arterial compliance by a novel advanced glycation end-product crosslink breaker, *Circulation 104*, 1464-1470.

204. Susic, D., Varagic, J., Ahn, J., and Frohlich, E. D. (2004) Crosslink breakers: a new approach to cardiovascular therapy, *Curr Opin Cardiol 19*, 336-340.

205. Desai, K., and Wu, L. (2007) Methylglyoxal and advanced glycation endproducts: new therapeutic horizons?, *Recent Pat Cardiovasc Drug Discov 2*, 89-99.

206. Yang, S., Litchfield, J. E., and Baynes, J. W. (2003) AGE-breakers cleave model compounds, but do not break Maillard crosslinks in skin and tail collagen from diabetic rats, *Arch Biochem Biophys 412*, 42-46.

207. Thornalley, P. J., Yurek-George, A., and Argirov, O. K. (2000) Kinetics and mechanism of the reaction of aminoguanidine with the alpha-oxoaldehydes glyoxal, methylglyoxal, and 3-deoxyglucosone under physiological conditions, *Biochem Pharmacol 60*, 55-65.

208. Chang, K. C., Tseng, C. D., Wu, M. S., Liang, J. T., Tsai, M. S., Cho, Y. L., and Tseng, Y. Z. (2006) Aminoguanidine prevents arterial stiffening in a new rat model of type 2 diabetes, *Eur J Clin Invest 36*, 528-535.

209. Huijberts, M. S., Wolffenbuttel, B. H., Boudier, H. A., Crijns, F. R., Kruseman, A. C., Poitevin, P., and Levy, B. I. (1993) Aminoguanidine treatment increases elasticity and decreases fluid filtration of large arteries from diabetic rats, *J Clin Invest 92*, 1407-1411.

210. Brownlee, M., Vlassara, H., Kooney, A., Ulrich, P., and Cerami, A. (1986) Aminoguanidine prevents diabetes-induced arterial wall protein cross-linking, *Science*

232, 1629-1632.

211. Chan, V., Hoey, A., and Brown, L. (2006) Improved cardiovascular function with aminoguanidine in DOCA-salt hypertensive rats, *Br J Pharmacol 148*, 902-908.

212. Misko, T. P., Moore, W. M., Kasten, T. P., Nickols, G. A., Corbett, J. A., Tilton, R. G., McDaniel, M. L., Williamson, J. R., and Currie, M. G. (1993) Selective inhibition of the inducible nitric oxide synthase by aminoguanidine, *Eur J Pharmacol 233*, 119-125.

213. Hong, H. J., Loh, S. H., and Yen, M. H. (2000) Suppression of the development of hypertension by the inhibitor of inducible nitric oxide synthase, *Br J Pharmacol 131*, 631-637.

214. Crijns, F. R., Struijker Boudier, H. A., and Wolffenbuttel, B. H. (1998) Arteriolar reactivity in conscious diabetic rats: influence of aminoguanidine treatment, *Diabetes 47*, 918-923.

215. Hill, M. A., and Ege, E. A. (1994) Active and passive mechanical properties of isolated arterioles from STZ-induced diabetic rats. Effect of aminoguanidine treatment, *Diabetes 43*, 1450-1456.

216. Rodriguez-Manas, L., Angulo, J., Vallejo, S., Peiro, C., Sanchez-Ferrer, A., Cercas, E., Lopez-Doriga, P., and Sanchez-Ferrer, C. F. (2003) Early and intermediate Amadori glycosylation adducts, oxidative stress, and endothelial dysfunction in the streptozotocin-induced diabetic rats vasculature, *Diabetologia 46*, 556-566.

217. Bucala, R., Tracey, K. J., and Cerami, A. (1991) Advanced glycosylation products quench nitric oxide and mediate defective endothelium-dependent vasodilatation in

experimental diabetes, *J Clin Invest 87*, 432-438.

218. Su, J., Lucchesi, P. A., Gonzalez-Villalobos, R. A., Palen, D. I., Rezk, B. M., Suzuki, Y., Boulares, H. A., and Matrougui, K. (2008) Role of advanced glycation end products with oxidative stress in resistance artery dysfunction in type 2 diabetic mice, *Arterioscler Thromb Vasc Biol 28*, 1432-1438.

219. Yu, P. H., and Zuo, D. M. (1997) Aminoguanidine inhibits semicarbazide-sensitive amine oxidase activity: implications for advanced glycation and diabetic complications, *Diabetologia 40*, 1243-1250.

220. Yildiz, G., Demiryurek, A. T., Sahin-Erdemli, I., and Kanzik, I. (1998) Comparison of antioxidant activities of aminoguanidine, methylguanidine and guanidine by luminol-enhanced chemiluminescence, *Br J Pharmacol 124*, 905-910.

221. Ruggiero-Lopez, D., Lecomte, M., Moinet, G., Patereau, G., Lagarde, M., and Wiernsperger, N. (1999) Reaction of metformin with dicarbonyl compounds. Possible implication in the inhibition of advanced glycation end product formation, *Biochem Pharmacol 58*, 1765-1773.

222. Beisswenger, P., and Ruggiero-Lopez, D. (2003) Metformin inhibition of glycation processes, *Diabetes Metab 29*, 6S95-103.

223. Tanaka, Y., Uchino, H., Shimizu, T., Yoshii, H., Niwa, M., Ohmura, C., Mitsuhashi, N., Onuma, T., and Kawamori, R. (1999) Effect of metformin on advanced glycation endproduct formation and peripheral nerve function in streptozotocin-induced diabetic rats, *Eur J Pharmacol 376*, 17-22.

224. Khouri, H., Collin, F., Bonnefont-Rousselot, D., Legrand, A., Jore, D., and

Gardes-Albert, M. (2004) Radical-induced oxidation of metformin, *Eur J Biochem 271*, 4745-4752.

225. Forbes, J. M., Thallas, V., Thomas, M. C., Founds, H. W., Burns, W. C., Jerums, G., and Cooper, M. E. (2003) The breakdown of preexisting advanced glycation end products is associated with reduced renal fibrosis in experimental diabetes, *FASEB J 17*, 1762-1764.

226. Peppa, M., Brem, H., Cai, W., Zhang, J. G., Basgen, J., Li, Z., Vlassara, H., and Uribarri, J. (2006) Prevention and reversal of diabetic nephropathy in db/db mice treated with alagebrium (ALT-711), *Am J Nephrol 26*, 430-436.

227. Demiot, C., Tartas, M., Fromy, B., Abraham, P., Saumet, J. L., and Sigaudo-Roussel, D. (2006) Aldose reductase pathway inhibition improved vascular and C-fiber functions, allowing for pressure-induced vasodilation restoration during severe diabetic neuropathy, *Diabetes 55*, 1478-1483.

228. Susic, D., Varagic, J., Ahn, J., and Frohlich, E. D. (2004) Cardiovascular and renal effects of a collagen cross-link breaker (ALT 711) in adult and aged spontaneously hypertensive rats, *Am J Hypertens 17*, 328-333.

229. Zieman, S. J., Melenovsky, V., Clattenburg, L., Corretti, M. C., Capriotti, A., Gerstenblith, G., and Kass, D. A. (2007) Advanced glycation endproduct crosslink breaker (alagebrium) improves endothelial function in patients with isolated systolic hypertension, *J Hypertens 25*, 577-583.

230. Coughlan, M. T., Thallas-Bonke, V., Pete, J., Long, D. M., Gasser, A., Tong, D. C., Arnstein, M., Thorpe, S. R., Cooper, M. E., and Forbes, J. M. (2007) Combination

therapy with the advanced glycation end product cross-link breaker, alagebrium, and angiotensin converting enzyme inhibitors in diabetes: synergy or redundancy?, *Endocrinology 148*, 886-895.

231. Tan, A. L., Sourris, K. C., Harcourt, B. E., Thallas-Bonke, V., Penfold, S., Andrikopoulos, S., Thomas, M. C., O'Brien, R. C., Bierhaus, A., Cooper, M. E., Forbes, J. M., and Coughlan, M. T. (2010) Disparate effects on renal and oxidative parameters following RAGE deletion, AGE accumulation inhibition, or dietary AGE control in experimental diabetic nephropathy, *Am J Physiol Renal Physiol 298*, F763-770.

232. Feng, L., Matsumoto, C., Schwartz, A., Schmidt, A. M., Stern, D. M., and Pile-Spellman, J. (2005) Chronic vascular inflammation in patients with type 2 diabetes: endothelial biopsy and RT-PCR analysis, *Diabetes Care 28*, 379-384.

233. Schmidt, A. M., Hori, O., Chen, J. X., Li, J. F., Crandall, J., Zhang, J., Cao, R., Yan, S. D., Brett, J., and Stern, D. (1995) Advanced glycation endproducts interacting with their endothelial receptor induce expression of vascular cell adhesion molecule-1 (VCAM-1) in cultured human endothelial cells and in mice. A potential mechanism for the accelerated vasculopathy of diabetes, *J Clin Invest 96*, 1395-1403.

234. Goh, S. Y., and Cooper, M. E. (2008) Clinical review: The role of advanced glycation end products in progression and complications of diabetes, *J Clin Endocrinol Metab 93*, 1143-1152.

235. Park, L., Raman, K. G., Lee, K. J., Lu, Y., Ferran, L. J., Jr., Chow, W. S., Stern, D., and Schmidt, A. M. (1998) Suppression of accelerated diabetic atherosclerosis by the

soluble receptor for advanced glycation endproducts, *Nat Med 4*, 1025-1031.

236. Schmidt, A. M., Vianna, M., Gerlach, M., Brett, J., Ryan, J., Kao, J., Esposito, C., Hegarty, H., Hurley, W., Clauss, M., and et al. (1992) Isolation and characterization of two binding proteins for advanced glycosylation end products from bovine lung which are present on the endothelial cell surface, *J Biol Chem 267*, 14987-14997.

237. Bucciarelli, L. G., Wendt, T., Rong, L., Lalla, E., Hofmann, M. A., Goova, M. T., Taguchi, A., Yan, S. F., Yan, S. D., Stern, D. M., and Schmidt, A. M. (2002) RAGE is a multiligand receptor of the immunoglobulin superfamily: implications for homeostasis and chronic disease, *Cell Mol Life Sci 59*, 1117-1128.

238. Sakatani, S., Yamada, K., Homma, C., Munesue, S., Yamamoto, Y., Yamamoto, H., and Hirase, H. (2009) Deletion of RAGE causes hyperactivity and increased sensitivity to auditory stimuli in mice, *PloS one 4*, e8309.

239. Brouwers, O., Niessen, P. M., Ferreira, I., Miyata, T., Scheffer, P. G., Teerlink, T., Schrauwen, P., Brownlee, M., Stehouwer, C. D., and Schalkwijk, C. G. (2011) Overexpression of glyoxalase-I reduces hyperglycemia-induced levels of advanced glycation end products and oxidative stress in diabetic rats, *J Biol Chem 286*, 1374-1380.

240. Schlotterer, A., Kukudov, G., Bozorgmehr, F., Hutter, H., Du, X., Oikonomou, D., Ibrahim, Y., Pfisterer, F., Rabbani, N., Thornalley, P., Sayed, A., Fleming, T., Humpert, P., Schwenger, V., Zeier, M., Hamann, A., Stern, D., Brownlee, M., Bierhaus, A., Nawroth, P., and Morcos, M. (2009) C. elegans as model for the study of high glucose- mediated life span reduction, *Diabetes 58*, 2450-2456.

241. Ranganathan, S., Walsh, E. S., and Tew, K. D. (1995) Glyoxalase I in detoxification: studies using a glyoxalase I transfectant cell line, *Biochem J 309 (Pt 1)*, 127-131.

242. Cameron, N. E., Cotter, M. A., Basso, M., and Hohman, T. C. (1997) Comparison of the effects of inhibitors of aldose reductase and sorbitol dehydrogenase on neurovascular function, nerve conduction and tissue polyol pathway metabolites in streptozotocin-diabetic rats, *Diabetologia 40*, 271-281.

243. Pethe, K., Sequeira, P. C., Agarwalla, S., Rhee, K., Kuhen, K., Phong, W. Y., Patel, V., Beer, D., Walker, J. R., Duraiswamy, J., Jiricek, J., Keller, T. H., Chatterjee, A., Tan, M. P., Ujjini, M., Rao, S. P., Camacho, L., Bifani, P., Mak, P. A., Ma, I., Barnes, S. W., Chen, Z., Plouffe, D., Thayalan, P., Ng, S. H., Au, M., Lee, B. H., Tan, B. H., Ravindran, S., Nanjundappa, M., Lin, X., Goh, A., Lakshminarayana, S. B., Shoen, C., Cynamon, M., Kreiswirth, B., Dartois, V., Peters, E. C., Glynne, R., Brenner, S., and Dick, T. (2010) A chemical genetic screen in Mycobacterium tuberculosis identifies carbon-source-dependent growth inhibitors devoid of in vivo efficacy, *Nat Commun 1*, 57.

244. Edgell, C. J., McDonald, C. C., and Graham, J. B. (1983) Permanent cell line expressing human factor VIII-related antigen established by hybridization, *Proc Natl Acad Sci U S A 80*, 3734-3737.

245. Riederer, I., Sievert, W., Eissner, G., Molls, M., and Multhoff, G. (2010) Irradiation-induced up-regulation of HLA-E on macrovascular endothelial cells confers protection against killing by activated natural killer cells, *PloS one 5*, e15339.

246. O'Connor, R. P., Madison, S. D., Leveque, P., Roderick, H. L., and Bootman, M. D.

(2010) Exposure to GSM RF fields does not affect calcium homeostasis in human endothelial cells, rat pheocromocytoma cells or rat hippocampal neurons, *PloS one 5*, e11828.

247. Lim, E. J., Smart, E. J., Toborek, M., and Hennig, B. (2007) The role of caveolin-1 in PCB77-induced eNOS phosphorylation in human-derived endothelial cells, *American journal of physiology. Heart and circulatory physiology 293*, H3340-3347.

248. Sakuma, S., Nishioka, Y., Imanishi, R., Nishikawa, K., Sakamoto, H., Fujisawa, J., Wada, K., Kamisaki, Y., and Fujimoto, Y. (2010) cis9, trans11-Conjugated Linoleic Acid Differentiates Mouse 3T3-L1 Preadipocytes into Mature Small Adipocytes through Induction of Peroxisome Proliferator-activated Receptor gamma, *J Clin Biochem Nutr 47*, 167-173.

249. Chaplen, F. W., Fahl, W. E., and Cameron, D. C. (1998) Evidence of high levels of methylglyoxal in cultured Chinese hamster ovary cells, *Proc Natl Acad Sci U S A 95*, 5533-5538.

250. Ahmed, N., Argirov, O. K., Minhas, H. S., Cordeiro, C. A., and Thornalley, P. J. (2002) Assay of advanced glycation endproducts (AGEs): surveying AGEs by chromatographic assay with derivatization by 6-aminoquinolyl-N-hydroxysuccinimidyl-carbamate and application to Nepsilon-carboxymethyl-lysine- and Nepsilon-(1-carboxyethyl)lysine-modified albumin, *Biochem J 364*, 1-14.

251. Dhar, A., Desai, K., Liu, J., and Wu, L. (2009) Methylglyoxal, protein binding and biological samples: are we getting the true measure?, *J Chromatogr B Analyt Technol*

Biomed Life Sci 877, 1093-1100.

252. Urbano, A. M., Gillham, H., Groner, Y., and Brindle, K. M. (2000) Effects of overexpression of the liver subunit of 6-phosphofructo-1-kinase on the metabolism of a cultured mammalian cell line, *Biochem J 352 Pt 3*, 921-927.

253. Umeda, M., Otsuka, Y., Ii, T., Matsuura, T., Shibati, H., Ota, H., and Sakurabayashi, I. (2001) Determination of D-sorbitol in human erythrocytes by an enzymatic fluorometric method with an improved deproteinization procedure, *Ann Clin Biochem 38*, 701-707.

254. Maeda, H., Fukuyasu, Y., Yoshida, S., Fukuda, M., Saeki, K., Matsuno, H., Yamauchi, Y., Yoshida, K., Hirata, K., and Miyamoto, K. (2004) Fluorescent probes for hydrogen peroxide based on a non-oxidative mechanism, *Angew Chem Int Ed Engl 43*, 2389-2391.

255. Li, Y., Bor, Y. C., Misawa, Y., Xue, Y., Rekosh, D., and Hammarskjold, M. L. (2006) An intron with a constitutive transport element is retained in a Tap messenger RNA, *Nature 443*, 234-237.

256. Wang, H., Meng, Q. H., Gordon, J. R., Khandwala, H., and Wu, L. (2007) Proinflammatory and proapoptotic effects of methylglyoxal on neutrophils from patients with type 2 diabetes mellitus, *Clin Biochem 40*, 1232-1239.

257. Chang, T., Untereiner, A., Liu, J., and Wu, L. (2010) Interactions of methylglyoxal and hydrogen sulfide in rat vascular smooth muscle cells, *Antioxid Redox Signal* 12, 1093-100.

258. Ramasamy, R., Yan, S. F., and Schmidt, A. M. (2006) Methylglyoxal comes of AGE,

Cell 124, 258-260.

259. Smith, J. M., Paulson, D. J., and Solar, S. M. (1997) Na+/K(+)-ATPase activity in vascular smooth muscle from streptozotocin diabetic rat, *Cardiovasc Res 34*, 137-144.

260. Agren, A., and Arnqvist, H. J. (1981) Influence of diabetes on enzyme activities in rat aorta, *Diabete Metab 7*, 19-24.

261. Heinz, F., Lamprecht, W., and Kirsch, J. (1968) Enzymes of fructose metabolism in human liver, *J Clin Invest 47*, 1826-1832.

262. Bode, C., Bode, J. C., Ohta, W., and Martini, G. A. (1980) Adaptative changes of activity of enzymes involved in fructose metabolism in the liver and jejunal mucosa of rats following fructose feeding, *Res Exp Med (Berl) 178*, 55-63.

263. Burant, C. F., and Bell, G. I. (1992) Mammalian facilitative glucose transporters: evidence for similar substrate recognition sites in functionally monomeric proteins, *Biochemistry 31*, 10414-10420.

264. Thornalley, P. J. (1988) Modification of the glyoxalase system in human red blood cells by glucose in vitro, *Biochem J 254*, 751-755.

265. Takagawa, Y., Berger, M. E., Hori, M. T., Tuck, M. L., and Golub, M. S. (2001) Long-term fructose feeding impairs vascular relaxation in rat mesenteric arteries, *Am J Hypertens 14*, 811-817.

266. Hwang, I. S., Ho, H., Hoffman, B. B., and Reaven, G. M. (1987) Fructose-induced insulin resistance and hypertension in rats, *Hypertension 10*, 512-516.

267. Nandhini, A. T., Thirunavukkarasu, V., and Anuradha, C. V. (2005) Taurine modifies insulin signaling enzymes in the fructose-fed insulin resistant rats, *Diabetes Metab 31*,

337-344.

268. Temple, R. C., Carrington, C. A., Luzio, S. D., Owens, D. R., Schneider, A. E., Sobey, W. J., and Hales, C. N. (1989) Insulin deficiency in non-insulin-dependent diabetes, *Lancet 1*, 293-295.

269. Hanssen, K. F. (1997) Blood glucose control and microvascular and macrovascular complications in diabetes, *Diabetes 46 Suppl 2*, S101-103.

270. Scalia, R., Gong, Y., Berzins, B., Zhao, L. J., and Sharma, K. (2007) Hyperglycemia is a major determinant of albumin permeability in diabetic microcirculation: the role of mu-calpain, *Diabetes 56*, 1842-1849.

271. Han, J., Mandal, A. K., and Hiebert, L. M. (2005) Endothelial cell injury by high glucose and heparanase is prevented by insulin, heparin and basic fibroblast growth factor, *Cardiovasc Diabetol 4*, 12.

272. Liu, J., Wang, R., Desai, K., and Wu, L. (2011) Upregulation of aldolase B and overproduction of methylglyoxal in vascular tissues from rats with metabolic syndrome, *Cardiovasc Res 92*, 494-503.

273. Singh, R., Barden, A., Mori, T., and Beilin, L. (2001) Advanced glycation end-products: a review, *Diabetologia 44*, 129-146.

274. Cai, H., and Harrison, D. G. (2000) Endothelial dysfunction in cardiovascular diseases: the role of oxidant stress, *Circ Res 87*, 840-844.

275. Laga, M., Cottyn, A., Van Herreweghe, F., Vanden Berghe, W., Haegeman, G., Van Oostveldt, P., Vandekerckhove, J., and Vancompernolle, K. (2007) Methylglyoxal suppresses TNF-alpha-induced NF-kappaB activation by inhibiting NF-kappaB

DNA-binding, *Biochem Pharmacol 74*, 579-589.

276. Yang, W. S., Seo, J. W., Han, N. J., Choi, J., Lee, K. U., Ahn, H., Lee, S. K., and Park, S. K. (2008) High glucose-induced NF-kappaB activation occurs via tyrosine phosphorylation of IkappaBalpha in human glomerular endothelial cells: involvement of Syk tyrosine kinase, *Am J Physiol Renal Physiol 294*, F1065-1075.

277. Park, J., Kwon, M. K., Huh, J. Y., Choi, W. J., Jeong, L. S., Nagai, R., Kim, W. Y., Kim, J., Lee, G. T., Lee, H. B., and Ha, H. (2011) Renoprotective antioxidant effect of alagebrium in experimental diabetes, *Nephrol Dial Transplant*.

278. Gabbay, K. H. (1973) The sorbitol pathway and the complications of diabetes, *N Engl J Med 288*, 831-836.

279. Yabe-Nishimura, C. (1998) Aldose reductase in glucose toxicity: a potential target for the prevention of diabetic complications, *Pharmacol Rev 50*, 21-33.

280. Lyles, G. A., and Chalmers, J. (1992) The metabolism of aminoacetone to methylglyoxal by semicarbazide-sensitive amine oxidase in human umbilical artery, *Biochem Pharmacol 43*, 1409-1414.

281. Nishikawa, T., Edelstein, D., and Brownlee, M. (2000) The missing link: a single unifying mechanism for diabetic complications, *Kidney Int Suppl 77*, S26-30.

282. Harrison, S. A., Buxton, J. M., and Czech, M. P. (1991) Suppressed intrinsic catalytic activity of GLUT1 glucose transporters in insulin-sensitive 3T3-L1 adipocytes, *Proc Natl Acad Sci U S A 88*, 7839-7843.

283. Cusin, I., Rohner-Jeanrenaud, F., Terrettaz, J., and Jeanrenaud, B. (1992) Hyperinsulinemia and its impact on obesity and insulin resistance, *Int J Obes Relat*

Metab Disord 16 Suppl 4, S1-11.

284. Henry, R. R. (1998) Type 2 diabetes care: the role of insulin-sensitizing agents and practical implications for cardiovascular disease prevention, *Am J Med 105*, 20S-26S.

285. Hardin, C. D., and Finder, D. R. (1998) Glycolytic flux in permeabilized freshly isolated vascular smooth muscle cells, *Am J Physiol 274*, C88-96.

286. Pelicano, H., Martin, D. S., Xu, R. H., and Huang, P. (2006) Glycolysis inhibition for anticancer treatment, *Oncogene 25*, 4633-4646.

287. Shepherd, P. R., Gibbs, E. M., Wesslau, C., Gould, G. W., and Kahn, B. B. (1992) Human small intestine facilitative fructose/glucose transporter (GLUT5) is also present in insulin-responsive tissues and brain. Investigation of biochemical characteristics and translocation, *Diabetes 41*, 1360-1365.

288. Berrone, E., Beltramo, E., Solimine, C., Ape, A. U., and Porta, M. (2006) Regulation of intracellular glucose and polyol pathway by thiamine and benfotiamine in vascular cells cultured in high glucose, *J Biol Chem 281*, 9307-9313.

289. Hutton, J. C., Williams, J. F., Schofield, P. J., and Hollows, F. C. (1974) Polyol metabolism in monkey-kidney epithelial-cell cultures. Sorbitol synthesis, *Eur J Biochem 49*, 347-353.

290. Hotta, N., Kakuta, H., Koh, N., Fukasawa, H., Yasuma, T., Awaya, S., and Sakamoto, N. (1991) In vitro retinal and erythrocyte polyol pathway regulation by hormones and an aldose reductase inhibitor, *Diabetes Res Clin Pract 14*, 29-35.

291. Saltiel, A. R., and Kahn, C. R. (2001) Insulin signalling and the regulation of glucose and lipid metabolism, *Nature 414*, 799-806.

292. Jia, X. (2010) Role of methylglyoxal in the pathogenesis of insulin resistance (Doctoral dissertation), University of Saskathewan.

293. Krief, S., Bazin, R., Dupuy, F., and Lavau, M. (1988) Increased in vivo glucose utilization in 30-day-old obese Zucker rat: role of white adipose tissue, *Am J Physiol 254*, E342-348.

294. Garpenstrand, H., Ekblom, J., Backlund, L. B., Oreland, L., and Rosenqvist, U. (1999) Elevated plasma semicarbazide-sensitive amine oxidase (SSAO) activity in Type 2 diabetes mellitus complicated by retinopathy, *Diabet Med 16*, 514-521.

295. Owen, O. E., Trapp, V. E., Skutches, C. L., Mozzoli, M. A., Hoeldtke, R. D., Boden, G., and Reichard, G. A., Jr. (1982) Acetone metabolism during diabetic ketoacidosis, *Diabetes 31*, 242-248.

296. Ghahary, A., Chakrabarti, S., Sima, A. A., and Murphy, L. J. (1991) Effect of insulin and statil on aldose reductase expression in diabetic rats, *Diabetes 40*, 1391-1396.

297. Kashiwagi, A., Obata, T., Suzaki, M., Takagi, Y., Kida, Y., Ogawa, T., Tanaka, Y., Asahina, T., Ikebuchi, M., Saeki, Y., and et al. (1992) Increase in cardiac muscle fructose content in streptozotocin-induced diabetic rats, *Metabolism 41*, 1041-1046.

298. Verma, S., Bhanot, S., Yao, L., and McNeill, J. H. (1997) Vascular insulin resistance in fructose-hypertensive rats, *Eur J Pharmacol 322*, R1-2.

299. Wang, Y., Cheng, K. K., Lam, K. S., Wu, D., Huang, Y., Vanhoutte, P. M., Sweeney, G., Li, Y., and Xu, A. (2011) APPL1 counteracts obesity-induced vascular insulin resistance and endothelial dysfunction by modulating the endothelial production of nitric oxide and endothelin-1 in mice, *Diabetes 60*, 3044-3054.

300. Tian, J. M., and Schibler, U. (1991) Tissue-specific expression of the gene encoding hepatocyte nuclear factor 1 may involve hepatocyte nuclear factor 4, *Genes Dev 5*, 2225-2234.